#106

U.S. Department of Transportation
Federal Railroad Administration

Thermal Effects and Mitigation Methods for Continuous Sheet Guideways

National Maglev Initiative
Washington, D.C. 20590

G. Samavedam
A. Purple

Foster-Miller, Inc.
350 Second Avenue
Waltham, MA 02154

DOT/FRA/NMI - 92/1

March 1992
FINAL REPORT

This document is available to the U.S. public through the National Technical Information Service, Springfield, Virginia 22161

11 - Advanced Systems

Technical Report Documentation Page

1. Report No.	2. Government Accession No.	3. Recipient's Catalog No.
DOT/FRA/NMI - 92/1		

4. Title and Subtitle	5. Report Date / 6. Performing Organization Code
Thermal Effects and Mitigation Methods for Continuous Sheet Guideways	5. Report Date: January 1992 6. Performing Organization Code: 30233
7. Author(s) G. Samavedam, A. Purple	8. Performing Organization Report No. DOT-0077-FM-9337-525
9. Performing Organization Name and Address Foster-Miller, Inc. 350 Second Avenue Waltham, MA 02154-1196	10. Work Unit No. (TRAIS) 11. Contract or Grant No. DTFR53-91-C-00077
12. Sponsoring Agency Name and Address U.S. Department of Transportation, Federal Railroad Administration 400 Seventh Street, SW Room 8222, Washington, D.C. 20590	13. Type of Report and Period Covered Final Report 14. Sponsoring Agency Code 5028-1

15. Supplementary Notes
COTR: Dr. A. Kish
U.S. Department of Transportation
Volpe National Transportation Systems Center
Kendall Square
Cambridge, MA 02142

16. Abstract

This final report summarizes work completed in the assessment and analysis of the thermal effects and mitigation methods for continuous sheet Maglev guideway structures. The thermal problems are identified and assessed in a literature search and review of design codes. Advanced heat transfer and structural analyses and parametric studies are performed to quantify the severity of these effects. Guideway deflections are found to be large and possibly inadmissible (if not mitigated) for Electromagnetic Suspension (EMS) systems. The adverse impact of thermal deflection on passenger ride comfort is also assessed. Continuous Sheet Guideway (CSG) thermal buckling, fatigue and fracture are addressed. Additional guideway heating effects due to vehicle induced eddy currents are found to be very significant in adversely affecting buckling and inducing cyclic thermal stresses. Techniques for controlling these thermal effects in both the primary structure and CSG are discussed. Alternating continuous support conditions and white surface coatings are shown to help in reducing thermal deflection in the primary structure. The use of expansion gaps and some innovative attachment and mitigation techniques for CSG are also presented. Requirements for design data and test validation of the advanced analysis are identified, and considered critical for the development of successful design methodology of Maglev structures.

17. Key Words	18. Distribution Statement
Maglev, guideway, thermal, continuous sheet, deflection, buckling, fracture, fatigue	Document is available to the U.S. public through the National Technical Information Service, Springfield, VA 22161

19. Security Classif. (of this report)	20. Security Classif. (of this page)	21. No. of Pages	22. Price
UNCLASSIFIED	UNCLASSIFIED	105	

Form DOT F 1700.7 (8-72) Reproduction of completed page authorized

PREFACE

The work in this report was sponsored by the United States Department of Transportation (DOT), Federal Railroad Administration (FRA), National Maglev Initiative (NMI) Program, under contract No. DTFR53-91-C-00077.

The report presents the results of an eight month research effort aimed at the identification and assessment of the thermal problem severity for Maglev continuous sheet guideways (CSGs) and the supporting primary structure, including methods to mitigate thermal effects.

The work herein directly supports the technology assessment objectives of NMI, and is expected to provide input to the system concept evaluation work.

Thanks are due to Dr. A. Kish of VNTSC, the COTR of this project for his technical comments and Mr. Y. Kyotani of Japan and Professor D. Wormley of MIT for their technical inputs as consultants.

The data supplied by Mr. Morton of the Florida Department of Transportation and by Prof. Ghali of the University of Calgary are gratefully acknowledged. Thanks are also due to Mr. D. Thompson, Dr. David Cope and Mr. Prem Pradhan of Foster-Miller for technical contributions to test plans, heat transfer analyses and finite element computational work.

Additional thanks are due to Dr. John Harding of the FRA for his review of the initial draft of this report.

TABLE OF CONTENTS

TABLE OF CONTENTS (Continued)

Section **Page**

LIST OF ILLUSTRATIONS

Figure **Page**

LIST OF ILLUSTRATIONS (Continued)

Figure **Page**

LIST OF ILLUSTRATIONS (Continued)

LIST OF ILLUSTRATIONS (Continued)

Figure **Page**

LIST OF TABLES

1. INTRODUCTION

Thermal considerations in the design of Maglev guideways are important for safe and economical operations of emerging Maglev systems. The issue is particularly significant in Maglev guideways which use continuous or segmented sheets. The sheet guideways, typically of aluminum, are proposed in many of the conceptual U.S. designs based on the electrodynamic system (EDS) (see Figure 1-1). They are preferred to the discrete coil arrangement due to their apparent cost savings in installation. The sheet guideway structural performance under thermal loads is critical for successful implementation of these designs.

A number of problems including buckling and tensile fracture could arise in continuous sheet guideways due to solar and vehicle induced heating. Further, the sheets cannot be directly bolted to the primary structure through drilled holes, as the holes act as stress raisers, thereby reducing fatigue life. The attachment of continuous sheets to the primary concrete structure poses a difficult problem which has not been addressed in the literature.

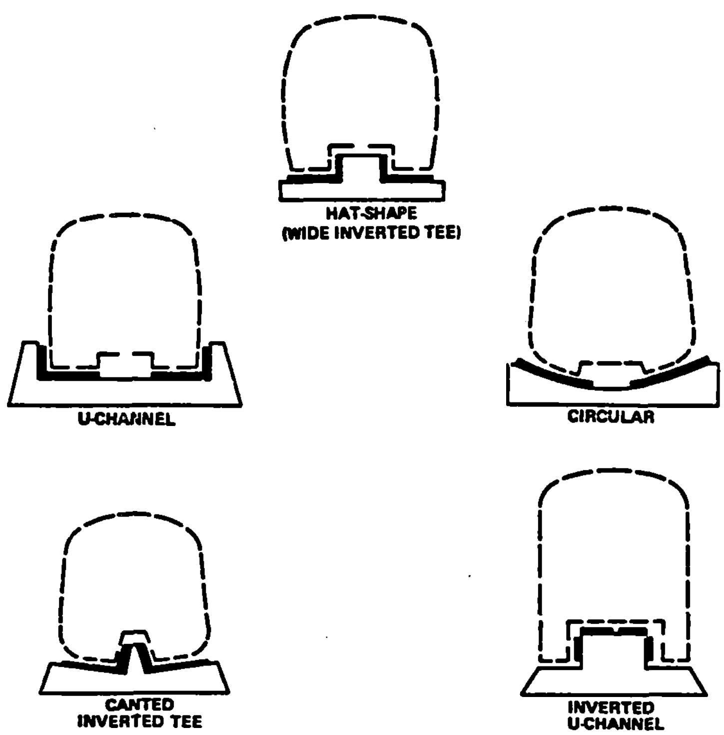

Figure 1-1. Typical Sheet Guideway Configurations

Adopting segmented guideways (with expansion gaps) in preference to continuous guideways to alleviate thermal forces may pose other problems. Loss of levitation and interruption of eddy current paths causing force transients could occur. This could affect ride quality and give rise to instabilities in the vehicle motion. Fatigue and quenching of supercooled magnets can occur, as pointed out in a recent work by Rossing, et al. (1) at Argonne National Laboratory.

The primary elevated structure which could be of concrete or steel will also experience undesirable thermal deformation due to the temperature gradient from top to bottom in the cross section. In the electromagnetic suspension systems (EMS) the transverse deflections, if not properly mitigated, can exceed the tight tolerances to which the guideways are designed. In addition to the potential interference with smooth passage of vehicles, ride quality will deteriorate as a result of the thermal deflections.

Although some foreign Maglev systems such as the German Transrapid have evolved to a reasonable operational stage, their published design method does not address the thermal problems. Although the thermal stress and deflection problems are recognized by the developers of the German electromagnet system and the Japanese superconducting electrodynamic system, it appears that there is no rational methodology, guidelines or design criteria to deal with this important technical issue of Maglev guideways.

What is missing to date is a comprehensive thermal load analysis for Maglev guideway and CSG systems. Currently available tools rely on very elementary calculations which are inadequate to predict critical loads, stresses and deformations. New analysis techniques are required not only for the CSG buckling and tensile failure predictions, but also for analyzing the supporting structure deformation behavior due to thermal loads, i.e., the thermal deflections resulting from depthwise temperature gradients particularly relevant to elevated Maglev structures.

Hence in view of the above, an important aspect of an improved Maglev guideway system design methodology is to have the advanced structural analysis tool and optimization capability to handle the thermal load effects so that strategies for the adequate mitigation of these influences could be developed.

1.1 Objectives

The overall objectives of the work reported here are: (1) identification of thermal problems associated with sheet guideways and support structures in Maglev transportation; (2) quantification of their severity through advanced thermal and structural analyses; (3) development of potential techniques to mitigate the thermal effects in Maglev structures; and (4) development of requirements for a design data software package, and for test validation of thermal analyses and possible mitigation concepts.

The foregoing objectives have been realized through the works presented in Sections 2 to 5. A brief description of accomplishments in each of the works is presented here. Conclusions of practical interest based on these works are presented in Section 6.

1.2 Accomplishments

Task 1 - Identification of Thermal Problems in Maglev Structures

This work, which is described in Section 2, presents a thorough discussion of temperature codes available in the U.S. and foreign countries. The New Zealand code on temperature due to diurnal solar heating is based on a fifth degree variation in depth direction and has been validated by tests. This code appears to be most appropriate for use on elevated Maglev primary structures. The literature search indicated that there is little published data, especially in the U.S., on vehicle induced heating in sheet guideways, which can be significant. There is also no adequate literature on attachment techniques of the sheet guideway to the primary structure.

Buckling due to temperature rise and tensile fracture due to temperature drop have also been identified as potential problems in sheet guideways.

Task 2 - Advanced Structural Analysis

The work performed under this task is presented in Section 3. The purpose of this work is to quantify the severity of thermal effects in CSG and primary Maglev structures, and to perform a parametric study using advanced analyses. This study has also been used to determine critical parameters influencing the structural performance under thermal loads.

Advanced analyses performed include: (1) heat transfer analysis in CSG and primary structure; (2) primary structural response under temperature gradient and its effect on ride quality; and (3) sheet guideway buckling and tensile fracture predictions, including strain transfer effects from the primary structure.

The heat transfer model for CSG includes the heating from eddy currents due to the passage of the superconducting magnet. This model predicts substantial increases in temperature in the sheet guideways.

Temperature distribution for the primary structure is evaluated using a two-dimensional unsteady state heat transfer model based on the Finite Element Method. The heat transfer considers diurnal solar input, radiation and convection losses, and heat carried away by conduction in the guideway cross section. The model facilitates the determination of the "worst" temperature distribution for any design of guideway to be erected in any geographical location.

The primary structural response of the guideway beam is evaluated using the beam theory with due regard to support conditions. Without some way of mitigating the response, the resulting deflections exceed the tolerance limits assumed in some guideway designs. The effect of thermal deflection on ride quality is evaluated using a simple dynamic model of the vehicle. Acceleration levels on the order of 0.05g are found in some cases, which may be considered to be significant from the ride quality viewpoint.

The buckling model developed predicts low buckling strengths for CSG, and therefore requires either a high neutral or stress free installation temperature (which could cause tensile fracture due to winter cooling), or a short fastener pitch (which could be prohibitively expensive).

Section 3 also presents an analysis of segmented sheets and optimum gap width and lengths for these sheets.

Task 3 - Mitigation Techniques for Control of Thermal Effects

This is presented in Section 4 of the report. Techniques for controlling thermal effects both in the primary structure and the CSG are discussed. The basis of the mitigation techniques is derived from the parametric study conducted using the advanced analysis presented in Task 2.

Primary structure mitigation techniques considered include use of white coatings and insulating concrete. Support conditions (simply supported vs alternating continuous) would also help in reducing thermal stress or deflection. The tradeoffs are also presented in this section.

Several mitigation techniques for control of thermal effects in CSG have been studied. These include known methods such as use of expansion gaps, and some innovative techniques. An innovative attachment technique using bonding is proposed. Use of innovative flexible structures to allow for longitudinal expansion has also been proposed.

Task 4- Design Data and Test Requirements

Requirements for tests to validate advanced analyses, and to facilitate development of a design/data software are presented in this section. The tests identified are critical for understanding fundamental issues related to thermal effects and for the development of successful design methodology of Maglev structures.

2. THERMAL PROBLEMS IN MAGLEV GUIDEWAY STRUCTURES

To assess the severity of the thermal problems in Maglev structures, a detailed search and review of U.S. and foreign literature and design data was conducted. This review included: data on available temperature distributions and codes for elevated structures; deflection, buckling, fracture and fatigue behavior under thermal loads; field and laboratory investigations of elevated structure and CSG designs; and current design guidelines and practices for thermal influence mitigation. The review encompassed literature from many countries, but concentrated on those active in Maglev design, development, analysis or operation, and included the U.S., Japan, Germany, the U.K. and Canada. The results of this review are discussed in the subsections below.

2.1 Thermal Loading and Temperature Distribution

The thermal loading in a Maglev structure is due both to the temperature distribution through the depth of the structure, and the temperature change from the neutral installation temperature, as shown in Figure 2-1. The primary guideway support structure experiences a thermal moment, M_T, caused by the depth-wise distribution of temperature. The guideway sheet experiences a direct load, P, due to temperature change. Both of these loadings can cause adverse effects, inducing excessive deflection, stress and fatigue.

The direct load P and the thermal moment M_T are given by

$$P = AE\,\alpha_S\,(T-T_0); \quad M_T = \int E\alpha_G\,T\,y\,dA$$

here

- A = cross sectional area
- E = Young's modulus
- α_S = sheet coefficient of thermal expansion
- α_G = guideway coefficient of thermal expansion
- T_0 = installation or stress free temperature
- T = temperature at depth, y

It is well known that a nonlinear temperature distribution induces thermal stresses in elevated structures even if complete freedom of end movements is allowed. The starting point in any thermal deflection and stress analysis is the determination of this temperature distribution.

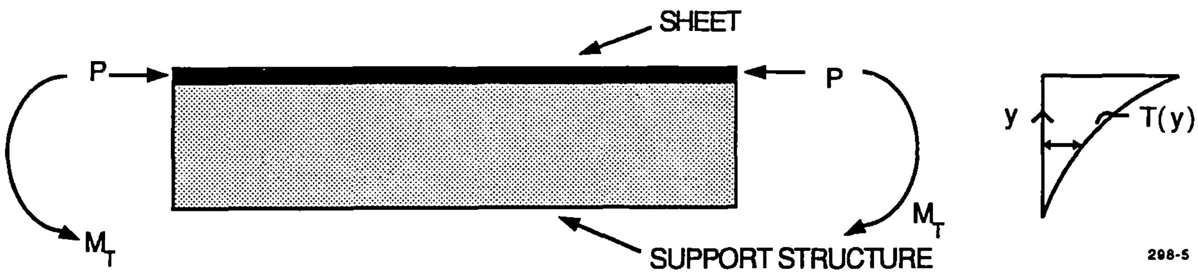

Figure 2-1. Thermal Loads

Several methods exist to determine the distribution of temperature through the depth of the structure. In all the literature, the temperature is assumed to be constant in the longitudinal direction. The temperature variations in both directions in the cross-sectional plane are of interest. Generally, the variation with depth, and the corresponding vertical deflection, are considered more important than variations in the lateral direction. The problem, then, is that of one-dimensional unsteady heat transfer. Even so, the problem is still complicated, as seen in the formulation. Figure 2-2 shows the heat transfer situation in the deck of a guideway structure. The input heat is due to incident solar radiation, as well as due to internal heating in the sheet guideway, generated from eddy currents caused by the moving magnets in the vehicle suspension. The heat loss consists of long wave emission and convection due to wind flow.

The differential equation for the unsteady state heat transfer is

$$K_i \frac{\partial^2 T}{\partial y^2} + \dot{q}_i = \rho_i C_i \frac{\partial T}{\partial t}$$

where

K_i = thermal conductivity of the i^{th} layer
C_i = specific heat of the i^{th} layer
ρ_i = mass density of the i^{th} layer
$\dot{q}_i$ = heat generated per unit volume of the i^{th} layer
t = time

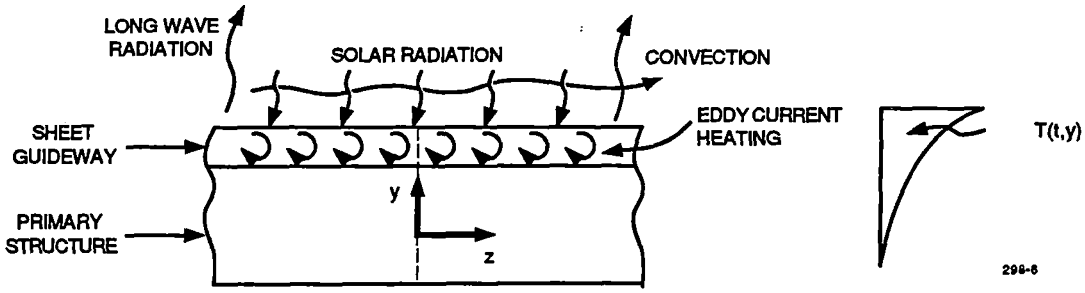

Figure 2-2. Heat Transfer in Elevated Maglev

The boundary condition at the top surface is

$$K_1 \frac{\partial T}{\partial y} = -(q_1 - q_2 - q_3)$$

where

q_1 = heat absorbed by solar radiation
q_2 = heat lost by convection
q_3 = heat lost by long wave radiation

Solution of the foregoing heat transfer problem (neglecting vehicle induced heating) has been attempted by several authors using analytical or finite element techniques. Additionally, several authors have conducted experimental studies on elevated bridge structures to determine the depth-wise temperature distribution. Priestley and others (2) wrote a general computer program using the one-dimensional heat transfer equation and also conducted various parametric studies on concrete bridges. Based on this work, Priestly recommended a fifth order variation in temperature through the depth of the structure, and this is reflected in the New Zealand design specification. Hoffman, et al., (3) conducted experimental temperature studies of a concrete bridge and concluded that the critical temperature distribution (i.e., that which produces maximum vertical deflection) can be approximated by a fifth order polynomial, as recommended by the New Zealand design code. This study also found very little temperature variation in the horizontal direction of the cross section, indicating that the problem is essentially one-dimensional.

Figure 2-3 shows the Finite Element and measured temperature distributions obtained on typical concrete bridge decks in New Zealand. The good agreement between the data indicates the realiability of the Finite Element method for the solution of unsteady state heat transfer equations presented in the earlier paragraph.

In New Zealand, laboratory work on concrete box beams was also carried out to evaluate deflection and stresses. Solar heating was simulated using radiant heat lamps. Using beam theory, Priestley and coworkers (2) made excellent predictions, as indicated in Figure 2-4.

Other experimental studies by the Florida Department of Transportation measured temperature distributions in cable-stayed bridges such as the Florida Skyway bridge (5). The bridge cross section was instrumented with thermocouples, as shown in Figure 2-5. Typical measured temperature distributions are shown in Figure 2-6. Based on the measured temperature data, it can be concluded that the temperature distribution followed the shape of the fifth degree parabola recommended by Priestly.

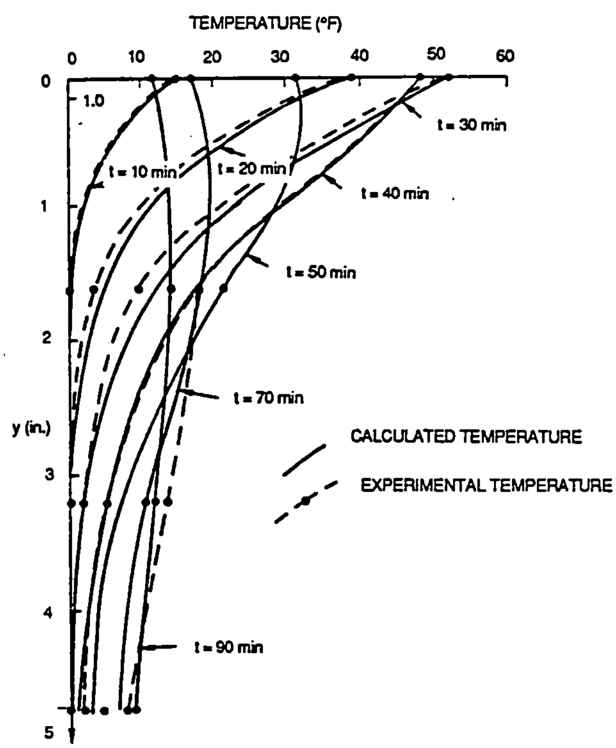

Figure 2-3. Calculated and Experimental Temperature Rises in Bridge Structures (4)

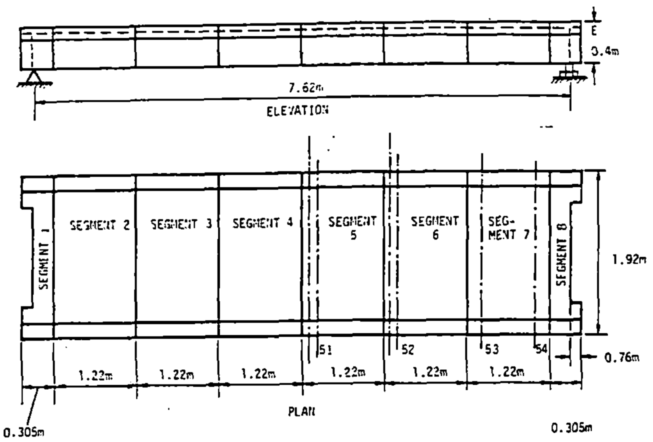

Model Bridge Used by Priestley and Buckle (2)

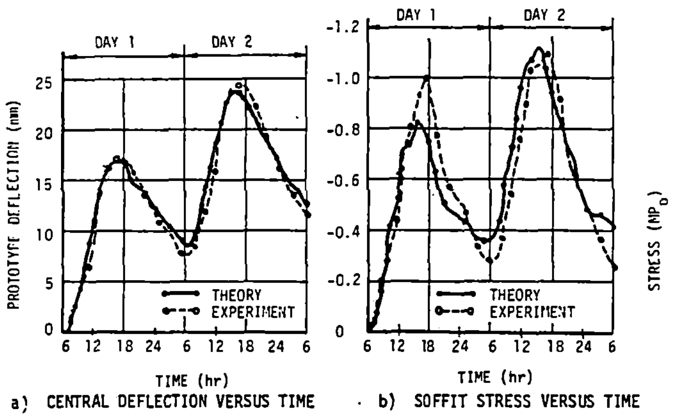

Figure 2-4. Beam Theory versus Experiment. Comparisons for Thermal Response of Quarter-Scale Prestressed Concrete Box Girder Model

2.2 Design Codes for Temperature Distribution

In addition to the New Zealand code mentioned above, various countries also have design codes which specify the temperature distribution for use in design problems of elevated structures. These design codes (discussed in the subsection below) were summarized by Podolny (6) and are illustrated on Figure 2-7.

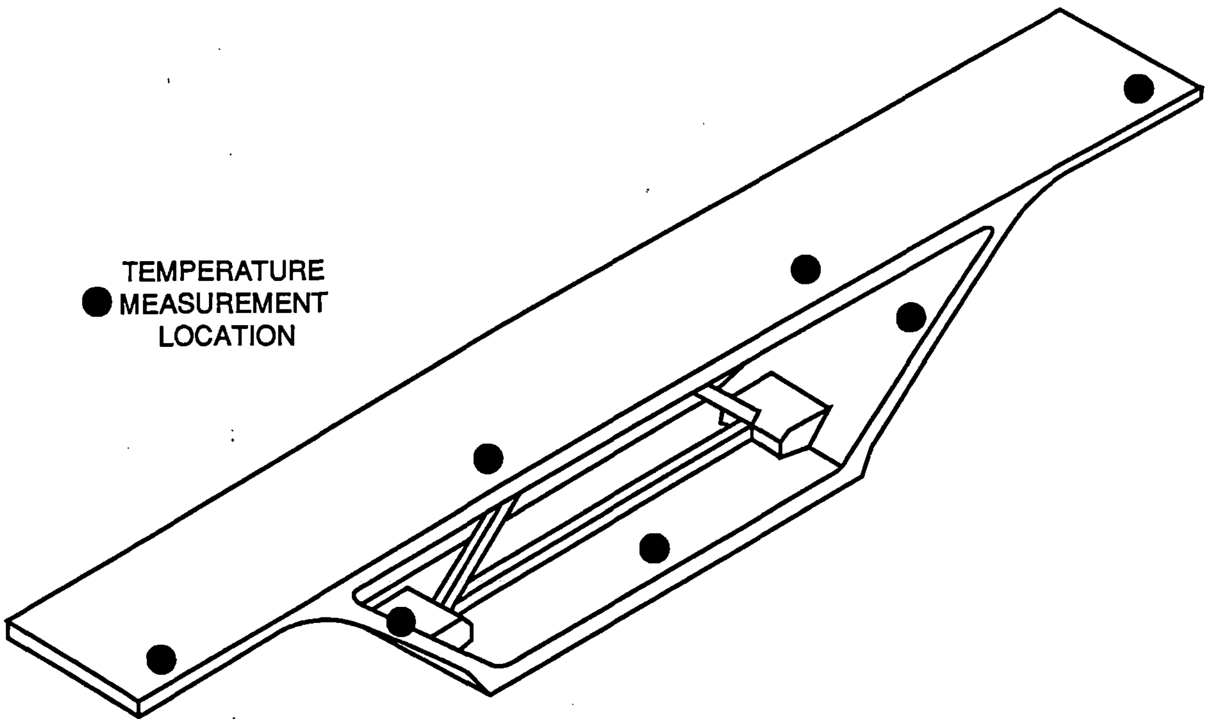

Figure 2-5. Bridge Segment and Thermocouple Locations Used in Florida DOT Skyway Bridge Thermal Study

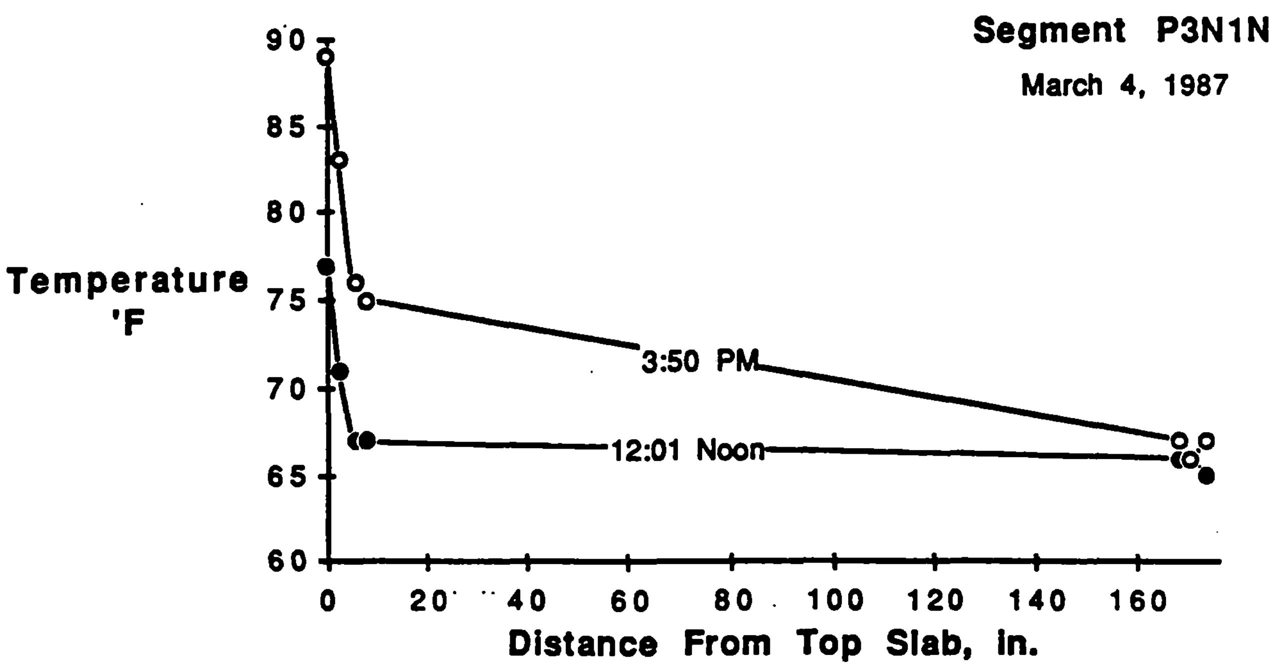

Figure 2-6. Measured Temperature Distribution in Bridge Segment

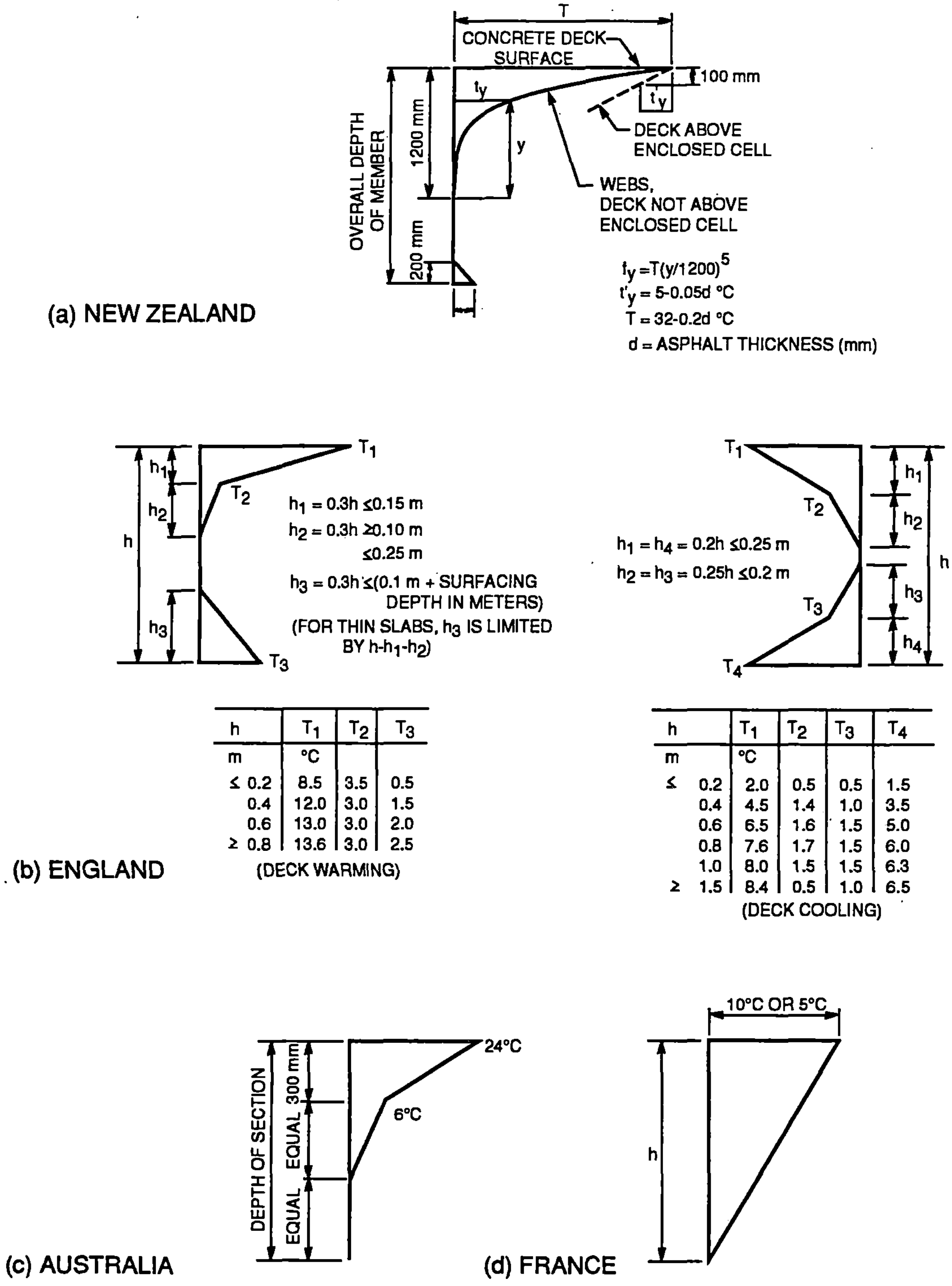

h	T_1	T_2	T_3
m	°C		
≤ 0.2	8.5	3.5	0.5
0.4	12.0	3.0	1.5
0.6	13.0	3.0	2.0
≥ 0.8	13.6	3.0	2.5

(DECK WARMING)

h	T_1	T_2	T_3	T_4
m	°C			
≤ 0.2	2.0	0.5	0.5	1.5
0.4	4.5	1.4	1.0	3.5
0.6	6.5	1.6	1.5	5.0
0.8	7.6	1.7	1.5	6.0
1.0	8.0	1.5	1.5	6.3
≥ 1.5	8.4	0.5	1.0	6.5

(DECK COOLING)

Figure 2-7. Thermal Gradients Used in Design Codes (6)

The purpose of this review of design codes is to bring out any deficiencies in the design codes for the Maglev design community and to suggest alternatives on which to base their design for improved Maglev performance.

New Zealand Code

As noted, the New Zealand code assumes a fifth order polynominal distribution through the depth of the section. In the slab above the box and in the soffit, a small linear distribution is assumed. As shown later, this code seems to represent the field conditions very closely.

British Codes

The British thermal gradient is bilinear in the upper region of the structure, with a linear distribution in the soffit. The distribution shown assumes deck warming; for a deck cooling condition, bilinear distributions are assumed for both the deck and soffit. The maximum temperatures used in the British code are much lower than the New Zealand code, and are not sufficient for the extreme thermal environment encountered in the U.S.

French Codes

The French code assumes a simple linear distribution of temperature through the entire depth of the structure. A linear distribution of temperature through a simply supported structure results in no thermal stress but does induce deflections. As such, this code is insufficient for complete and accurate assessment of thermal response.

Australian Codes

Similar to the British code, the Australian code assumes a bilinear temperature distribution through the upper section of the structure. The soffit is assumed to remain at the neutral temperature. Again, this code is considered insufficient for use in Maglev design purposes, due to the low maximum temperatures.

In addition to the codes summarized by Podolny, other countries specify design standards for thermal effects, but do not necessarily recommend a temperature distribution, as described below.

German Codes

No explicit gradient in the cross section is given in German Industrial Standard (DIN) 1072. A variance of ±30°C is to be used in calculating the thermal movements at bearings and expansion joints for concrete bridges with an assumed erection temperature of 10°C. A nonuniform temperature of ±5°C is to be considered in the design. Austria, Sweden and Japan have similar codes to Germany.

United States Codes

The current AASHTO Specifications do not consider the temperature gradients. They simply state:

Provision shall be made for stresses or movements resulting from variations in temperature. The rise and fall in temperature shall be fixed for the locality in which the structure is to be constructed and shall be figured from an assumed temperature at the time of erection. Due consideration shall be given to the lag between air temperature and the interior temperature of massive concrete members or structures. The range of temperature shall generally be as follows:

Concrete Structures	Temperature Rise	Temperature Fall
Moderate climate	16.7K (30°F)	22.2K (40°F)
Cold climate	19.4K (35°F)	25K (45°F)

These guidelines are generally insufficient for Maglev design purposes. No explicit temperature gradient is given, and the temperature range is too narrow.

Japanese Codes

As mentioned above, the Japanese codes are similar to the German design codes in that no explicit temperature gradient is specified. However, literature in Japan has shown temperature data for alternate elevated configurations used in long span bridges. In addition to the more typical span and arch construction, the long span bridges shown in Figure 2-8 can also be supported by struts or cables, which are also subject to thermal loading. For example, a maximum bridge deck deflection of -9 mm is allowed when the truss and cable supports are subjected to a temperature

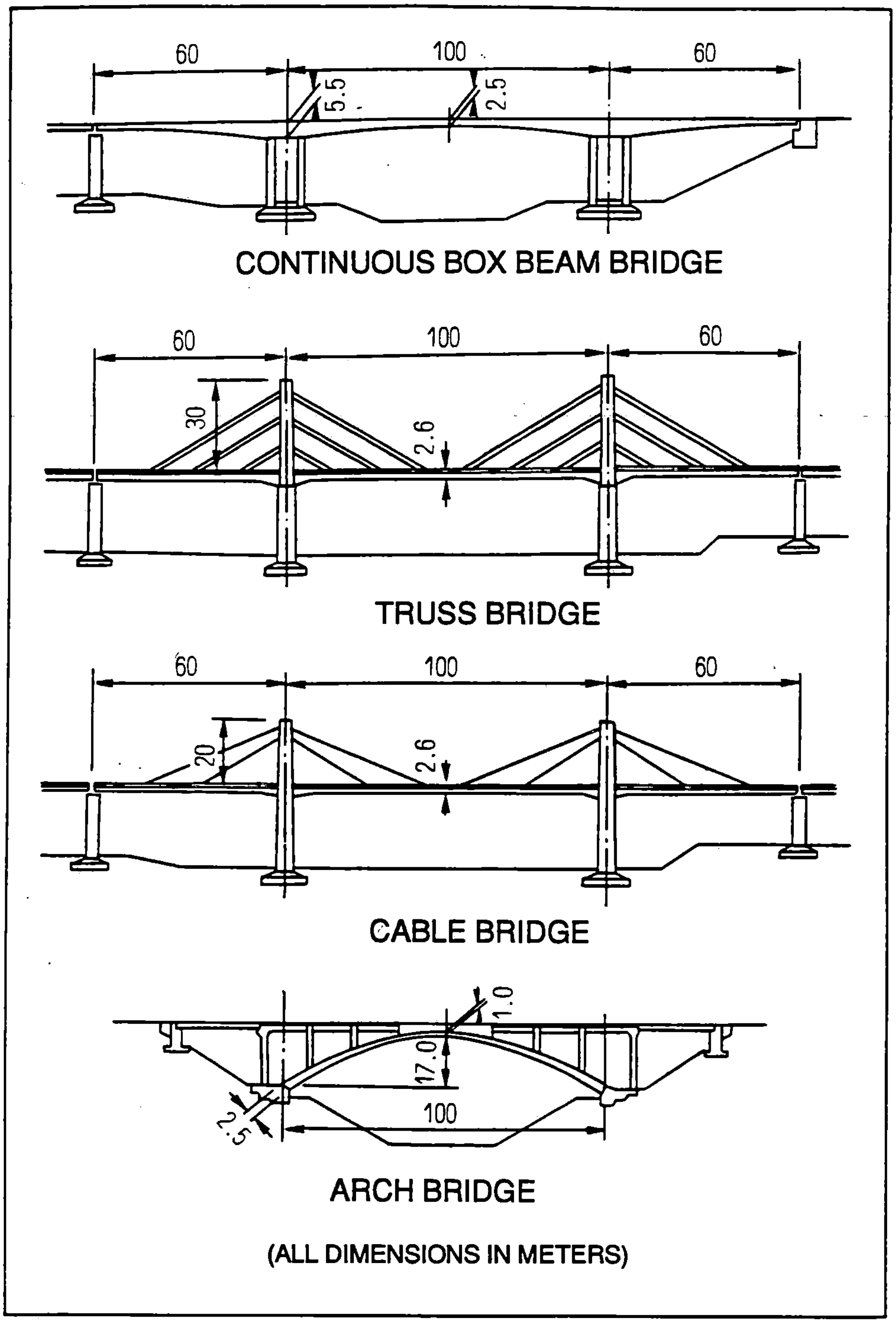

Figure 2-8. Types and Specifications of Long Span Bridges

increase of 5K. Figure 2-8 is included in this report, as it represents candidate segments in elevated Japanese Maglev routes (7).

2.3 Thermal Response of the Primary Structure

In the literature, considerable attention has been focussed on the deflection of Maglev guideway structures. Deflections typical of standard elevated structures may be tolerated by conventional transportation vehicles, but may pose problems for Maglev vehicles, especially those operated on tight tolerances, based on the attractive principle of levitation. Even those based on repulsive levitation will be affected by thermal deflections in regard to ride quality.

If the temperature distribution is known, the thermal moment and resulting thermal deflection and stresses can be calculated using beam theory. The severity of the various temperature gradients proposed by the design codes listed in the sections above were examined. The results verified that thermal deflections and stress are strongly dependent upon the temperature distribution. The thermal deflections of a Maglev system using a steel guideway under various thermal gradients are shown in Table 2-1 (from 8). The results show that the deflection for a fifth order temperature distribution can be several times larger than the deflection produced by the other temperature gradients.

The New Zealand type fifth order temperature distribution thus provides a basis for the worst case scenario thermal deflection analysis. The deflections resulting from this worst case are quite large (1.55 cm for a steel-guideway 25m span) and could violate design tolerances or affect passenger ride comfort. A more detailed discussion of this analysis of thermal deflection and stress will be presented in later sections.

2.4 Vehicle Induced Heating

In an EDS system, movement of the vehicle superconducting magnets will induce eddy currents in the guideway sheet. These eddy currents dissipate as heat, raising the temperature of the guideway sheet and primary structure. Little has been done in the literature to address this important issue.

Table 2-1. Deflection of an EMS Type Steel Guideway Due to Various Temperature Gradients (8)

Thermal Gradient	δ (cm)
Linear 10°C through section (French code)	0.53
Linear 10°C through top slab	0.32
New Zealand Code (5th order)	1.55

One Japanese study (9) did analyze the effects of eddy current heating on an aluminum CSG. Using finite difference techniques, the temperature increase in the sheet was calculated for positions at or near a Maglev station. Trains of 10 cars each were assumed, operating at 2 minutes headway with in-station stops lasting 15 seconds. The ambient temperature was assumed to be 293K (20°C). The results are shown in Figure 2-9. The maximum temperature increase due to the passage of 30 trains at short headway (rush hour) is approximately 105K. Passage of 45 trains will cause a temperature increase of 120K, as predicted in Ref. 9. The theoretical predictions were also verified through testing in this work.

Eddy current heating is then a very important issue, since a large increase in sheet temperature can result, which as shown in Section 3 can induce buckling and cyclic thermal fatigue.

2.5 Thermal Buckling, Fracture and Fatigue

In addition to the thermal moment generated by the variation of temperature through the section depth, the temperature change from the neutral installation temperature can cause a thermal compression or tension load in the continuous guideway sheet. If this load becomes excessive, the sheet can buckle from compressive load in hot weather or possibly fracture due to the tensile load in cold weather. The daily and seasonal cyclic variation of temperature can also introduce thermal fatigue problems, particularly in weldments, where tensile and fatigue strength is significantly reduced.

Significant problems of buckling and weldment failures are well known in continuous welded rail (CWR) and other transportation structures. Buckling and weldment failures also occurred on the T-shaped aluminum reaction rail used in a 5 km (3 mile) test track at the

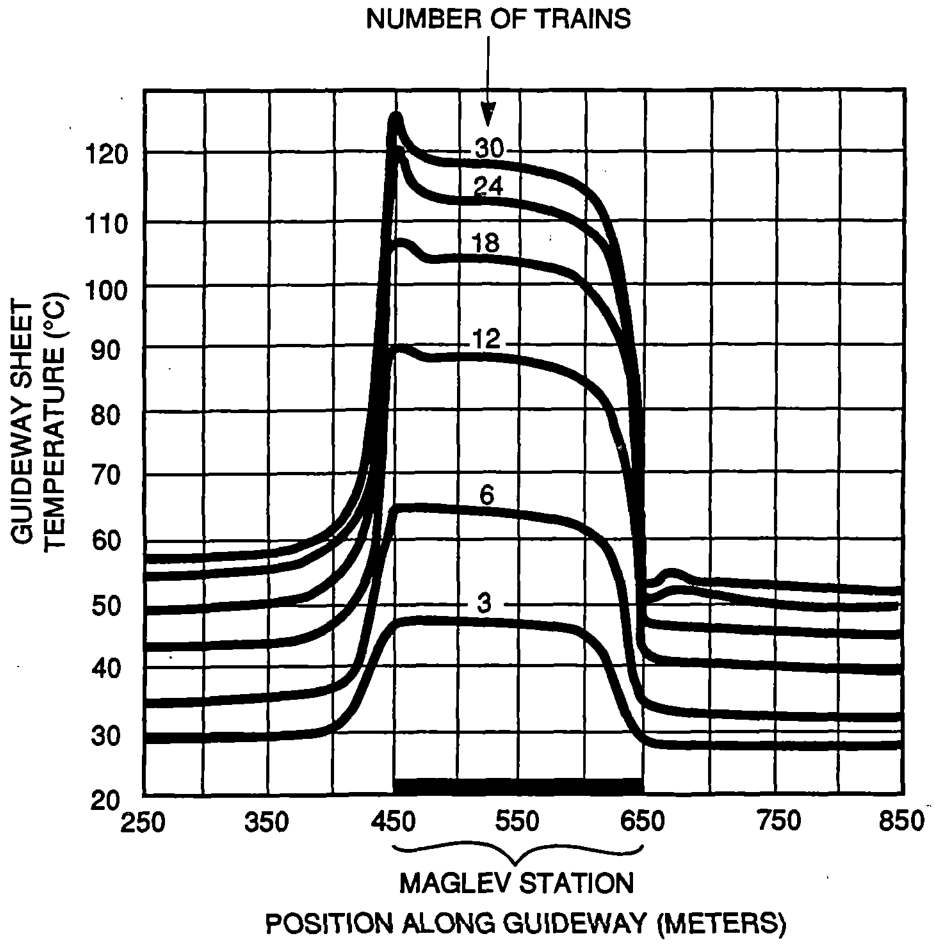

Figure 2-9. Calculated CSG Temperature due to Eddy Current Heating (9)

Transportation Test Center, (TTC) in Pueblo, Colorado. The early Garrett LIMRV was tested on this track.

Extensive work done on the analysis of CWR thermal buckling (10, 11) can be applied to a similar analysis of thermal buckling in continuous sheet guideways. Since the cross-sectional inertia (and buckling resistance) of a flat sheet is relatively small, thermal buckling could be a severe problem for CSG design. These effects can be mitigated by installation of the sheet at elevated temperatures or by using destressing techniques similar to CWR practice. This, however, can induce problems in colder weather, due to possible fracture and fatigue at weldments. Some type of design optimization procedure will be required.

2.6 Attachment Techniques

An important issue in the use of CSG is in regard to its attachment to the primary structure. Assuming the CSG material to be aluminum and the primary structure to be concrete, bonding, bolting or other fasteners pose certain problems. Bolting through the aluminum sheet gives rise to stress concentrations at the holes due to thermal load cycles. If fasteners such as clips driven in concrete and holding the CSG at the edges through friction type pads are used, the required longitudinal resistance may not be adequate. The fasteners will have to be non-metallic (which may increase costs) to reduce the magnetic drag. Designing the fastener heads to be flush with the sheet guideway can also be a problem, and may increase costs.

Bonding of large aluminum sheets to concrete is not easy, and bond failures may occur in service conditions due to vibrations and thermal cycles.

It appears that the mechanical attachment of CSG to the primary structure is a challenging technical problem which is not addressed in the Maglev literature to date. This is addressed along with some new potential solutions in Section 4.

2.7 Summary of Thermal Problem Assessment

Based on the review of U.S. and foreign literature and on the initial analysis conducted by Foster-Miller, the results of the thermal problem assessment are as follows:

- Thermal movements can occur in both continuous sheet guideways and primary Maglev structures supporting the sheet guideways. The longitudinal movements are essentially due to the overall temperature increase, whereas the vertical displacements are due to temperature gradients through the thickness. Control of both movements will be required for efficient operations and safety of Maglev guideways.

- Existing experimental data for elevated bridge structures correlate well with the temperature distribution of the New Zealand design code. A fifth order distribution similar to the New Zealand design code seems to provide a basis for the worst case scenario. However, these data do not include vehicle induced heating, which is important in Maglev structures. Therefore, an advanced heat transfer analysis is required.

- Without adequate countermeasures, the thermal deflections resulting from this worst case could be unacceptably large and affect ride quality.

- Eddy current heating of CSG has received comparatively little attention, but is a very important issue and warrants further study. A Japanese work indicated significant temperature rise due to this phenomenon.

- Existing work on the buckling of continuous structures indicates that thermal buckling of CSG is an extremely important issue and needs to be rigorously studied for effective control.

- Fracture and fatigue can also occur due to weldments in the manufacture of CSG and need to be mitigated by proper design.

- Attachment of CSG to the primary structure itself poses several problems and has not been sensibly addressed in the literature. Reliable engineering solutions for attachment are needed.

3. ADVANCED ANALYSES

In the following subsections advanced heat transfer, stress and deflections analyses of the CSG and primary structure are presented with the following objectives:

- Quantify the severity of thermal problems identified in the previous section;
- Identify critical parameters influencing heat transfer, sheet guideway buckling and fatigue, and the primary structural response through a parametric study; and
- Develop a rational basis for the mitigation methods for the thermal problems, which are discussed in Section 4.

3.1 Heat Transfer Analysis

As noted in previous sections, heat transfer occurring in the Maglev guideway is due not only to atmospheric radiation and convection, but also stems from the vehicle induced eddy current heating of the continuous guideway sheet. The guideway is subject to solar heating from the environment, which is conducted through the CSG and guideway structure. Heat loss occurs due to convective cooling and long wave radiation. This is shown in Figure 2-2. The problem will be studied in two parts. In the first part, the presence of the sheet guideway will be ignored and attention will be focussed on the primary structure. In the second part, the sheet guideway will be analyzed to include eddy current heating.

3.1.1 Primary Structure Temperature Analysis

For the thermal analysis of the primary structure, analytical solutions are difficult because of the complex cross sectional shape. The heat transfer includes radiation, convection and conduction, which is further complicated by the presence of enclosed cells of still air in the guideway cross section. A finite element method is the preferred approach. A transient, 2-D finite element analysis has been done by Foster-Miller using the FE code FETAB (12) for the candidate Foster-Miller concrete guideway design.* The resulting temperature distribution has been evaluated, and the parametric effects of candidate mitigation techniques have also been studied.

*The Foster-Miller guideway does not use continuous sheets, hence, CSG is not included in this analysis.

The finite element model is shown in Figure 3-1. This model simulates one-half of the symmetric Foster-Miller baseline, and consists of approximately 250 nodes. The properties used are typical of concrete. (Thermal conductivity =1.5 W/m-K; coefficient of thermal expansion = 8 x 10^{-6} K^{-1}; and solar absorbtivity = 0.5.) The analysis examined a worst case condition of a summer environment at 42.5 deg latitude. Maximum daytime temperature was assumed to be 308K (35°C), with a minimum night temperature of 283K (10°C). The diurnal variation of temperature was assumed to be sinusoidal.

Figure 3-2 shows the computed temperature distribution in the guideway at several time intervals. Typical temperature distributions for midnight, 9 a.m. and 2 p.m. are shown. The worst case temperature distribution corresponds to 2 p.m. This worst case temperature distribution agrees closely with the fifth order distribution of the New Zealand design code shown in Figure 2-7. The maximum temperature differential between the section web and the upper slab is 37K, whereas a value of 32K is specified by the New Zealand code. The distribution at midnight shows the effects of guideway cooling, as the internal temperature of the guideway is warmer than the surrounding air. Due to the relatively low thermal conductivity of concrete and the continuously changing ambient conditions, the guideway temperature distribution is not uniform, and does not achieve steady-state conditions.

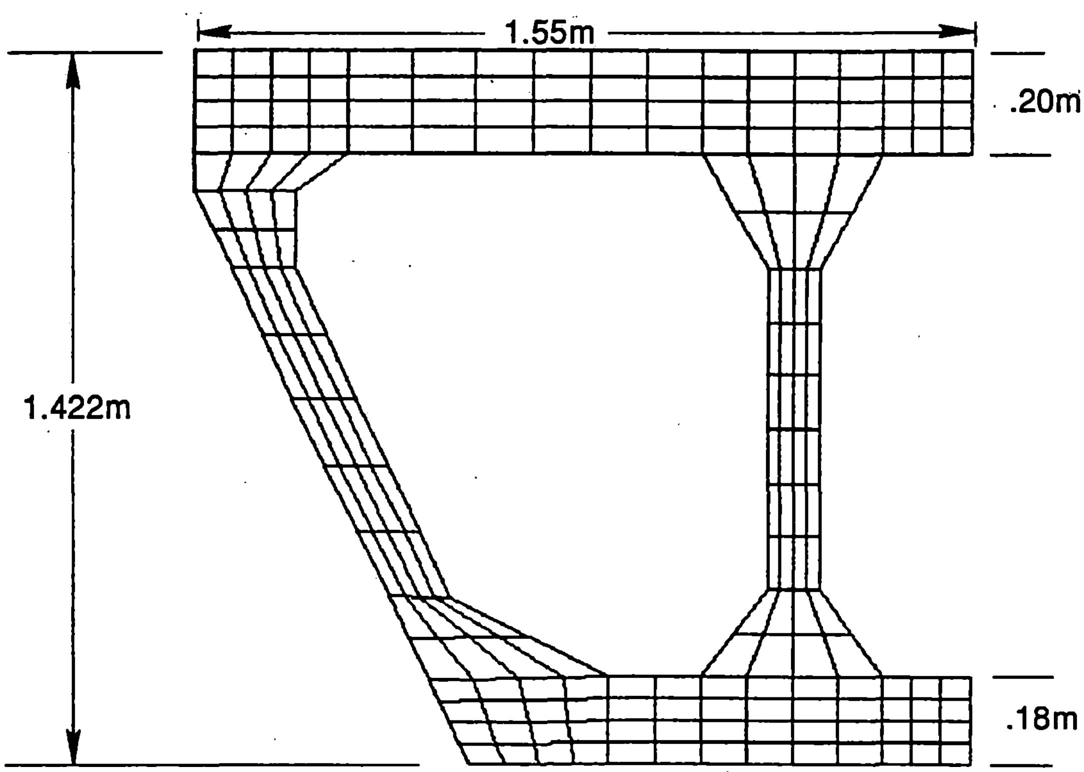

Figure 3-1. FE Model of Foster-Miller Concrete Section

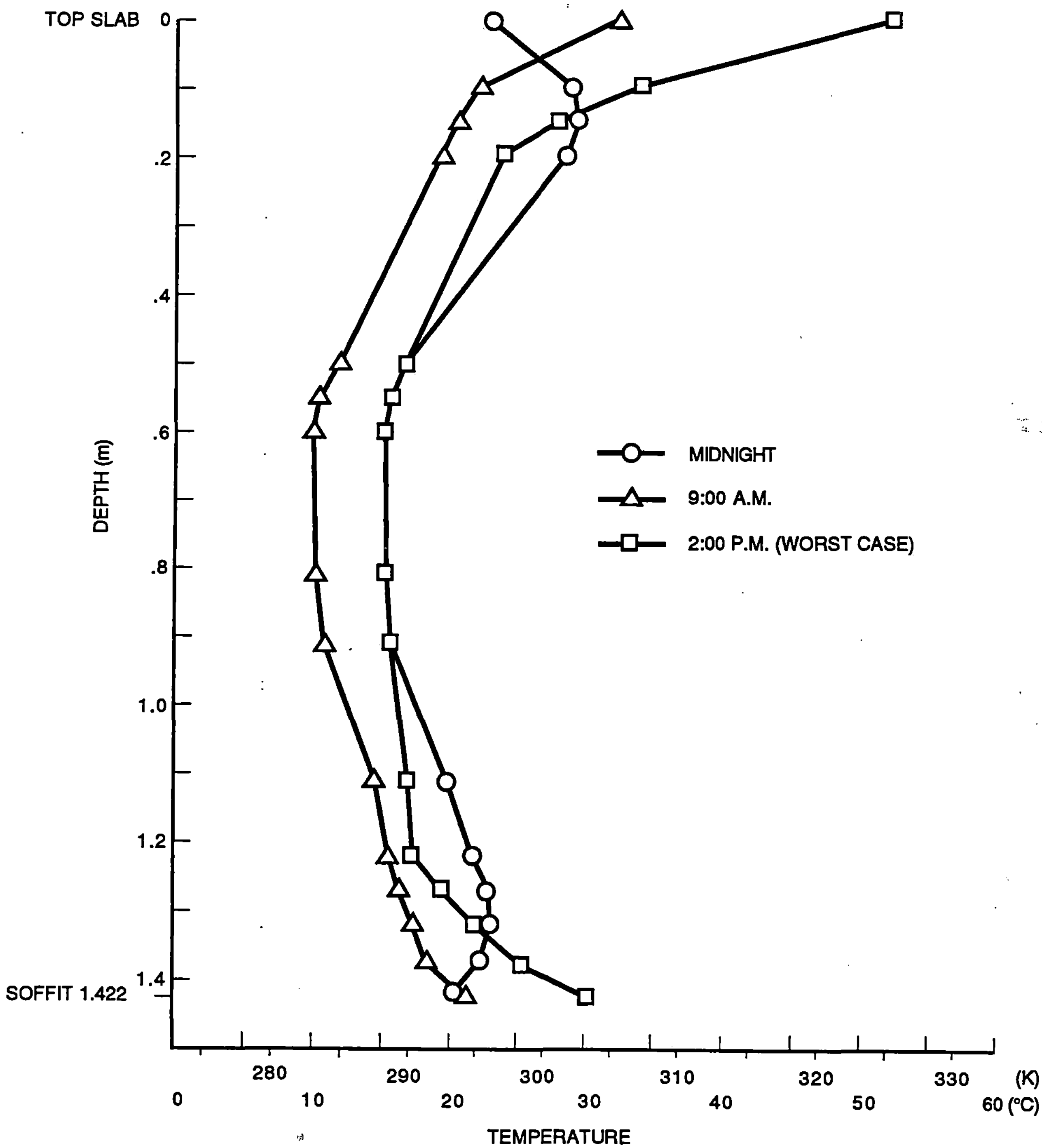

Figure 3-2. FE Model Results Showing Variation of Temperature with Time

The effects of white coatings and insulating layers of concrete were also studied using the finite element method. Their impact on the resulting temperature distribution and their potential to mitigate thermal effects were assessed. A thin layer of aerated, low conductivity concrete on the upper surface of the top slab was modeled. This insulating concrete assumed a 67 percent reduction in the typical value of concrete thermal conductivity, while the white reflective coating was assumed to reduce the absorbed solar radiation by 75 percent (13,16).

The results of this study are shown in Figure 3-3. In comparison to the untreated guideway, the insulating layer of concrete actually causes an increase in the upper slab top surface temperature. The insulated guideway absorbs as much solar radiation as the untreated guideway. However, the insulating layer cannot efficiently transmit this absorbed heat to the rest of the guideway. As a result, the top slab temperature is increased, while the internal temperature of the insulated guideway is reduced in comparison to the untreated guideway. The white coating has a much more dramatic effect, in that the temperature throughout the upper half of the structure is markedly reduced. The combined effects of insulation and white coating show a similar result.

Since the temperature distribution strongly affects the resulting thermal response of the guideway, the white reflective coating, or the coating combined with the insulating concrete layer, should significantly reduce thermal deflection and stress. The effect of the insulating layer alone is not as significant. The white reflective coating should have a similar mitigating effect on steel guideways as well.

3.1.2 CSG Temperature Analysis

Several conceptual Maglev designs exist which use CSG. They can be analyzed in a manner similar to that described above. Solar heating effects can be easily predicted, and are generally comparatively small, resulting in a small daytime temperature increase above ambient. However, as shown in subsection 2.4, eddy current heating effects are very significant, and require advanced analysis.

The eddy current heating effects are determined by calculating the total power dissipated in the guideway sheet due to induced currents that create lift and drag. The Maglev vehicle is modelled in 2-D, as shown in Figure 3-4. Magnetic levitation coils are positioned at each corner of the vehicle; each magnetic coil is represented by two bars. For convenience, the interaction between bars is ignored. The magnetic field intensity for any position x on the guideway sheet is calculated as shown in Figure 3-5. The x- and y-direction magnetic fields are given by

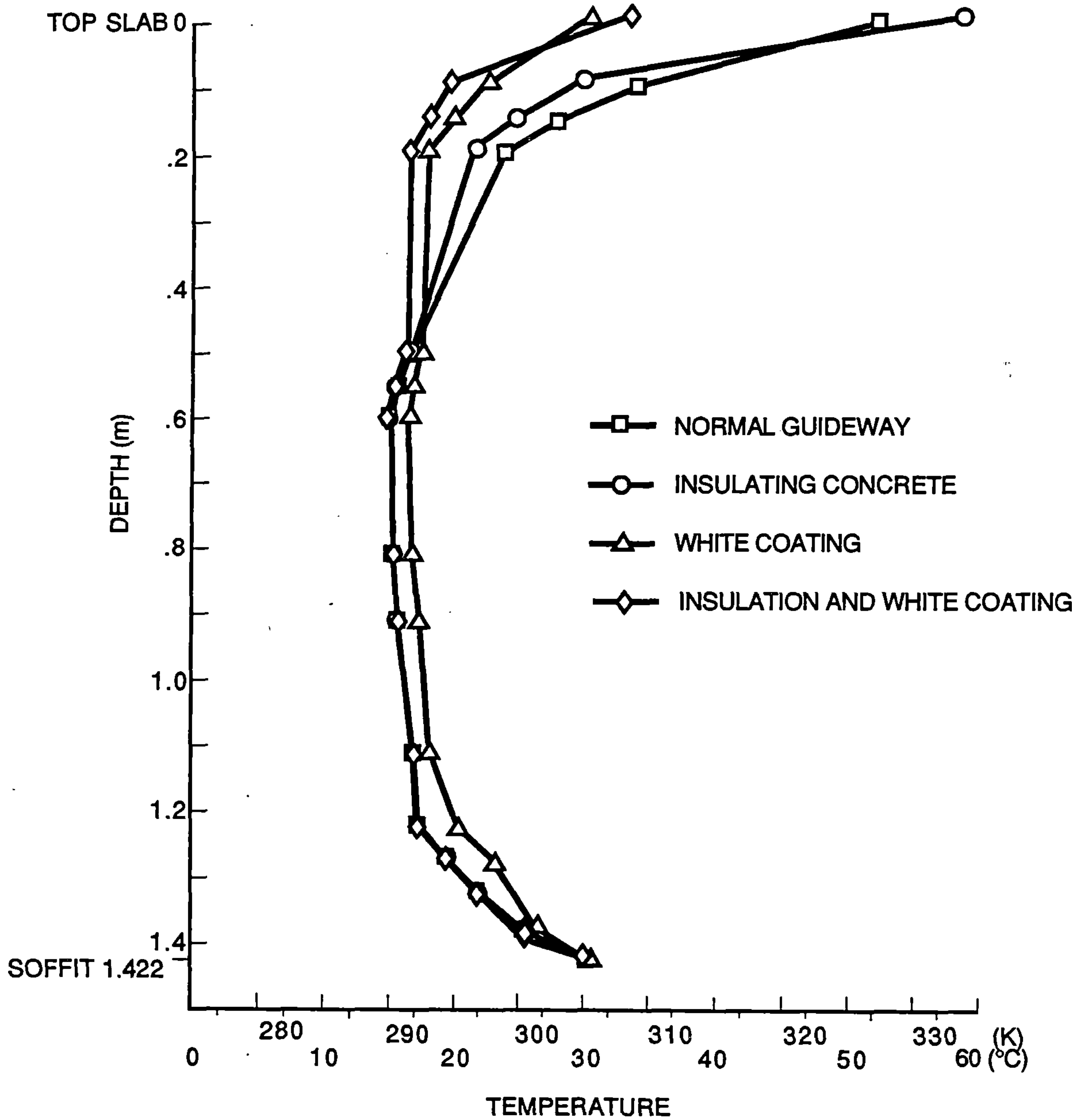

Figure 3-3. FE Model Results Showing Effects of Candidate Mitigation Methods

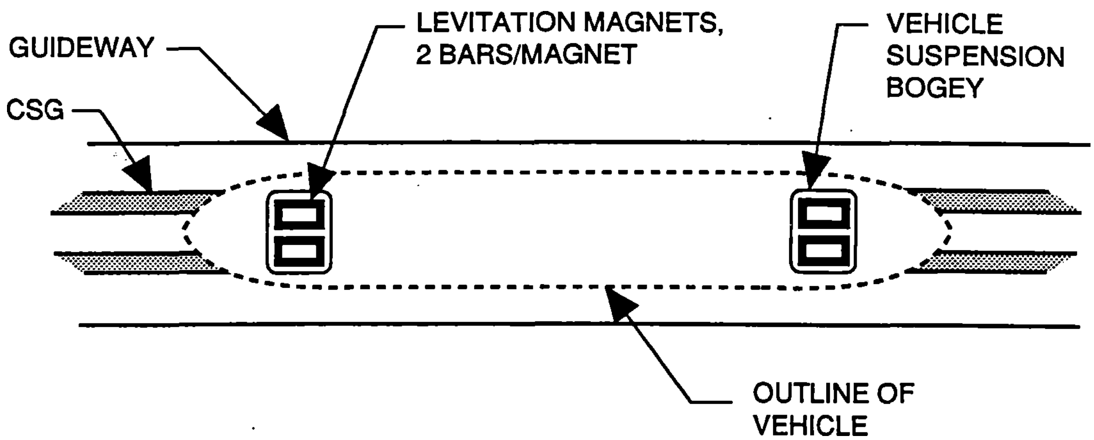

Figure 3-4. Schematic of Vehicle Model

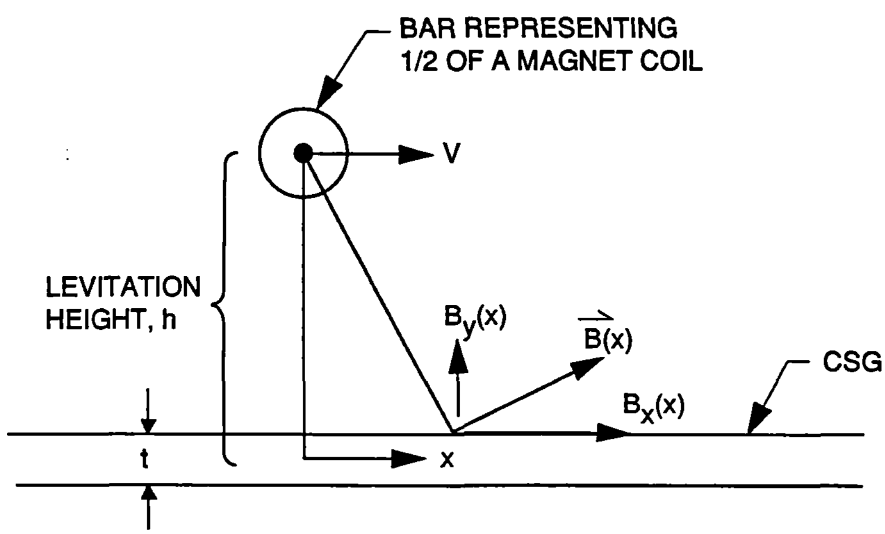

Figure 3-5. Magnetic Fields in CSG

$$B_x = \frac{\mu_o Ih}{2\pi \left(x^2+h^2\right)}$$

$$B_y = \frac{\mu_o Ix}{2\pi \left(x^2+h^2\right)}$$

where

I = coil current turns
h = levitation height
μ_o = permeability constant = $4\pi \times 10^{-7}$ H/m

The induced current K (x) in the sheet per magnetic bar is then calculated from

$$K(x) = \frac{2V}{\mu_o W} \frac{\left(B_y + B_x \frac{V}{W}\right)}{\left(1 + \frac{V^2}{W^2}\right)}$$

where

V = velocity
W = characteristic velocity = $\frac{2R}{\mu_o t}$

R = sheet resistivity

To levitate the vehicle, the total induced vertical force must equal the vehicle weight; the horizontal, x-direction force is then the drag. The vertical and horizontal forces per magnet bar are given by

$$F_y = \int_{-\infty}^{\infty} b\, K(x)\, B_x\, dx$$

$$F_x = \int_{-\infty}^{\infty} b\, K(x)\, B_y\, dx$$

where

b = sheet width

The power dissipated in the sheet is then calculated from

$$P_{DIS} = \frac{Rb}{t} \int_{-\infty}^{\infty} K^2 (x)\, dx$$

For a vehicle with N bars, the total dissipated power is

$$P_{TOT} = N \cdot P_{DIS}$$

This power is assumed to be uniformly dissipated into the guideway sheet (i.e., skin depth effects are ignored). Assuming a constant vehicle speed, V, the total energy dissipated per unit of sheet volume is then given by

$$E = \frac{P_{TOTAL}}{Vbt}$$

This energy is manifested as an increase in the sheet temperature. The temperature increase can be calculated from

$$\Delta T = \frac{E}{\rho C}$$

where

ρ = mass density

C = sheet specific heat capacity

The equation above determines the sheet temperature increase due to the passage of a single vehicle. If trains of several cars are used, the total dissipated power and increase in temperature are correspondingly greater. Maglev system design requirements assume that multiple car vehicles will be used, each operating at a headway as small as a few minutes. Assuming a long series of multi-car vehicles, each evenly separated by the vehicle headway, a quasi steady state thermal condition is reached in which the eddy current power dissipated in the sheet is balanced by the heat transfer out of the sheet to the surroundings as shown in Figure 3-6. Ignoring radiation and conduction to the concrete guideway, the temperature of the sheet can then be calculated from

$$\Delta T = \frac{P_{TOTAL}}{hA}$$

where

A = exposed sheet area between vehicles
= V • b • headway
h = convective heat transfer coefficient

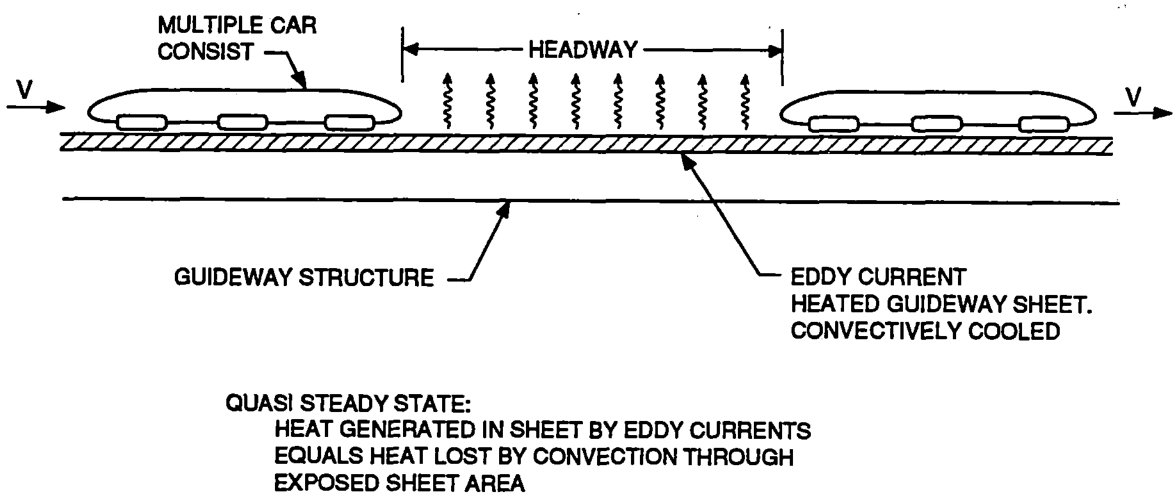

Figure 3-6. Heat Transfer in CSG due to a Series of Multiple Car Vehicles with Short Headway

Numeric Results

An in-house computer program was developed to calculate the vehicle-induced eddy currents, forces and dissipated powers. It represents a two-dimensional model of the passing of the magnet over the track. This assumption ignores sheet edge effects. For simplicity, only the current elements which are transverse to the guideway are considered. For convenience and to retain a simple model, skin depth effects were neglected. The effect of skin depth could be estimated with the model by calculating the skin depth, using that value for the sheet thickness and calculating the dissipated electrical power. The power is then uniformly distributed over the total sheet thickness by thermal conduction.

To quantify the eddy current heating effects, typical values for vehicle and sheet parameters (14,15) were assumed, as follows:

Vehicle weight (1 car):	383 kN (85,800 lbs)
Magnets per vehicle:	8, with 2 bars each
Sheet geometry:	2 parallel aluminum sheets, 1m wide and 0.01m thick, one on each side of the vehicle centerline
Sheet resistivity:	2.7×10^{-8} Ohm-m
Magnet levitation height:*	0.30m

To determine the resulting eddy current and thermal effects, the preceding equations were solved iteratively, varying the magnetic coil current until the proper total levitation force (equal to the vehicle weight) was achieved. The total dissipated power and corresponding temperature increase were then calculated for a range of vehicle velocities, including the velocity at which the dissipated power per unit of sheet volume was maximized. A parametric study was then undertaken to examine effects of vehicle velocity, multiple vehicles and vehicle headway (in terms of passengers per hour). The results of this parametric study are discussed below.

Effects of Vehicle Velocity

The effects of vehicle velocity were examined using a single passage of an eight-car Maglev consist. The resulting initial temperature increase in the sheet is shown in Figure 3-7. The

*This value represents the levitated height of the superconducting levitation coil centerline above the guideway sheet. The actual vehicle-guideway clearance (air gap) for this design is approximately 0.19m (please see Reference 15, page 4-15).

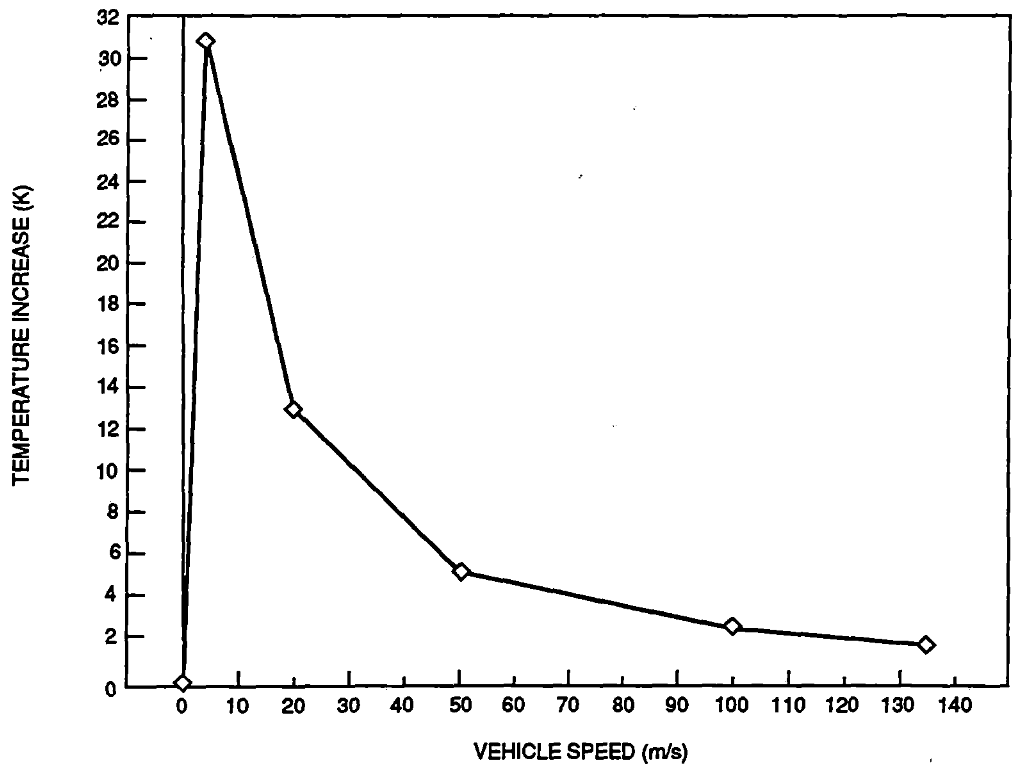

Figure 3-7. CSG Eddy Current Heating Effect of a Single 8-Car Train

maximum power dissipation and temperature increase occur at V = 4.3 m/s, well below the nominal vehicle lift-off speed of approximately 20 m/s. In a worst case situation (at or near a station), the passage of an eight-car vehicle could thus increase the local sheet temperature by 30K. At lift-off speed the increase is 13K. These effects are magnified by the passage of many vehicles at short headway, as described below.

Effects of Passenger Capacity

Using a long series of eight-car Maglev consists (each car carrying 75 passengers), the resulting steady state sheet temperature was calculated for different headways corresponding to 4000, 6000 and 12,000 passengers per hour. The results, shown in Figure 3-8, indicate that at low speeds, the resulting temperature increase could be very high. The maximum temperature increase occurs at very low speeds, well below the vehicle lift-off speed. Since the model assumes constant vehicle speed, the temperature extremes shown in Figure 3-8 for V = 4.3 m/s will probably not occur in practice. It is more reasonable to assume an average vehicle speed near a station equal to the lift-off speed (20 m/s). At this speed, the temperature increase could be in

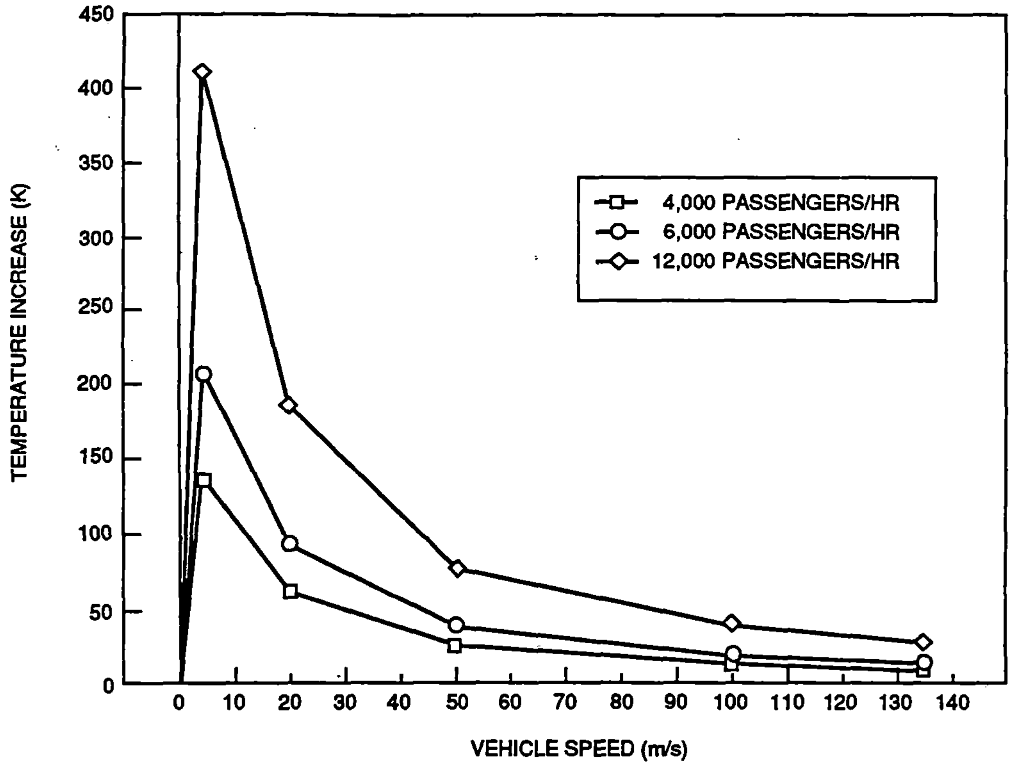

Figure 3-8. CSG Eddy Current Heating Effect of Passenger Capacity

excess of 100K, as was also predicted in Reference (9) (see Section 2). Even at cruise speeds, the increase in temperature can be significant.

The analysis and results presented here indicate that the potential impact of eddy current heating on CSG is very significant. Eddy current heating could raise CSG temperatures substantially higher than the heating produced by solar and ambient effects, and must be considered in any design of CSG. It should be noted here that this eddy current heating analysis is generally applicable to EDS systems only. EMS systems (such as the German Transrapid) use laminated reaction rails in place of CSG. Eddy currents thus do not play a significant role in EMS systems.

3.2 Primary Structure Response

The thermal deflection and stress response of the primary support structure will now be examined. The effects of the temperature distribution and support conditions will be analyzed. Parametric studies will quantify these effects.

3.2.1 Analytical Procedure

Assuming the temperature distribution through the depth of the primary structure is known, the thermal moment and resulting thermal deflection and stresses can be calculated using beam theory. The non-uniform temperature distribution gives rise to a thermal moment, M_T, as given by

$$M_T = \int E \alpha T y dA$$

where T is the temperature at the depth y. The differential equation for the vertical deflection, v, is

$$EI_z \frac{d^2 v}{dx^2} = -(M_T + M)$$

where the following definitions are used:

M = bending moment due to loads or constraints
M_T = thermal bending moment, defined above
I_z = moment of inertia about the z-axis

The equation above can be integrated to find the resulting thermal deflection. Boundary conditions consistent with the span supports (simple or continuous) must be applied.

The thermal stress in the cross section is given by

$$\sigma_x = -E\alpha T + \frac{P_T}{A} + \frac{M_T y}{I_z} + \frac{My}{I_z}$$

where

$$P_T = \int E \alpha T dA$$

Based on the above theory it can be shown that a constant or linear temperature distribution in simply supported spans will produce no thermal stresses, although the linear distribution will result in thermal deflection.

Knowledge of the temperature distribution is thus critical to the evaluation of the primary structure response. As noted in previous sections, the literature indicates that the fifth order temperature gradient specified by the New Zealand code provides a worst case assessment of thermal response. This distribution can be approximately represented by

$$T = \Delta T \left(\frac{y}{C}\right)^5$$

where

C = distance from section centroid to the top of the upper slab

In this gradient, shown schematically in Figure 3-9, the linear distributions of the New Zealand code in the top slab and soffit are ignored for the sake of simplicity. The parameter ΔT is the maximum temperature differential between the section centroid (assumed to be at neutral temperature) and the top surface of the upper flange.

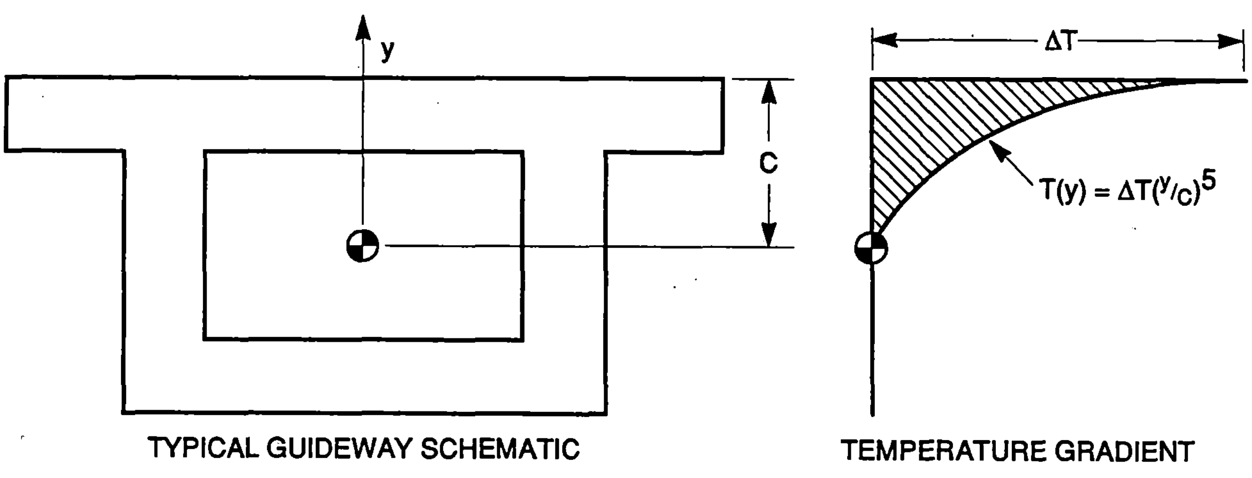

Figure 3-9. Fifth Order Temperature Distribution

3.2.2 Numerical Results

A parametric study was used to study the effects of ΔT, and to compare maximum deflection (δ_{max}) and stress for cases of simple and continuous span supports. The results are discussed below.

Effects of ΔT

In the New Zealand code for a guideway with no asphalt deck topping, a value of $\Delta T = 32K$ is prescribed. As noted, previous work has shown that this code provides a good assessment of the temperature gradient and resulting thermal deflection for bridges in a moderate thermal environment. However, even greater temperature extremes (with larger values of ΔT) may be found in the proposed Maglev locations of Florida and southern California.

Using simply supported steel and concrete guideways for an EMS attractive principle Maglev (shown in Figure 3-10), the thermal deflections for several span lengths were calculated. It was assumed that the guideway self-weight deflection was cancelled by the initial guideway camber. At the neutral temperature, the guideway thus has no vertical deflection. In each case, the fifth order temperature distribution of Figure 3-9 was assumed; the parameter ΔT was varied over a reasonable range. The results of this study are presented in Figure 3-11 and 3-12, which show that thermal deflections of several centimeters are possible, particularly for the steel guideway. These results are in agreement with the work of Campbell and Siu (8) and the CIGGT (16), who examined the typical guideways proposed for use in the southern California-Las Vegas corridor using transient finite element techniques.

Clearly, the deflections in the single spans are large and may be inadmissible from an operational point of view. The deflections can be reduced by using alternating continuous spans, as shown below.

Effects of Support Conditions

The parametric studies described above were also applied to alternating continuous span (or double span) designs. The thermal deflection in these spans is generally smaller than found in single spans, due to bending moment continuity at the middle support. This is shown schematically in Figure 3-13. Theoretically, the maximum deflection due to a thermal moment in a double span is only 30 percent of that found in a single span. The results of the parametric study

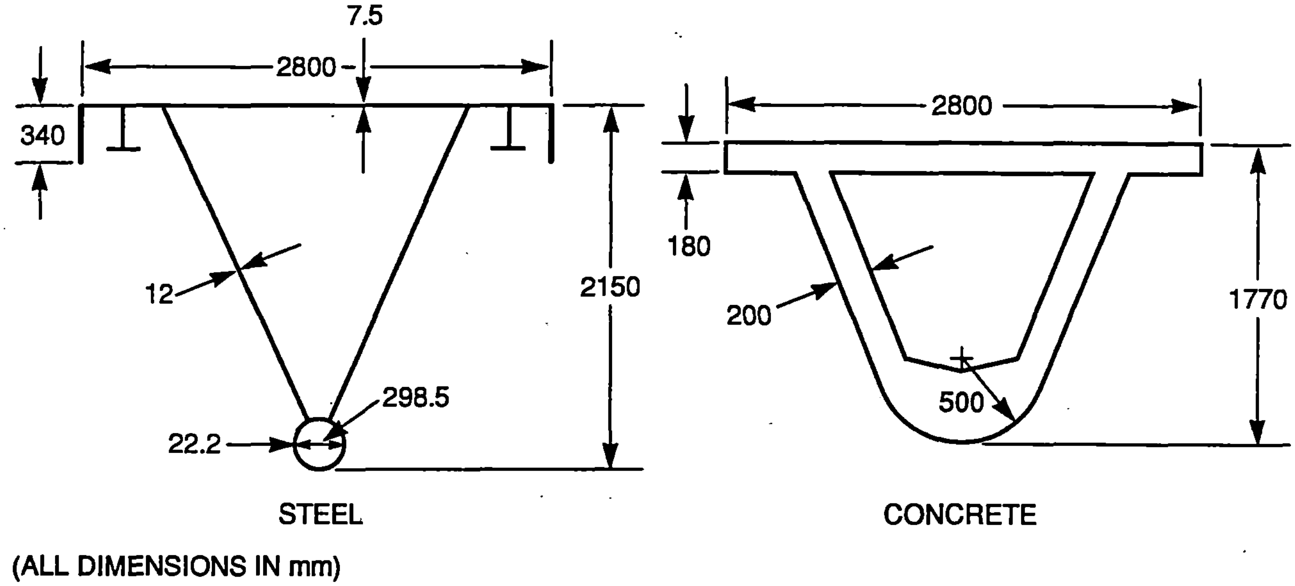

Figure 3-10. Typical EMS Guideways Used in Deflection Analysis

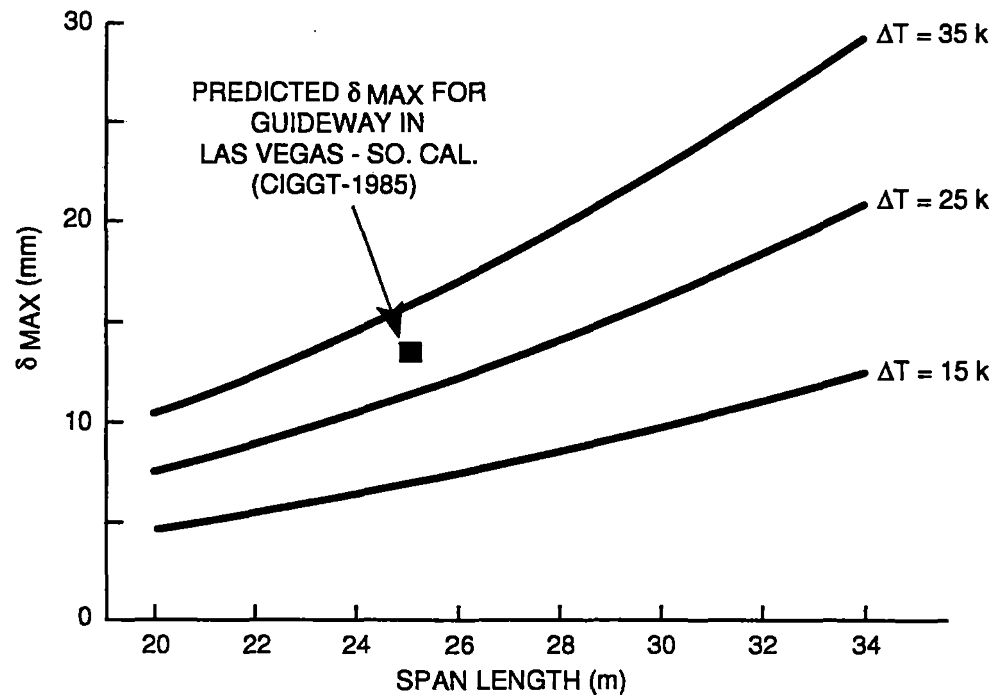

Figure 3-11. Thermal Deflection of EMS Steel Guideway (Single Span)

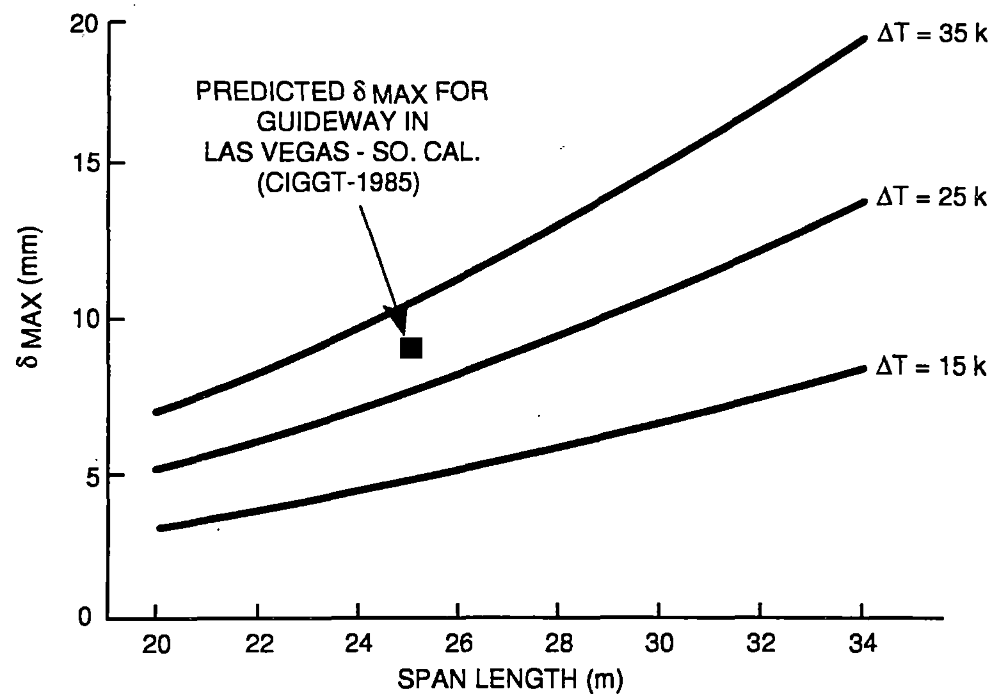

Figure 3-12. Thermal Deflection of EMS Concrete Guideway (Single Span)

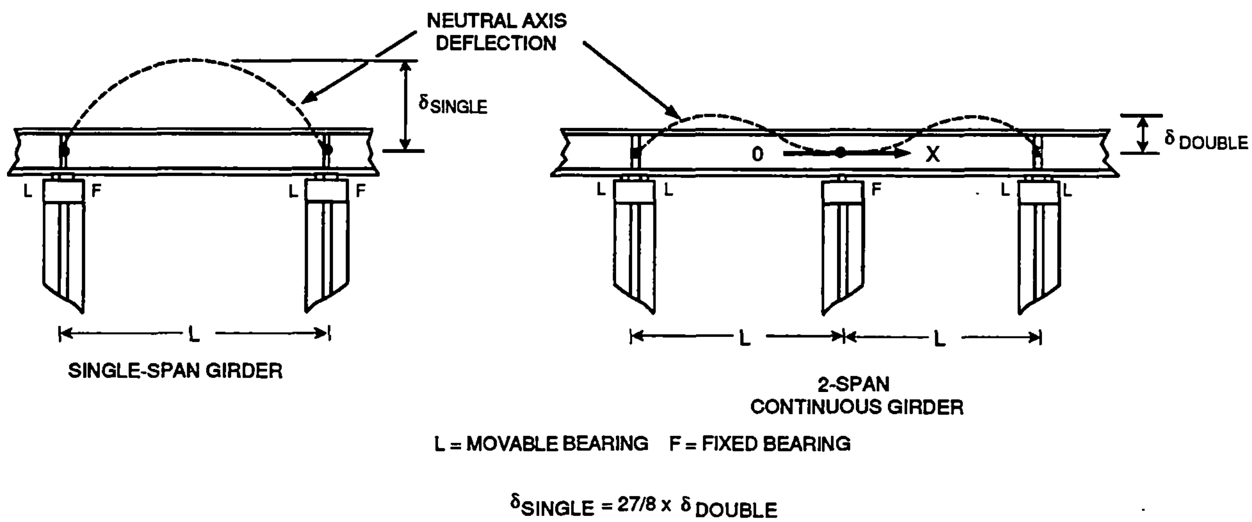

Figure 3-13. Thermal Deflection in Single and Double Spans

are shown in Figures 3-14 and 3-15 for the steel and concrete guideways, respectively. Here the deflections are generally less than 1 cm, even for the longer spans.

This analysis was also applied to several other Maglev guideway designs, including an EDS concrete design presented in (14), and several candidate design variations of the Foster-Miller U-shaped EDS concrete guideway. These guideway designs are diagrammed in Figures 3-16 and 3-17. In this analysis, particular emphasis was placed on use of the guideways in U.S. urban corridors. Here not only the thermal environment can be quite severe, but guideway spans of considerable length (30m or more) are usually required. The resulting thermal deflections can be quite large.

The thermal deflection results of this study are shown in Table 3-1, for single and double spans of 30m with $\Delta T = 32K$. Thermal stress results are presented in Table 3-2. As previously stated, these are thermal deflections and stresses only. The self-weight deflections are assumed to be cancelled by initial camber. The additional stresses due to self-weight, prestressing and post-tensioning are not considered here. In the single spans, the maximum compressive stress generally occurs at the top fiber, with maximum tensile stress occurring at the section centroid. In double

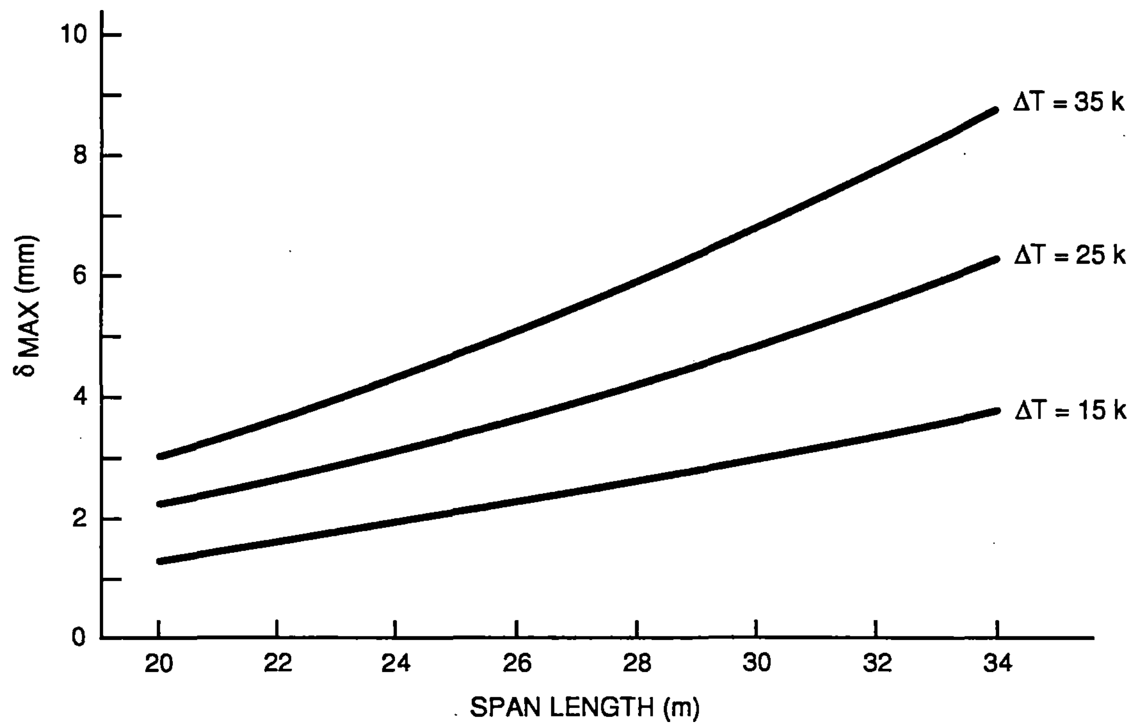

Figure 3-14. Thermal Deflection of EMS Steel Guideway (Double Span)

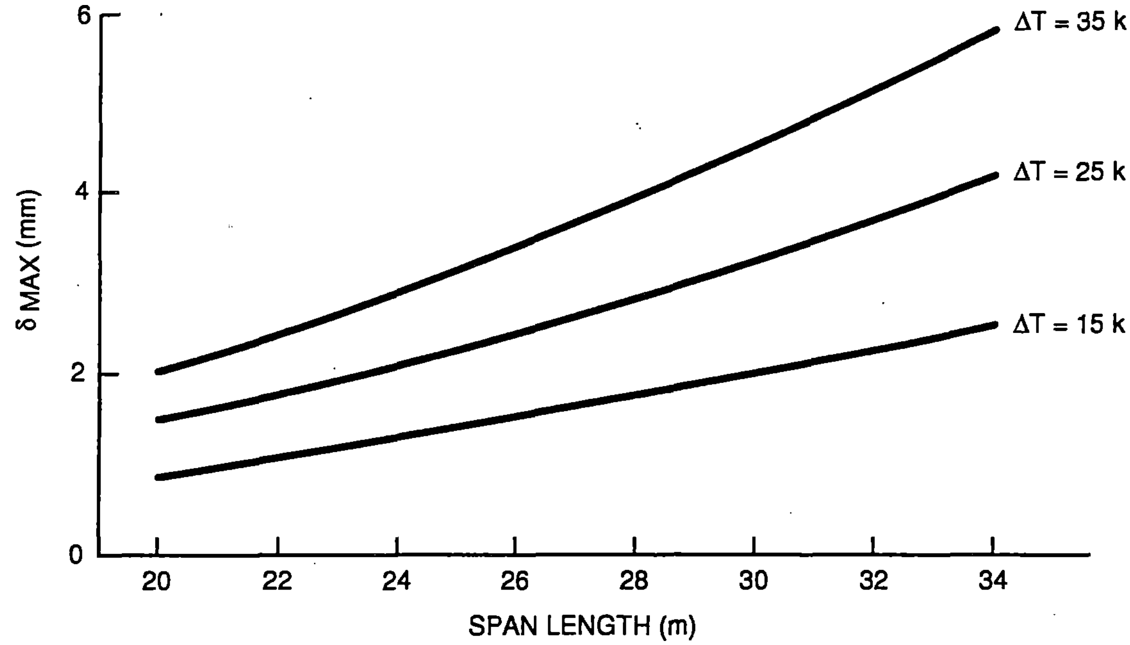

Figure 3-15. Thermal Deflection of EMS Concrete Guideway (Double Span)

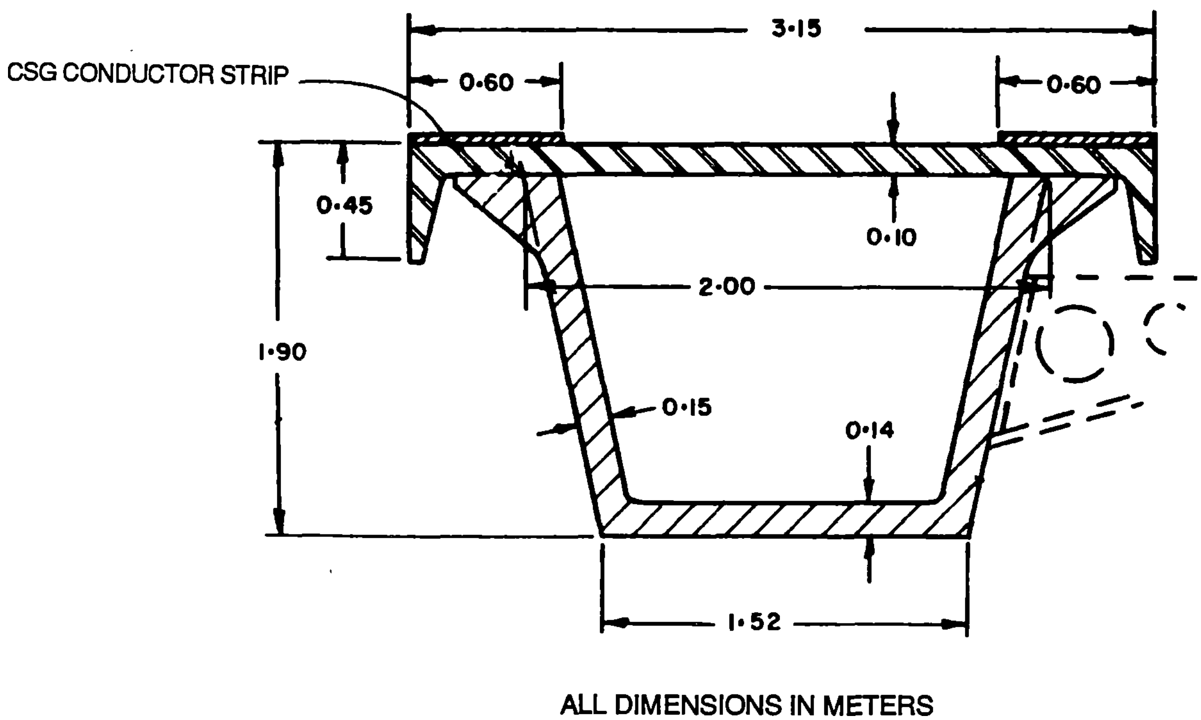

Figure 3-16. Concrete EDS Guideway (14)

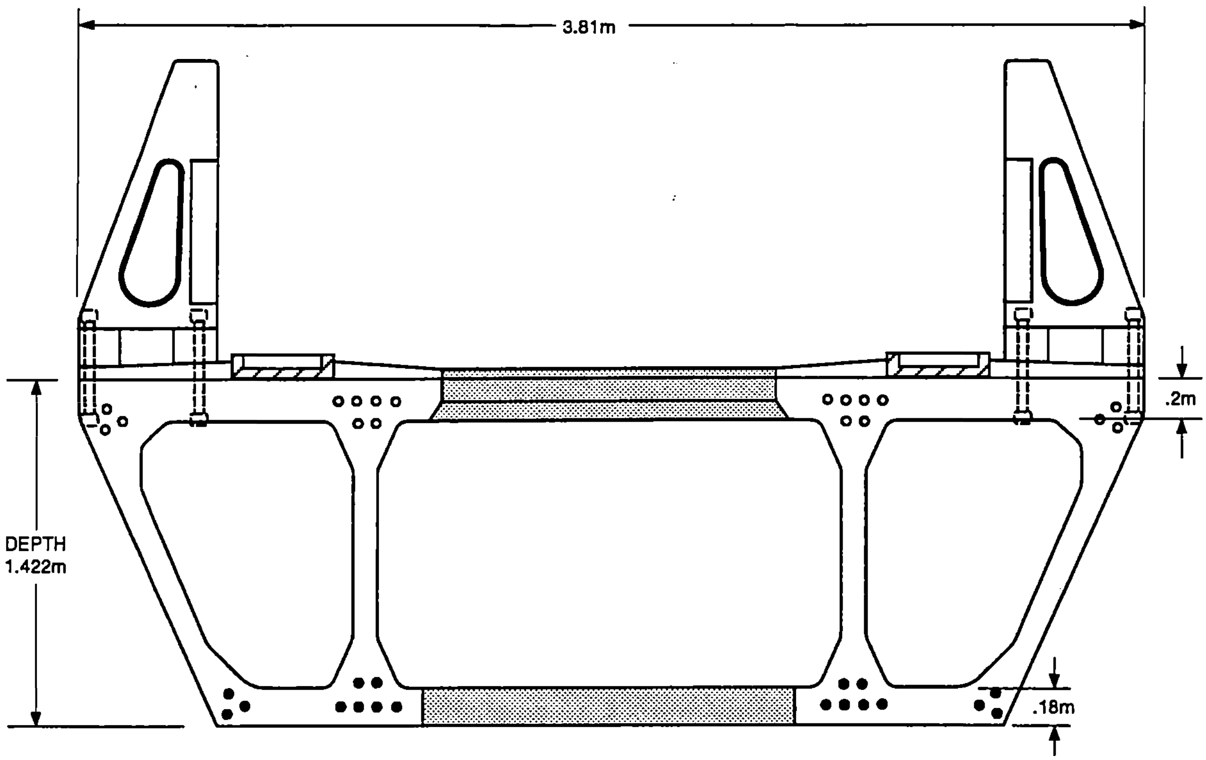

Figure 3-17. Foster-Miller Baseline EDS Concrete Guideway

Design	Thermal Deflection cm (in.)			
	Single Span		Double Span	
EMS				
Steel	1.97	(0.78)	0.58	(0.23)
Concrete	1.41	(0.56)	0.42	(0.16)
EDS				
Concrete	1.53	(0.60)	0.46	(0.18)
Foster-Miller Candidate Designs*				
A (depth = 1.83m)	1.33	(0.52)	0.39	(0.15)
B (depth = 1.68m)	1.41	(0.56)	0.42	(0.16)
C (depth = 1.52m)	1.49	(0.59)	0.44	(0.17)

*Designs reflect variations in depth in the baseline design.

Table 3-1. Comparison of Thermal Deflections for Various Designs ($L = 30m$, $\Delta T = 32K$)

	Single Span				Double Span			
	Max Tension		Max Comp.		Max Tension		Max Comp.	
EMS								
Steel	32.0	(4640)	-18.1	(-2625)	55.0	(7980)	-60.9	(-8830)
Concrete	2.1	(300)	-5.0	(-730)	3.4	(500)	-8.8	(-1270)
EDS								
Concrete	2.9	(415)	-3.9	(-560)	5.0	(720)	-8.1	(-1170)
Foster-Miller Candidate Designs* (Concrete)								
A (depth = 1.83m)	2.4	(345)	-4.2	(-615)	4.0	(580)	-8.6	(-1250)
B (depth = 1.68m)	2.3	(340)	-4.3	(-620)	3.9	(570)	-8.7	(-1260)
C (depth = 1.52m)	2.1	(305)	-4.6	(-660)	3.6	(520)	-8.9	(-1290)

Units are MPa or (PSI)
*Designs reflect variations in depth in the baseline design.

Table 3-2. Comparison of Thermal Stress for Various Designs (L = 30m, ΔT = 32K)

spans, the maximum compressive stress occurs in the top fiber over the continuous support, and the maximum tensile stress occurs in the bottom fiber over the continuous support.

The EMS steel guideway is most susceptible to large thermal deflection, particularly for simply supported spans. Double spans provide considerable benefit for the reduction of thermal deflection, but they also experience a corresponding increase in thermal stress. The thermal stresses are greatest in the steel section, due to its larger thermal moment and smaller cross sectional moment of inertia. In the concrete sections, additional reinforcement may be required to compensate for the tensile stresses caused by the thermal loads.

Aside from the possibility of exceeding deflection design tolerances due to the thermal bending of the Maglev primary support structure, these deflections can also adversely affect passenger ride comfort.

To examine these effects, a simple dynamic model was employed to estimate the maximum vertical accelerations that a passenger might experience due to thermal deflections in the guideway. As shown in Figure 3-18, the model assumes a fixed sinusoidal deflection in the guideway with a

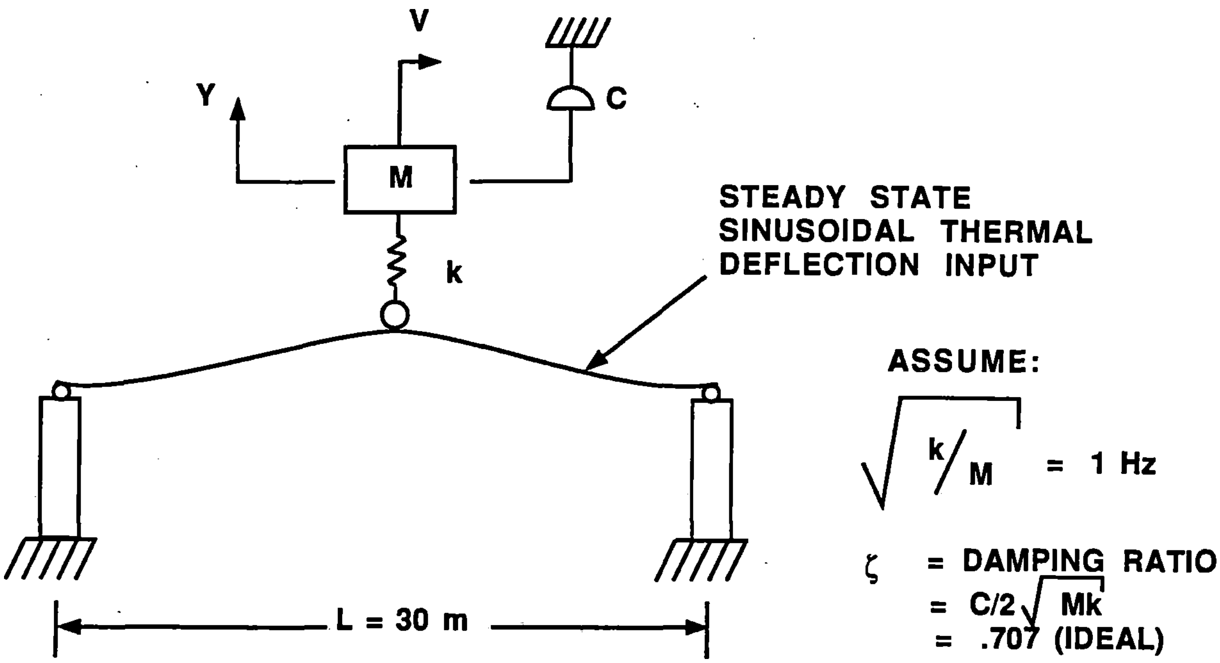

Figure 3-18. 1 D-O-F Model for Heave Acceleration

maximum peak-to-peak amplitude equal to the maximum thermal deflection. The sinusoidal deflection is input to the 1 degree-of-freedom vehicle model, which assumes a suspension natural frequency of 1 Hz (considered typical), with ideal damping. The maximum steady-state heave acceleration $\ddot{y}_{max}$ is calculated from

$$\ddot{y}_{max} = \frac{\left(\frac{\delta_{max}}{2}\right)\left(\frac{2\pi V}{L}\right)^2}{\sqrt{\left(1-r^2\right)^2 + 4\zeta^2 r^2}}$$

where

$$r = \frac{2\pi V}{L} / \Omega_N \, ; \, \Omega_N = \sqrt{k/M} \, ; \, \zeta = \text{damping ratio} = 0.707$$

The acceleration increases with velocity. However, for large velocities, a limiting steady-state maximum heave acceleration is achieved, and is given by

$$\bar{y}_{max} = \frac{\delta_{max}}{2} \left(\Omega_N\right)^2$$

A parametric study was performed using the EMS steel guideway on both single and double spans. Variations in the parameter ΔT were examined for a range of suitable vehicle speeds. The results of this study are presented in Figures 3-19 and 3-20. For large ΔT, the thermal deflection is quite large and produces vertical accelerations on the order of 0.04 to 0.05g in the simply supported span.

A steady, continuous heave acceleration of 0.02 to 0.05g could have an adverse effect on passenger comfort. Similar studies by Philco-Ford (17) estimated that 0.02g was a useful vehicle acceleration limit for this type of analysis based on the unconservative nature of the model. This acceleration could also be compounded by the deflection transients induced by changes in thermal deflection from span to span due to emergence from tunnels or shaded areas.

The alternating continuous spans thus have considerable advantage over simply supported spans: thermal deflection is reduced, and the resulting influence on ride comfort is less severe. Thermal stresses are greater with the double span design, but should not be a problem for steel guideways. For concrete guideways, standard techniques of pre- or post-stressing should mitigate these effects.

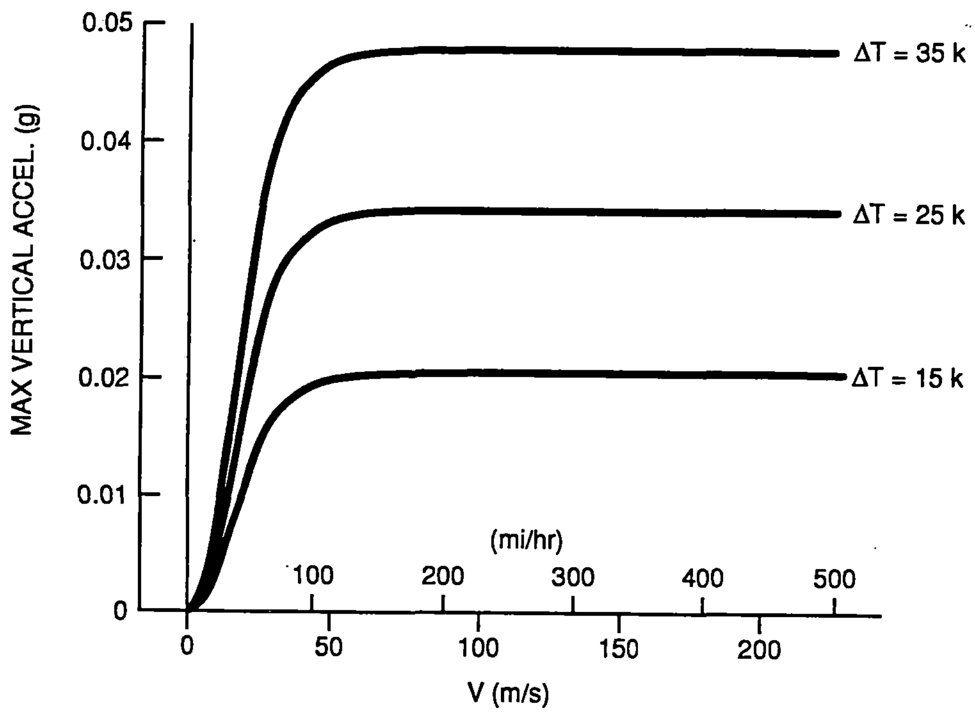

Figure 3-19. Heave Acceleration due to Thermal Deflection (Single Span)

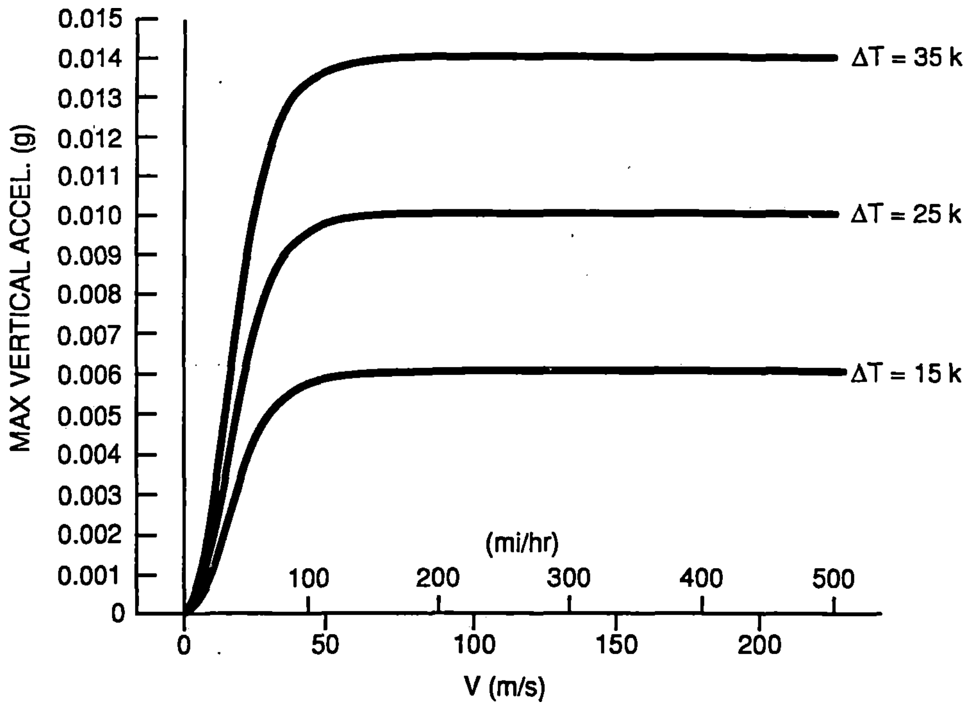

Figure 3-20. Heave Acceleration due to Thermal Deflection (Double Span)

3.3 Sheet Guideway Response

In this section, rigorous analyses for buckling strength of CSG, thermal movement of segmented sheet guideways, and fracture and of CSG will be presented. A detailed parametric study will be carried out to facilitate optimization of CSG design.

3.3.1 Buckling of Continuous Sheet Guideways

The sheet is assumed to be fastened to the guideway by clip-type fasteners (Figure 3-21), and is held in place longitudinally by the friction force acting at the fasteners.

If the temperature of the sheet is raised above its neutral reference temperature, an axial stress will develop. At some critical temperature the sheet could buckle upwards over a buckled length 2L, as shown in Figure 3-22. This buckled length is limited to a maximum value, equal to the fastener pitch, $2L_p$. As a result of this buckle there will be a force drop. The sheet guideway moves longitudinally towards the center of the buckle, opposing the longitudinal resistance force of the fasteners, f_o.

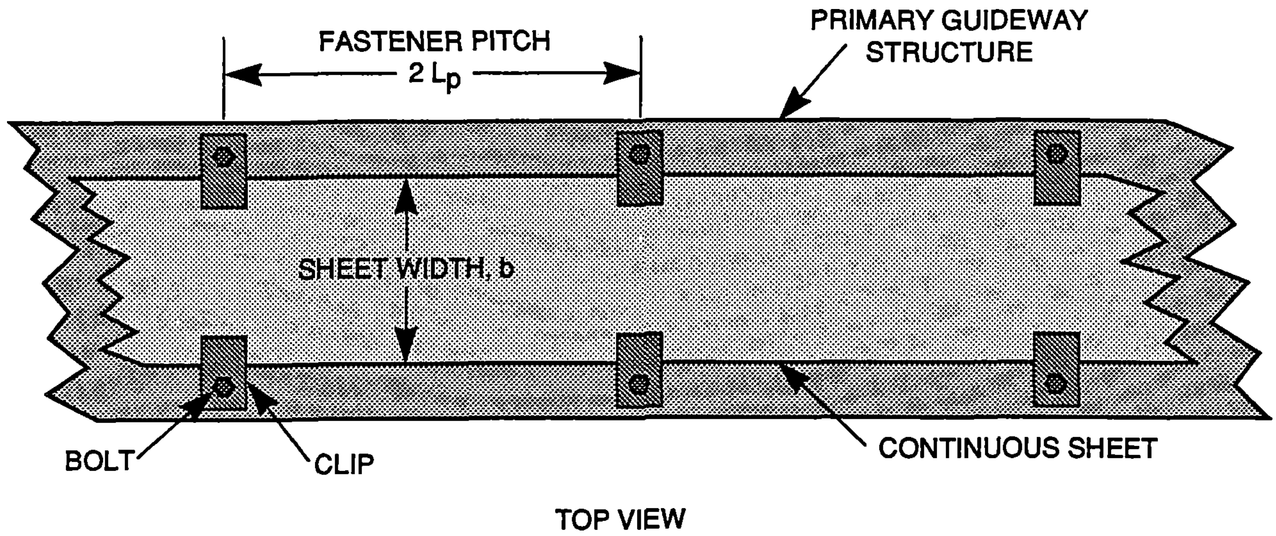

Figure 3-21. CSG Model for Buckling Analysis

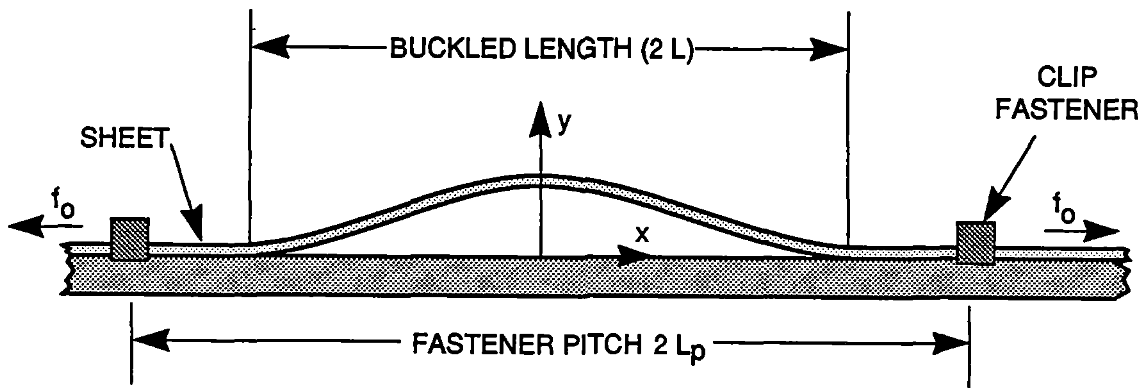

Figure 3-22. Buckled Guideway Sheet

The differential equation for the buckled zone has been derived by Samavedam in previous works (10,11).

$$EIw'''' + P w'' = -Mg$$

where EI is the bending rigidity of the sheet in the vertical plane, w is the buckling deflection, P is the force in the buckled zone, Mg is the weight of sheet guideway per unit length and the primes denote derivatives with respect to x. The boundary conditions are:

$$\begin{aligned} x = 0:\quad & w' = 0 \text{ (zero slope)} \\ & w''' = 0 \text{ (zero shear)} \\ x = L:\quad & w = 0 \\ & w' = 0 \\ & w'' = 0 \end{aligned}$$

The differential equations for the longitudinal equilibrium are:

Buckled Zone

$$AE\, U'' = 0 \quad (0 \leq x \leq L)$$

where U = longitudinal displacement in the buckled zone

Adjoining Zone

$$AE\, u'' = f_0 \quad (L < x < \infty)$$

where u = longitudinal displacement in the adjoining zones and f_0 = constant longitudinal resistance force. The continuity conditions at $x = \pm L$ are

$$\begin{aligned} U &= u \\ U' &= u' \end{aligned}$$

At

$$\begin{aligned} x &= 0 \\ U = u' &= 0 \end{aligned}$$

As can be shown, at large distances the force in the sheet guideway is given by

$$P_\infty = AE\alpha T$$

Solution of the foregoing equations can be obtained along the same procedures as used by Samavedam in earlier works (10).

Briefly, the solution of this differential equation can be obtained in terms of trigonometric series. The buckled deflection and vertical resistance (self weight) are expressed as

$$w(x) = \sum_{1,3,5}^{\infty} A_m \cos (m\pi x/2L)$$

$$Mg = \sum_{1,3,5}^{\infty} a_m \cos (m\pi x/2L)$$

Four of the five boundary conditions specified above are automatically satisfied by these series expressions. By Fourier analysis,

$$a_m = \frac{4Mg}{m\pi} \sin (m\pi/2)$$

$$A_m = -4L^4 a_m \Big/ \left[EI\, \pi^2 m^2 \left(\left(\frac{m\pi}{2}\right)^2 - \beta \right) \right]$$

where the remaining boundary condition (w' = 0) is satisfied if

$$\beta = PL^2/EI = 20.19$$

The buckling temperature is determined from

$$T = \frac{1}{EA\alpha} \left(P + \sqrt{2AEf_o Z} \right)$$

where

$$Z = \frac{L}{4} \sum_{1,3,5}^{\infty} A_m^2 (m\pi/2L)^2$$

The corresponding maximum buckled deflection, w_{max}, is given by

$$w_{MAX} = \sum_{1,3,5}^{\infty} A_m$$

Using the foregoing analysis, the buckling temperature increase above neutral, T, can be determined as a function of the fastener pitch, $2L_p$. A typical CSG buckling response is shown in Figure 3-23. For a fastener pitch corresponding to position A on Figure 3-23, the sheet can buckle only at temperatures greater than T_A. Buckling at temperatures less than T_A requires a buckled length (2L) greater than the fastener pitch ($2L_{PA}$), which is not possible. Thus, T_A is defined to be the buckling temperature for this case.

For a fastener pitch corresponding to position C on Figure 3-23, it is apparent that the sheet can buckle at any temperature greater than T_B since the buckled length at this temperature is smaller than the fastener pitch ($2L_{PC}$). It follows then that for any fastener pitch greater than $2L_{PB}$, the buckling temperature is given by T_B. Any further increase in temperature beyond T_B means only that the buckle will increase in length, until limited by the fastener pitch.

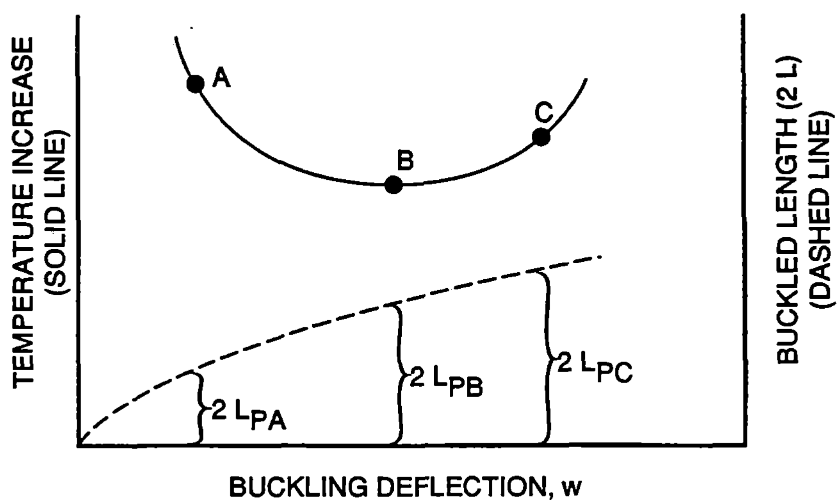

Figure 3-23. Typical CSG Buckling Response

Parametric Study

To study the effects of sheet material and geometry, fastener pitch, and fastener longitudinal resistance upon the buckling temperature, parametric studies were performed. In these studies a range of acceptable values for each parameter was determined. Flat aluminum sheets of rectangular cross section were assumed. Aluminum is generally considered to be the most economical choice for sheet guideways. Other metals, such as steel or copper, are either too electrically resistive, or too expensive to be cost effective. Various alloys of aluminum, showing some variation in mechanical and thermal properties, were examined. Sheet cross sectional dimensions were also varied. The longitudinal resistance force of the fasteners (f_o) was estimated, based on the assumed tightening and frictional forces of the bolts and clips. This was also compared to the longitudinal tractive forces exerted on the sheet by the accelerating vehicle. The fasteners must exert at least this force to prevent the sheet from slipping.

The results of these parametric studies are presented in Figures 3-24 to 3-27. Each figure shows the sheet buckling temperature for a range of fastener pitch lengths ($2L_p$). The results are discussed below.

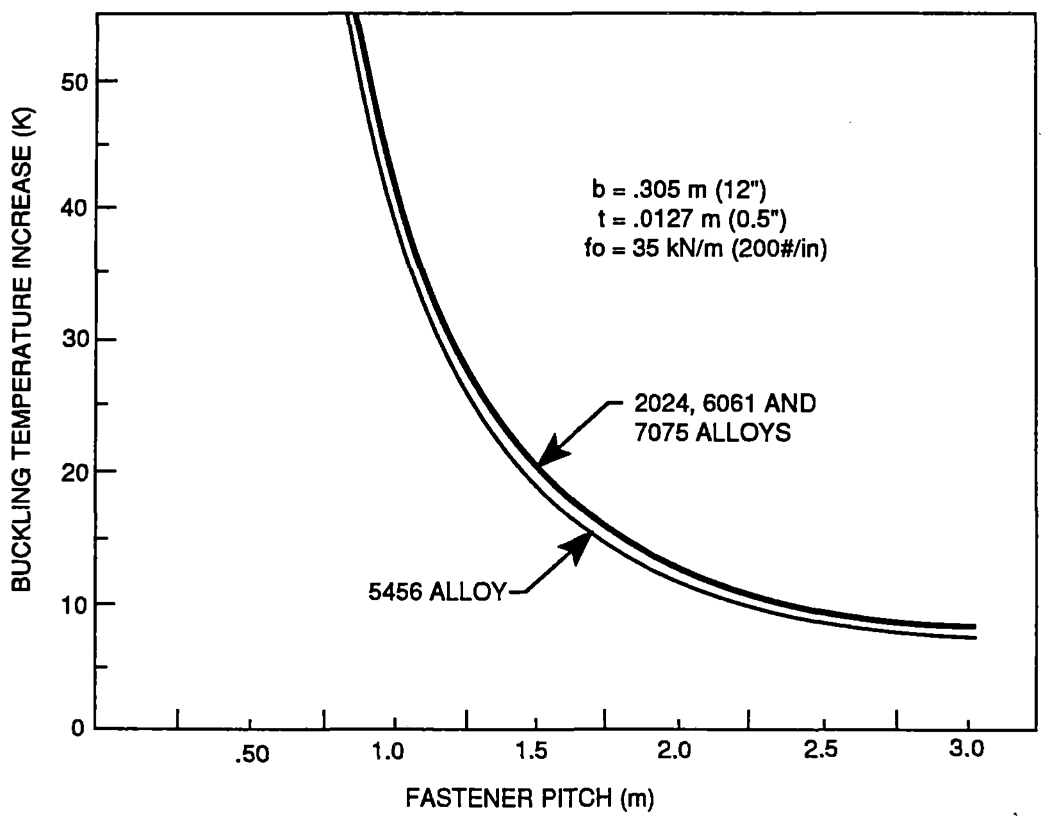

Figure 3-24. Effect of Material Properties on CSG Buckling

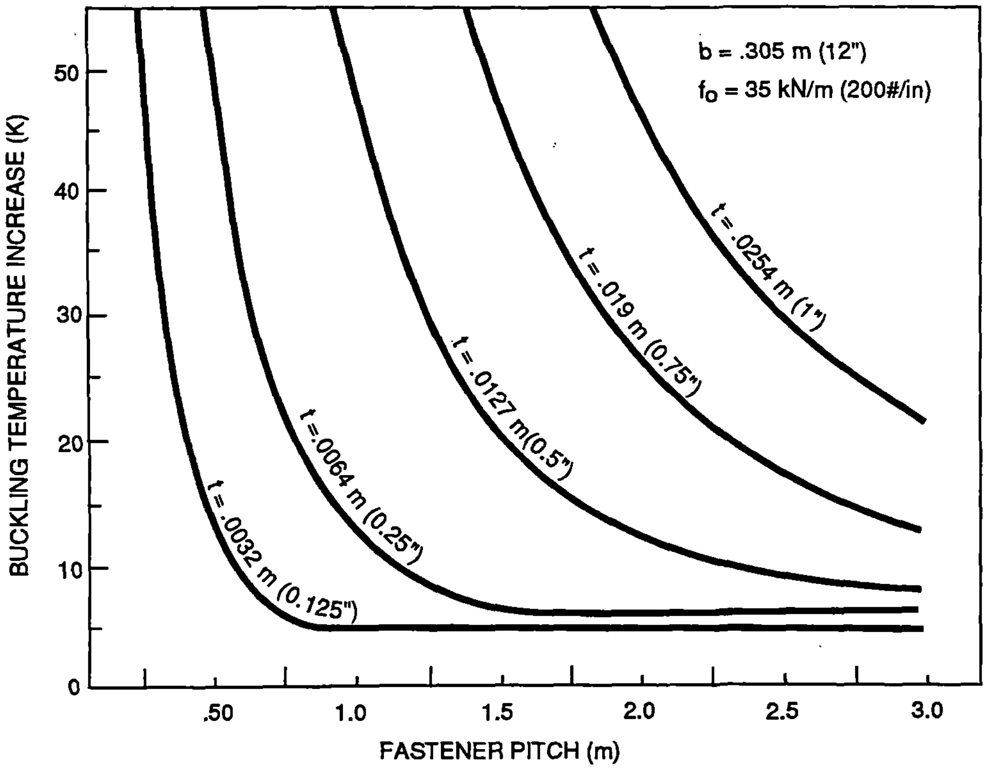

Figure 3-25. Effect of Sheet Thickness on CSG Buckling

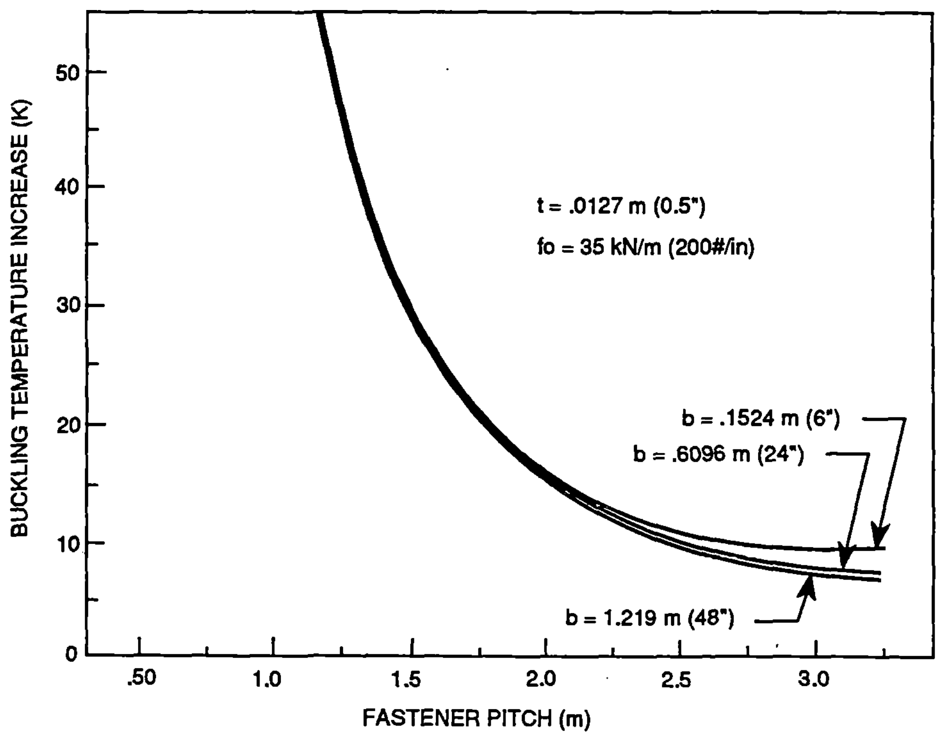

Figure 3-26. Effect of Sheet Width on CSG Buckling

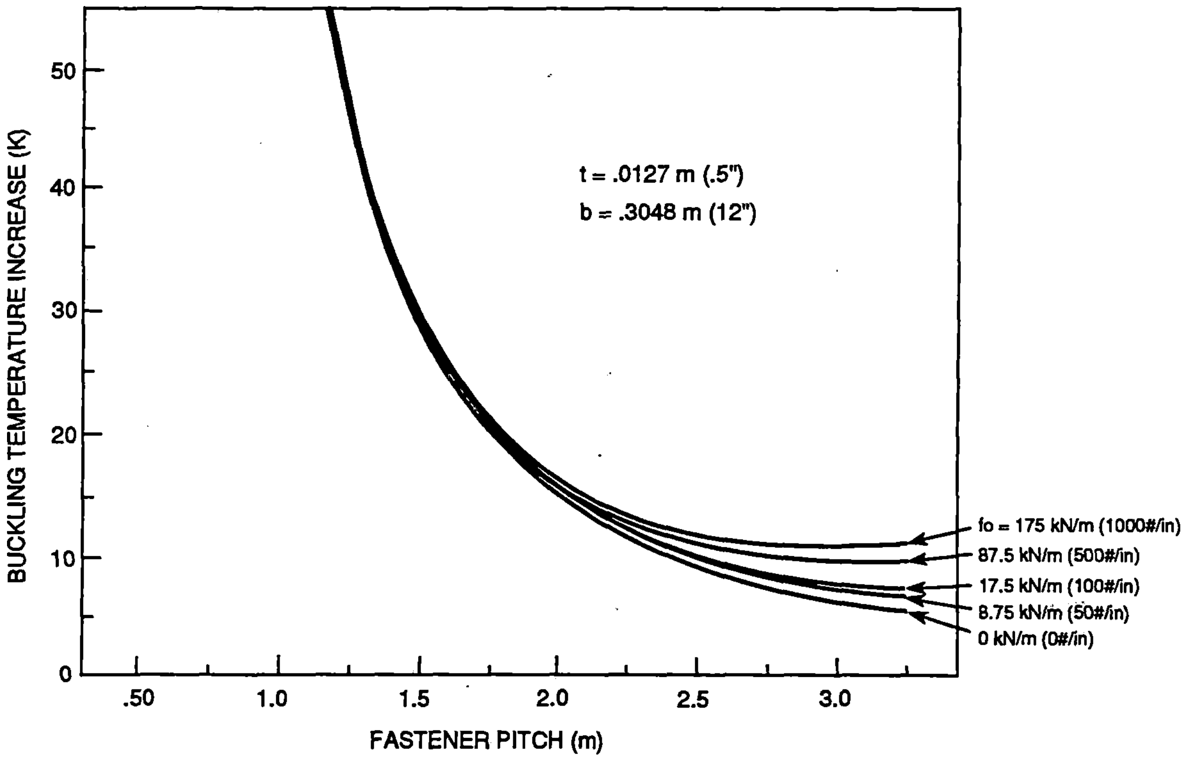

Figure 3-27. Effect of Longitudinal Resistance on CSG Buckling

Effects of Material Properties

Figure 3-24 shows the thermal buckling response for several typical aluminum alloys: 2024, 5456, 6061, and 7075. These alloys were selected because they provide a reasonable variation in mechanical and thermal properties, as summarized in Table 3-3. The buckling results indicate that there is very little variation in the buckling temperature among the candidate materials. Thus, for the remainder of this analysis, typical aluminum material properties were assumed, as follows:

E = 72.4 GPa
α = 22.5 x 10^{-6}/K
ρ = mass density = 2700 kg/m^3

However, the choice of sheet guideway material, even in the aluminum family, is important from fatigue and fracture strength considerations. This is discussed in subsection 3.3.3.

Table 3-3. Typical Mechanical and Thermal Properties of Aluminum Alloys

Alloy	E (Pa)	α (1/K)	ρ (kg/m³)
2024	75.87E9	22.59E-6	2.77E3
5456	71.74E9	24.21E-6	2.66E3
6061	69.66E9	22.77E-6	2.71E3
7075	72.43E9	22.41E-6	2.80E3

Effects of Sheet Thickness

In contrast to the results described above, there is a marked effect on the buckling temperature due to changes in the sheet thickness. These effects are primarily due to changes in the sheet cross sectional moment of inertia. Figure 3-25 shows that very thin sheets will buckle at temperatures less than 10K (18°F) above neutral, unless the fastener pitch is very short. Grumman (15) determined that the most economical sheet thicknesses for their Maglev design were in the range of 0.76 to 1.27 cm (0.3 to 0.5 in.). Similarly, the Canadian design study (14) used a flat aluminum sheet 1 cm (0.4 in.) thick. The results in Figure 3-25 show, however, that even a 1.27 cm (0.5 in.) thick sheet can buckle at low temperature if the fastener pitch is not kept sufficiently small.

Effects of Sheet Width

Figure 3-26 shows the effects of sheet width upon buckling temperature for a 1.27 cm (0.5 in.) thick sheet. These effects are not appreciable unless the fastener pitch is quite large (2.4m or more). Since the longitudinal resistance is held constant, increasing the sheet width decreases the longitudinal resistance per unit width of the sheet. The result is that increasing the sheet width slightly decreases the buckling temperature.

Effects of Longitudinal Resistance

Similar to the effects of sheet width, the buckling temperature in a 1 cm thick sheet is relatively insensitive to changes in longitudinal resistance (f_0), unless the fastener pitch is quite large. Increasing f_0 then increases the buckling temperature, as shown on Figure 3-27. From a practical standpoint, this implies that buckling strength is most easily increased by use of a small fastener pitch. Increasing the longitudinal resistance is comparatively ineffective, unless a large fastener pitch is required.

Additional Compressive Stress Due to Strain Transfer

The multiple vehicle static and dynamic loads on the guideway cause bending moments which put the upper fibers of a simply supported guideway in compression. Assuming the sheet is securely fastened to the guideway, the strain of the upper guideway fibers is also present in the guideway sheet, resulting in compressive sheet stress.

The strain induced in the top fibers of the guideway is calculated from the bending moment as

$$\varepsilon = \frac{Mc}{E_G I}$$

where

M = bending moment
E_G = Young's modulus of guideway
c = distance to upper fiber
I = section moment of inertia

This strain is transferred to the guideway sheet; the resulting stress in the sheet is then given by

$$\sigma_s = E_s \left(\frac{Mc}{E_G I} \right)$$

where

E_S = Young's modulus of sheet

This compressive stress can be represented as an equivalent increase of sheet temperature, as given by

$$\Delta T = \frac{\sigma_s}{\alpha E_s}$$

The bending moment is determined from a concentrated load at the midspan of 445 kN (100,000 lb). This represents a worst case assumption for the vehicle static and dynamic loads. Additionally, the following were assumed for this analysis:

$E_G = 27.6$ GPa
$E_S = 72.4$ GPa
$\alpha = 22.5 \times 10^{-6}$/K

The resulting stress and temperature increase due to strain transfer are shown in Figure 3-28 for typical guideway geometries. The results show that a considerable equivalent increase in sheet temperature can be attributed to strain transfer. This additional increase of temperature should be considered in the design of CSG, as described below.

Numeric Example

The results of the above parametric studies can be used to determine the best combination of sheet dimensions and fastener pitch. From an economic standpoint, thin sheets with a very large fastener pitch are desirable. However, as noted above, this will result in very low buckling

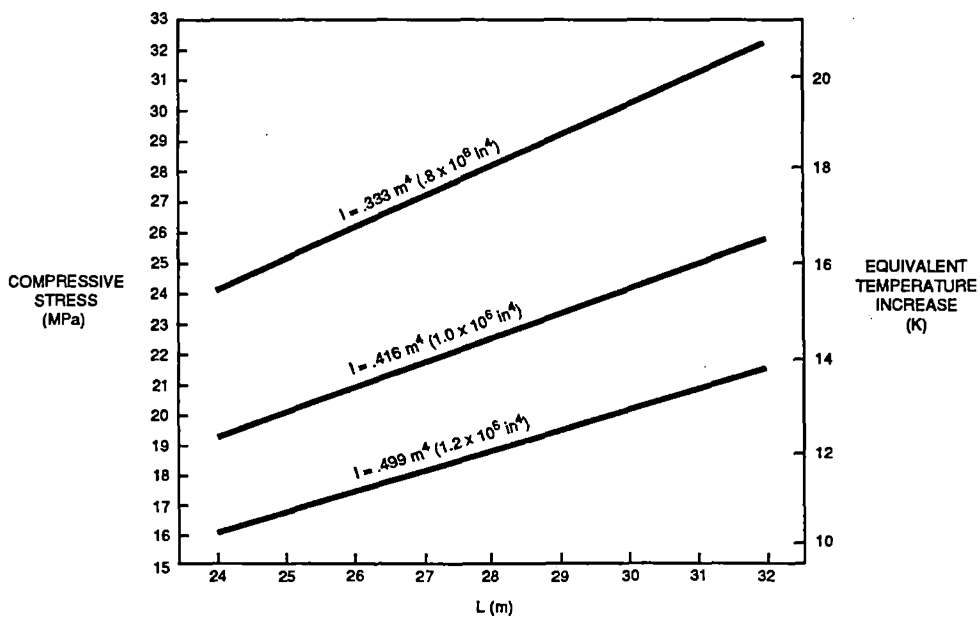

Figure 3-28. CSG Compressive Stress Due to Strain Transfer

strength. A thicker sheet can markedly increase the buckling strength, but still requires careful control of fastener pitch. For example, a 1 cm thick sheet with a fastener pitch of 1m will buckle at a temperature increase of approximately 47K (84°F). In practice, however, some fasteners could be worn out or missing, such that the local fastener pitch could increase to 2m (or more); the buckling temperature then drops dramatically to 12K (22°F) or less. This problem is further magnified by the potentially large sheet temperature increase due to eddy current heating, and the equivalent sheet temperature increase caused by strain transfer from the primary structure. In practice, it may be necessary to design with considerable margin allowed for these effects. This may then require very thick sheets, or a very small fastener pitch, neither of which is economically attractive.

Other Sheet Designs

There exist CSG designs which use L-shaped cross sections rather than flat sheets. A typical example is shown in Figure 3-29 (14). The beam-type buckling strength of these sheets is increased due to the increased moment of inertia. However, each flange of the L-section is subject to localized thermal buckling and can be analyzed as a flat plate with one edge (at the bend of the L-section) simply supported, the other free. The equation governing plate buckling of the flanges is given by

$$\sigma_{CR} = k \frac{\pi^2 D}{b^2 t}$$

where

D = plate flexural rigidity
b = plate width
t = thickness
k = numerical factor, based on width and length (18).

The equivalent temperature increase corresponding to this stress is

$$\Delta T = \frac{\sigma_{CR}}{\alpha E}$$

The buckling stress and critical temperature increase for several flange width and fastener pitch lengths were calculated and are shown in Figure 3-30. The results show that buckling can occur

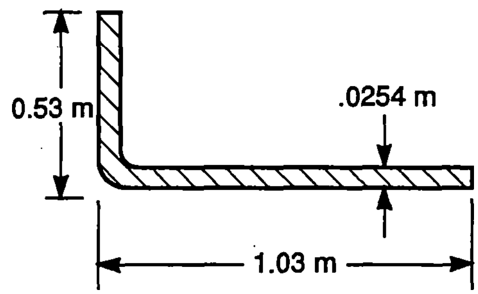

Figure 3-29. Typical L-Section CSG Design

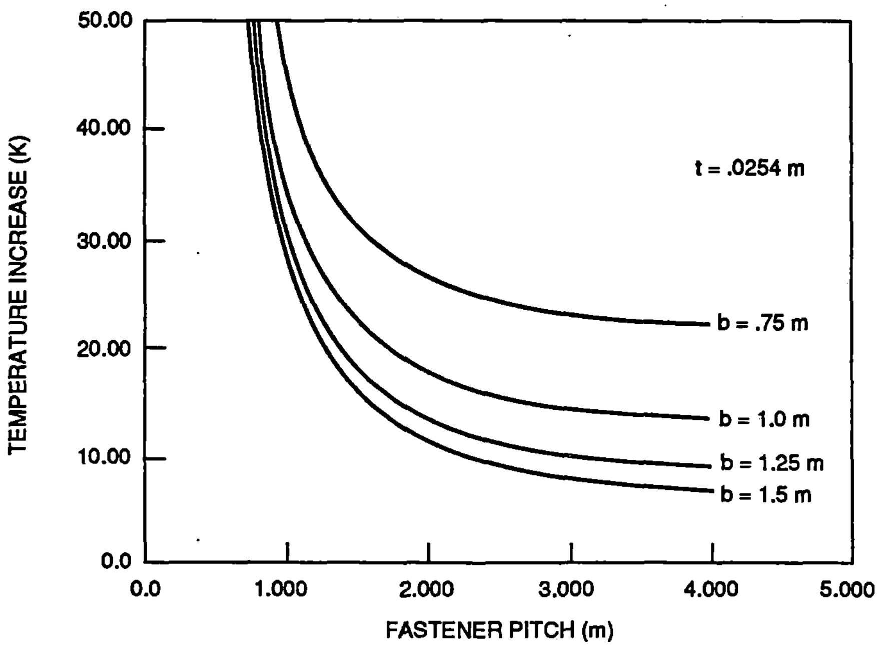

Figure 3-30. Critical Temperature for Local Buckling of L-Section CSG

for a temperature increase less than 10K, unless the fastener spacing is kept small. Thus, thermal buckling cannot be avoided simply by use of L-shaped sections; thermal buckling analysis must be considered in any CSG design.

3.3.2 Analysis of Segmented Sheet Guideways

The simplest means of mitigating the thermal buckling effects described in the section above is to use segmented sheets, which use gaps to allow for thermal expansion. However, an expansion joint creates a discontinuity in the eddy currents generated in the sheet, which causes magnetic force perturbations on the vehicle levitation magnets. Generally, the force transient on a magnet moving over an expansion joint consists of three components: a loss of lift, a longitudinal attractive and retarding force, and an increase in drag. The longitudinal force attracts the vehicle toward the discontinuity, producing both thrust and conservative retarding forces as the vehicle moves toward and away from the joint. These forces are distinct from the non-conservative drag force, which arises due to increased power dissipation in the sheet near the joint.

Experiments measuring the force transients at high speeds (19) have shown that the lift and longitudinal force transients increase with increasing gap size, while the drag force transient actually decreases. These results are shown in Figures 3-31 to 3-33. Reference 19 suggests that the optimum tradeoff between the longitudinal and drag force transients occurs for a 2 cm gap, but a gap of this size still produces a 20 percent transient loss of lift. Figure 3-31 shows that even a 0.1 cm butt joint gap can produce a large transient (> 15 percent) in lift force. Additional work from reference 20 (Figure 3-34), shows that very large force transients can occur at both high and low speeds.

The expansion joints of segmented sheet guideway are also subject to thermal effects. The gap should be as small as possible but still allow free expansion without butting forces that can lift off the free edges. Ideally the ends of the adjacent sheet guideways should just butt on a hot summer day, and must have limited thermal contraction in winter. These conditions can be accomplished by optimum installation temperature and fastener resistance. For the segmented sheet guideway shown in Figure 3-35, the governing differential equation is

$$U'' = \frac{f_o}{AE}$$

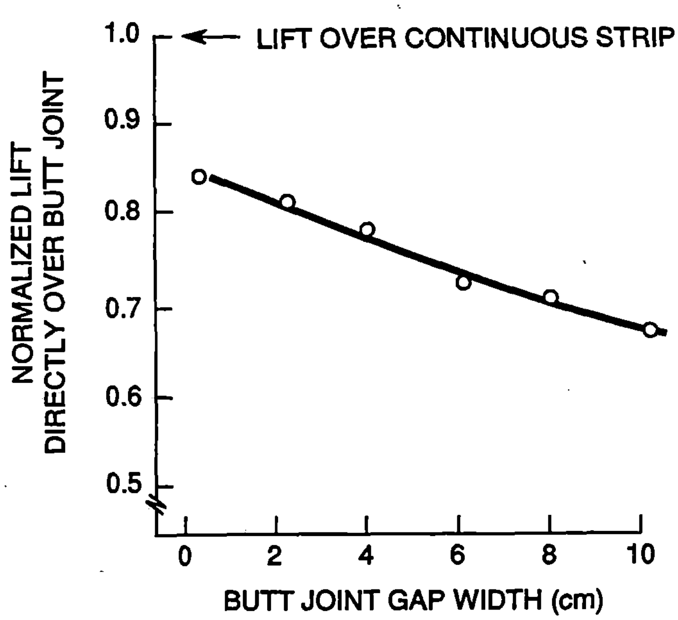

Figure 3-31. Variation of Lift Force with Gap Size (19)

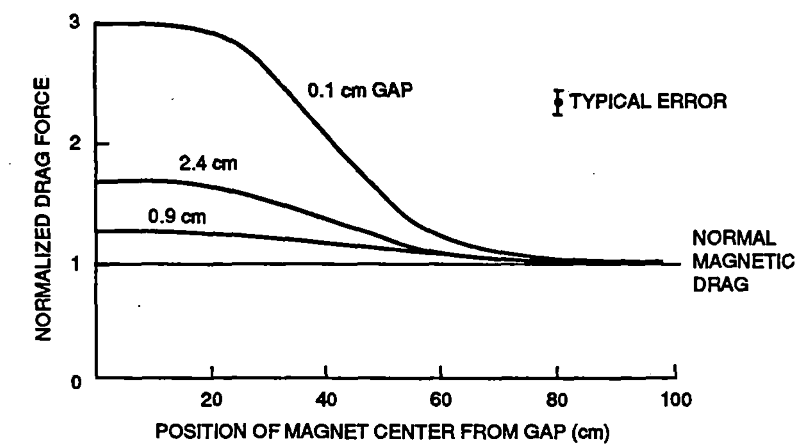

Figure 3-32. Variation of Drag Force with Gap Size (19)

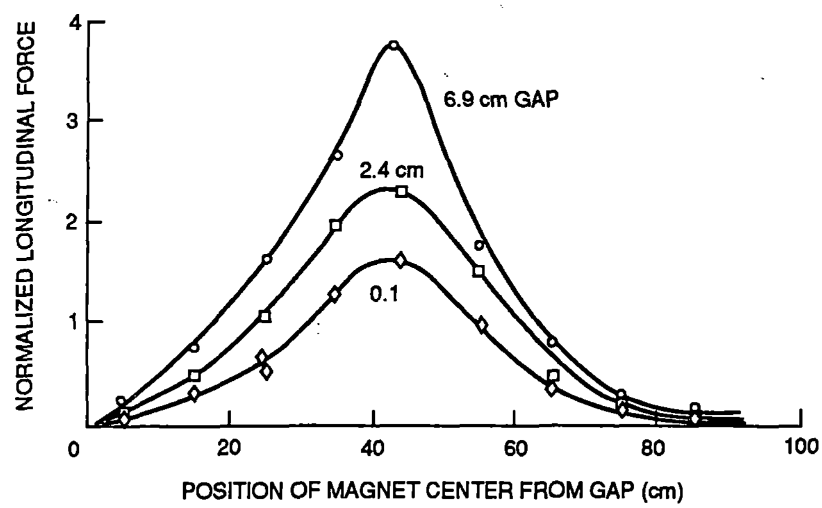

Figure 3-33. Variation of Longitudinal Force with Gap Size (19)

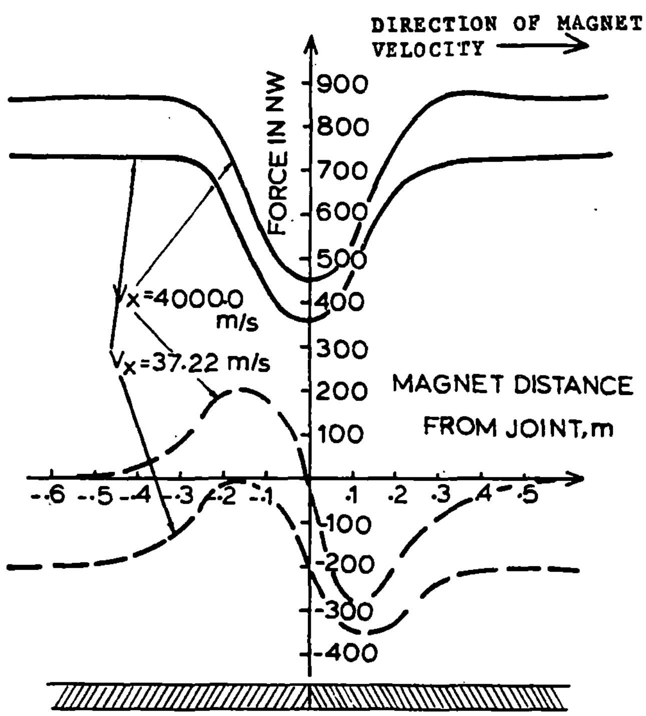

Figure 3-34. Variation of Lift and Drag (Broken Lines) Forces at Speeds 4000.0 and 37.22 m/s as the Magnet Crosses Over a Butt Joint

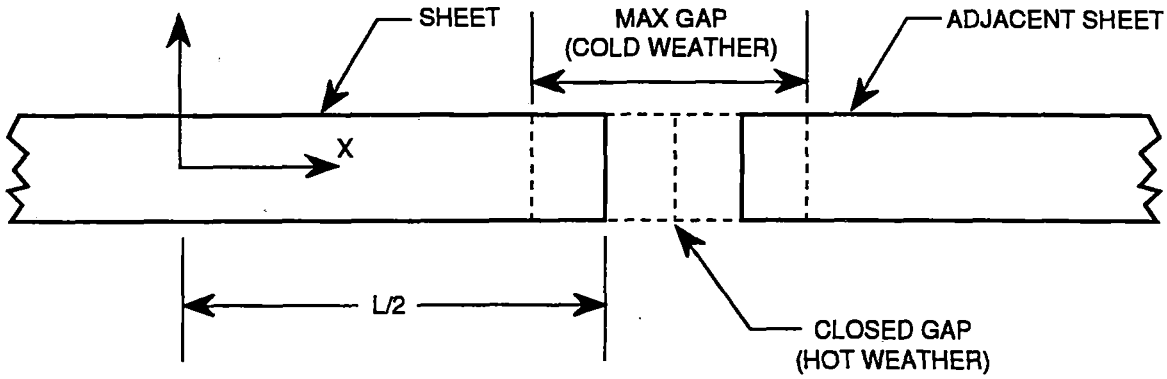

Figure 3-35. Thermal Movement of Segmented Sheet Guideways

The boundary conditions are

$$x = 0: \quad u = 0$$
$$x = L/2 \quad \sigma_x = E(U' - \alpha \Delta T) = 0$$

The resulting longitudinal displacement at position x=L/2 in hot weather is

$$\delta_H = -\frac{f_o L^2}{4AE} + \alpha L\left(T_H - T_o\right)$$

where T_0 = neutral installation temperature.

In cold weather, this displacement is given by

$$\delta_C = \frac{f_o L^2}{4AE} + \alpha L\left(T_C - T_o\right)$$

Thus, the total displacement is

$$\delta_{MAX} = \delta_H - \delta_C = -\frac{f_o L^2}{2AE} + \alpha L \left(T_H - T_C\right)$$

The stress at any position x is given by

$$\begin{aligned}\sigma_x &= E\,(U' - \alpha \Delta T) \\ &= \frac{f_o}{A}(X - L/2)\end{aligned}$$

which has a maximum value at x=0 of $-f_0L/2A$.

Numeric Example

Assuming reasonable temperature extremes, ignoring eddy current heating, of 248K (-25°C or -13°F) and 333K (60°C or 140°F), then for a desired maximum gap size, the corresponding length of the aluminum sheet segment can be calculated. The results of this analysis for a 1 cm thick, 0.6m wide aluminum sheet are shown in Figure 3-36. For a desired gap width of 2 cm (0.79 in.), the allowable maximum sheet lengths are in the range of 10 to 16m. If the fastener resistance is very large, even longer lengths may be used.

However, if a high fastener resistance and long segment lengths are used, then stress levels may become inadmissible, especially in winter months. Very long sheet segments may require welding and assembly from shorter sheet lengths. These weldments are subject to fatigue and fracture in winter.

The maximum tensile stresses in a 1 cm thick, 0.6m wide segmented sheet are shown in Figure 3-37. For very long segments with high fastener resistance, the stress can approach 220 MPa (31.9 ksi) or more, which exceeds the tensile strength of 6061 aluminum in weldments. Shorter segments (≈15m) can produce lower stress levels (100 MPa, 15 ksi), but the resulting fatigue life is limited.

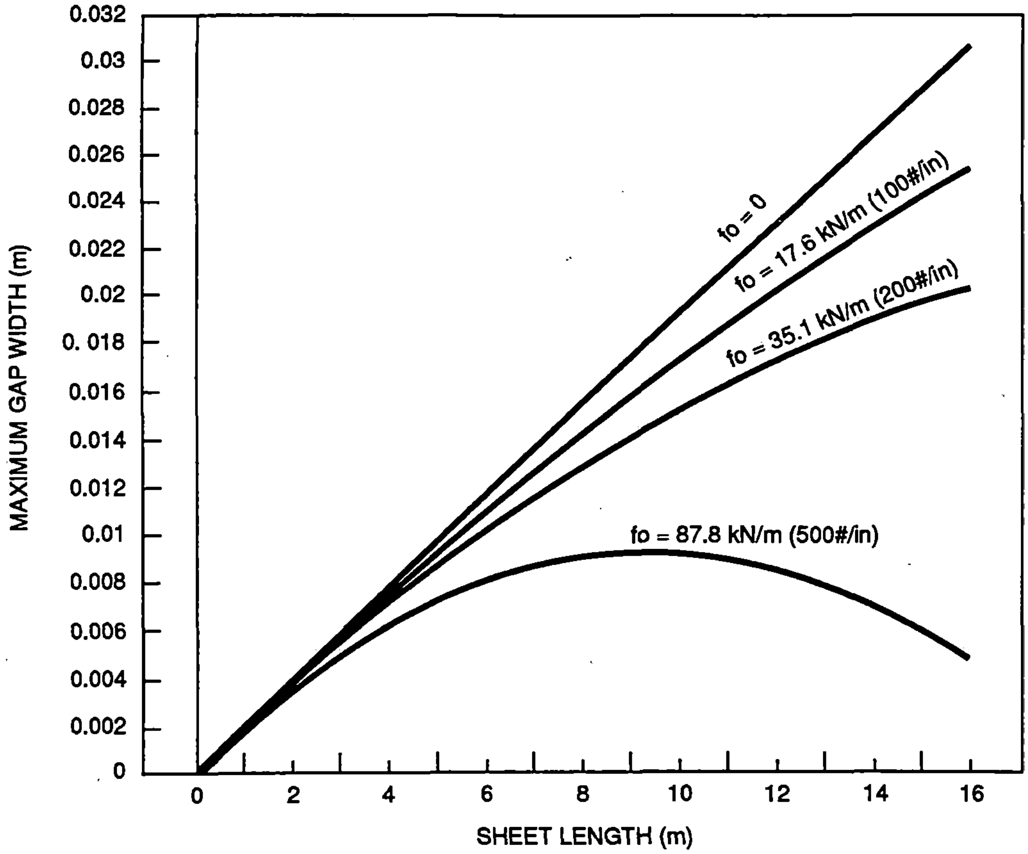

Figure 3-36. Maximum Allowable Gap Widths in Segmented Sheet Guideways

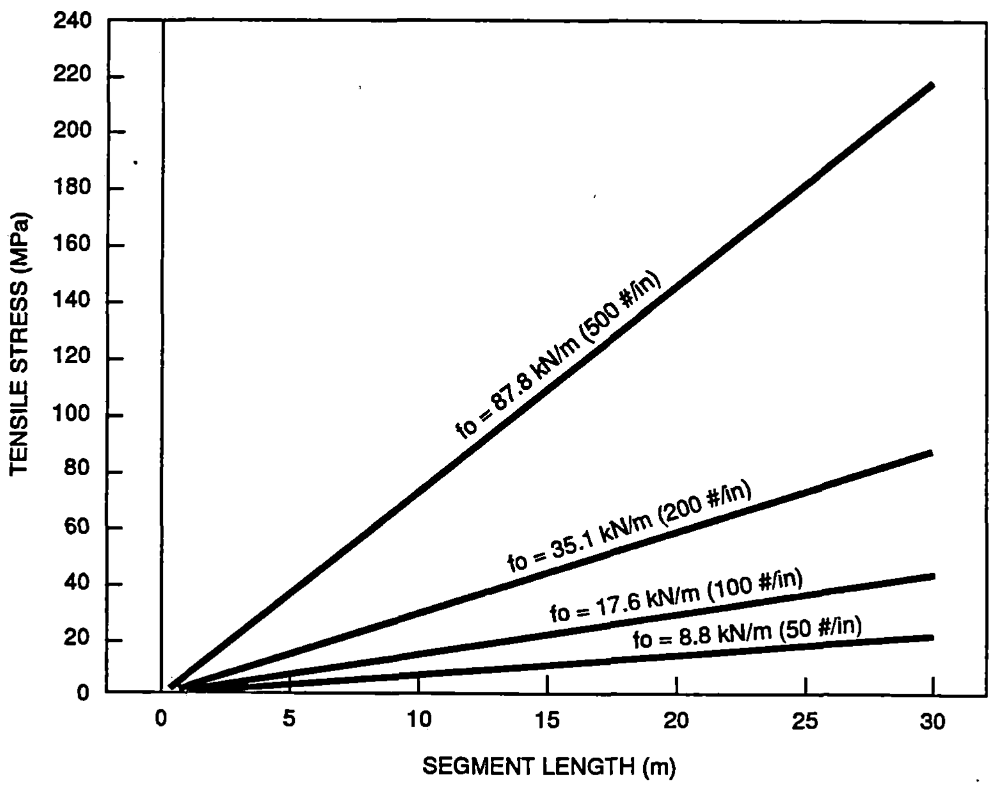

Figure 3-37. Tensile Stress in Segmented Sheet Guideways

In addition, segmented sheets in service can slide due to wear of the fasteners, etc., possibly closing the expansion gaps (causing end lift or buckling) or opening the gaps beyond the desired tolerance. Debris could also lodge in the gaps, precipitating buckling. Since the magnetic force transients are strongly related to the gap size, special joint designs, such as strapped or overlapping joints, may be required which could also increase costs.

3.3.3 Fracture and Fatigue

Given the susceptibility of sheet guideways to thermal buckling, it may become necessary to install continuous sheet guideways at elevated temperatures, or by using destressing techniques similar to those used on CWR. This, however, can induce excessive tensile stress in the sheet during colder weather. The weldments of continuous or segmented sheet guideways are particularly weak and could fail in direct tensile fracture or due to cyclic thermal loading at the weld. Selection of sheet materials, even within the aluminum family, then becomes considerably important, as will be shown.

3.3.3.1 Tensile Fracture

Due to tensile stressing and the reduced strength of weldments, CSG or segmented sheet guideway can fail in tensile fracture. Typical tensile yield and ultimate strengths for 6061 T-6 aluminum sheet are 240 MPa and 290 MPa, respectively. Yield and ultimate strength in weldments are considerably lower, at approximately 138 MPa (20 ksi) and 165 MPa (24 ksi), respectively (17). At these reduced strengths, a CSG temperature decrease of 89K (160°F) from neutral will cause yielding, and a decrease of 107K (192°F) will cause failure. Unless CSG is installed at artificially high temperatures, tensile fracture will be avoided. (However, as will be discussed, fatigue life will be shortened.)

Other typical alloys of aluminum have similar or greater yield and ultimate strengths than 6061. However, some of the less common alloys, such as the 1000 series of aluminum, might be considered due to their increased electrical conductivity. These materials do not exhibit good fatigue and ultimate strengths in weldments, and are more subject to thermal ultimate strength failure. For example, the yield and ultimate strengths of 1100-H14 alloy in weldments are 31 MPa (4.5 ksi) and 76 MPa (11 ksi) respectively (17). At these strengths, a CSG temperature decrease of 20K (36°F) from neutral will cause yielding, and a decrease of 49K (88°F) will cause fracture. Due to the expected extreme thermal environment and cyclic loading of the Maglev guideway sheet, these materials are thus not useful for continuous or segmented guideway sheets.

3.3.3.2 Fatigue

The sheet guideway is subject to many sources of cyclic thermal and mechanical loading. These sources include:

- Transient heating due to vehicle induced eddy currents;
- Diurnal thermal cycles;
- Vehicle mechanical loading and strain transfer; and
- Stress concentrations.

These sources, and their impact on the fracture and fatigue of sheet guideways will now be addressed.

Transient Vehicle Heating

As shown in previous sections, eddy current heating can raise the temperature of the sheet guideway by several degrees, even in regions where vehicle speed is high. The heat transfer due to vehicle passage is transient, and since the sheet has finite thickness, an initial depth-wise temperature gradient forms. This temperature gradient can induce transient thermal stresses, compressive and tensile, in the sheet. Since this phenomenon can occur with every vehicle passage, several hundred cycles per day are possible.

Diurnal Thermal Cycles

The daily variation in sheet temperature can be significant. If an installed neutral temperature of 311K (38°C or 100°F) is assumed with an average nightly minimum temperature of 283K (10°C or 50°F), then the daily cycle of tensile stress is 43 MPa (6.3 ksi). In winter, when the minimum temperature could drop to 248K (-25°C or -13°F) or below, tensile stresses of 97 MPa (14 ksi) are achieved.

Strain Transfer

Similar to the strain transfer of compressive load (described in the previous sections), spans which use continuous supports can transfer tensile load into the guideway sheet. Vehicle static and dynamic loads cause bending moments which put the upper fibers of the guideway over the continuous support in tension, as shown in Figure 3-38. Assuming the sheet is securely fastened to the guideway, the strain of the upper guideway fibers is also present in the guideway sheet, resulting in tensile sheet stress. The strain, stress and equivalent temperature change in the sheet can be calculated. Here the stress induced in the sheet is tensile, and the equivalent temperature change reflects a decrease from the neutral temperature. This is shown in Figure 3-39 for typical guideway geometries.

Stress Concentrations

An important source of stress concentration occurs at the expansion joints between adjoining guideway girders. As shown in Figure 3-40, the guideway sheet is continuous over this joint. However, the slope of the girder deflection is not continuous at the joint, and a cusp is formed. The CSG is thus subjected to large bending loads in this region due to the thermal, static and dynamic flexure of the adjoining girders. Additionally, a small length of the sheet is unsupported over the joint, which will cause large localized bending stresses when the vehicle passes.

Other important sources of stress concentration include sheet guideway designs which are comprised of L-shaped sections of aluminum sheet, as shown in Figure 3-41. As the sheet flexes due to thermal and mechanical loads, it will experience high stresses due to the stress concentration at the bend of the L-section. This stress concentration could seriously affect the fatigue life of the sheet. Additional stress risers could occur at any bends, cuts or holes made in the sheet by various joint techniques.

Fatigue Life Estimation

Estimates of the tensile stress levels found in CSG due to eddy current heating and strain transfer are generally less than 34 MPa (5 ksi). These cycles occur with each vehicle passage.

For a passenger capacity of 12,000 passengers per hour over an 18 hour day, approximately 1 million cycles per year are achieved. Since the stress levels are low, fatigue life should not be affected, even with a large number of cycles.

However, the additional stress due to the diurnal thermal cycles and any stress concentrations could greatly increase the stress levels, precipitating fracture or a shortened fatigue life. To avoid this, the cyclic stress due to daily temperature changes should be kept as small as possible. The cyclic thermal stress levels can be minimized by proper selection of the sheet installation (neutral) temperature, as will be discussed in the following section.

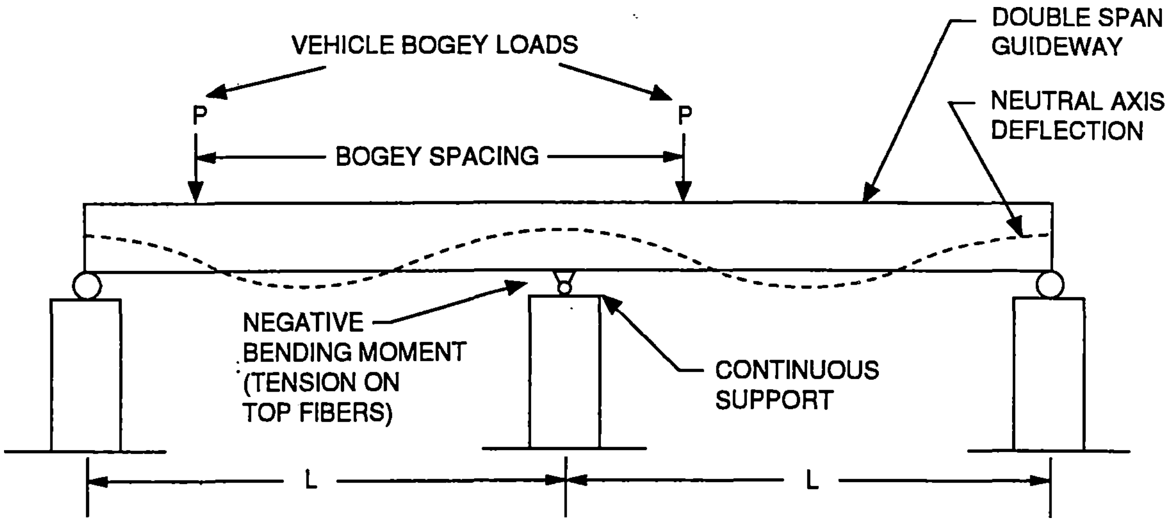

Figure 3-38. Bending Moment and Strain Transfer in Double Span Guideways

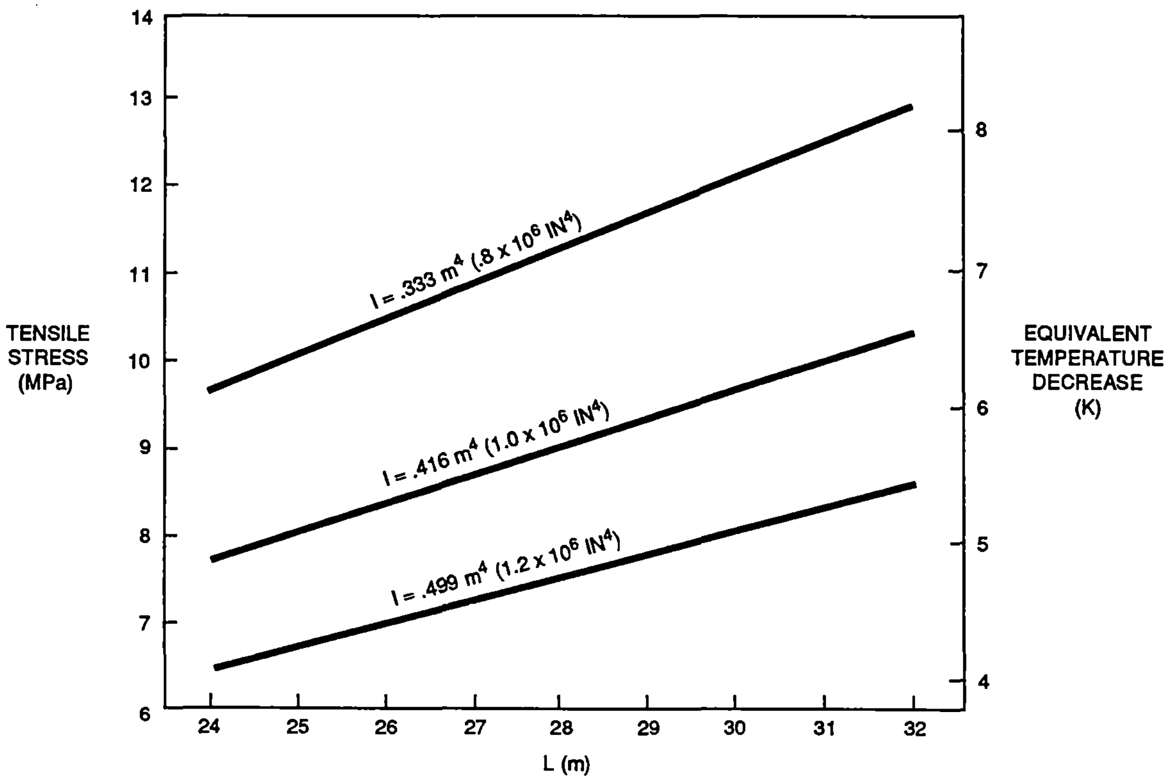

Figure 3-39. CSG Tensile Stress Due to Strain Transfer

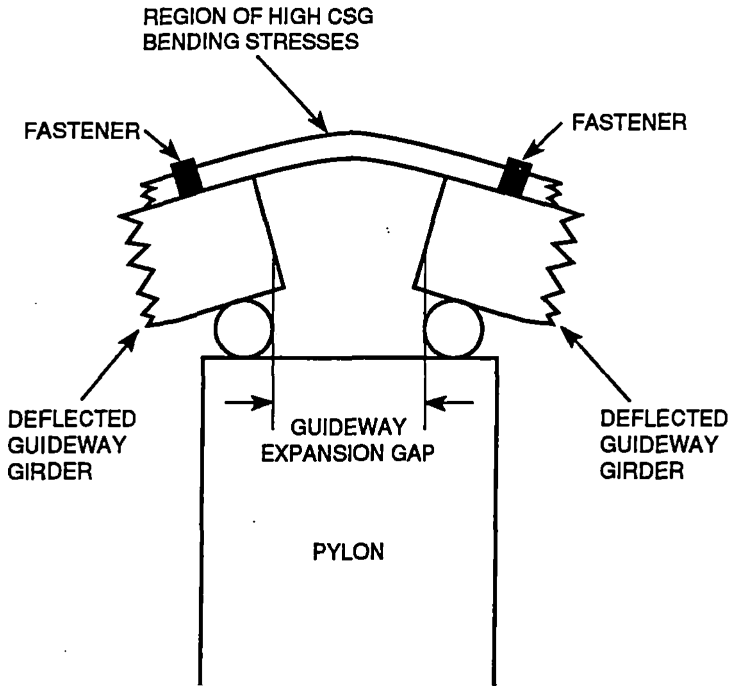

Figure 3-40. CSG Stress Concentration at Guideway Expansion Joint

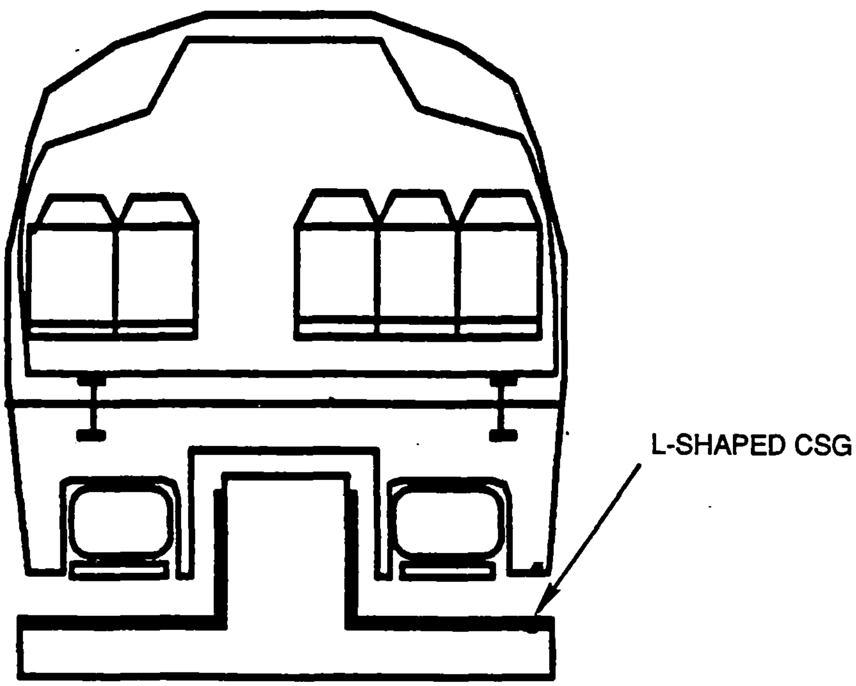

Figure 3-41. L-Shaped CSG Design (15)

4. MITIGATION TECHNIQUES FOR CONTROL OF THERMAL EFFECTS

The analyses in previous sections indicate that serious problems can arise due to temperature changes in the continuous sheet guideways and supporting primary structures. The problems can range from buckling and fatigue and fracture to undesirable deflections affecting ride comfort. It is important to eliminate or reduce the severity of the thermal problems in Maglev structures for smooth, and cost efficient operations. Potential techniques for mitigation of thermal effects in these structures are discussed in this section. Preliminary evaluations indicate that at present there is no single cost effective and reliable technique for control of thermal effects in CSG. Further research will be required to identify and develop an acceptable mitigation method.

4.1 Primary Structure Mitigation Techniques

Thermal effects can induce large deflections of the primary structure. The analysis presented here has shown that these thermal deflections can exceed desired design tolerances, and have an adverse impact upon passenger ride comfort.

Possible means of mitigating these effects include:

- The use of alternating continuous spans in place of simply supported spans;
- Passive heat transfer control by means of white coatings or insulating layers of concrete on the guideway; and
- Active heat transfer control, using active cooling of the guideway.

These methods are discussed in the following sections.

4.1.1 Alternating Continuous Spans

Any spans used in a Maglev guideway, regardless of support or continuity, must include expansion joints for the relief of thermal longitudinal expansion, as is standard practice in elevated bridge and highway construction. However, as noted previously, the temperature gradient through the guideway structure induces large thermal deflection. The use of alternating continuous spans in place of simply supported single spans (as shown in Figure 3-13) can mitigate this effect, reducing the resulting deflections by approximately 70 percent. Concurrent with this reduction is an increase in bending stress, which may require additional reinforcement in concrete structures. The extra costs incurred in the construction of continuous supports and use of reinforcement must then be considered in any Maglev guideway design.

4.1.2 White Coatings and Insulating Concrete

The analysis presented in this study (subsection 3.1.1) has shown that the use of white coatings or insulating concrete on the guideway can lessen the thermal effects, thereby reducing the thermal deflection.

Of these two methods of controlling heat transfer, the white coating produces the greatest reduction of thermal bending moment and can possibly provide substantial reduction of thermal deflections. The use of white coatings on an EMS guideway, such as the Emsland Transrapid, is thus a useful means of thermal deflection mitigation.

However, in an EDS guideway using continuous sheets, the effects of white coatings are less direct. The aluminum sheets can cover a significant portion of the guideway surface. The heating of the aluminum sheet, via solar radiation and, more importantly, eddy current heating, can be transferred to the guideway and reduce the mitigating effects of the white coatings. EDS guideways using discrete coils are less subject to eddy current heating, and should not have this effect.

4.1.3 Active Guideway Cooling

The temperature gradient in the box beam type guideway can be reduced by means of active convective fan cooling (Figure 4-1). Such a technique has been apparently conceptualized for an Emsland type guideway. The fans can be automatically turned on at a preset temperature rise on the top surface of the guideway. Clearly, this method is not cost effective for the entire guideway, but may be used at limited locations vulnerable to high temperature change.

4.2 CSG Thermal Mitigation Techniques

As discussed in previous sections, the thermal effects on CSG are a potentially greater problem than the effects on the primary guideway structure. Due both to ambient heat transfer and the even greater effects of eddy current heating, very high temperatures can be induced in the guideway sheet. And as shown, these effects can cause cyclic stress and thermal buckling.

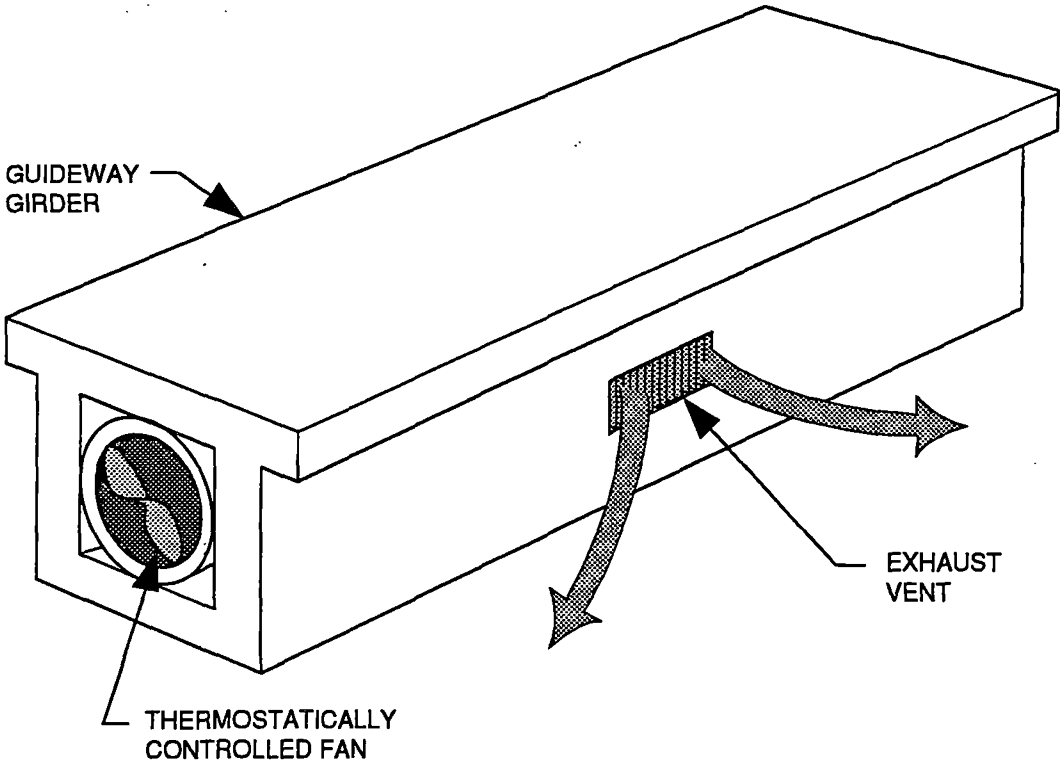

Figure 4-1. Active Guideway Cooling

Possible mitigation methods for these effects include:

- Use of expansion joints;
- Optimization of installation temperature;
- Use of novel CSG attachment techniques;
- Use of innovative joints;
- Active temperature control; and
- Passive temperature control.

These methods are discussed in the following subsections.

4.2.1 Expansion Joints

Expansion joints seemingly provide the most straightforward method of relieving thermal buckling stress and relief of sheet bending stress at girder expansion joints. However, the magnetic force transient caused by gaps in the sheet are undesirable and could affect passenger ride comfort. Since the sheet is likely to be subjected to in-plane forces, it can slide under worn fasteners in service conditions, closing the gaps and causing edges to lift off. The sheet can eventually buckle upwards. (Buckles do occur in jointed railroad rails due to movement under braking and vehicle traction.) Debris could also lodge in the expansion joints and precipitate buckling. These effects could then require costly periodic inspection and maintenance to ensure proper gap size.

Reference 1 has also shown that fatigue and quenching of supercooled magnets can occur due to the force transients caused by expansion joints. Joints using backing plates were also shown by (1) to be ineffective.

4.2.2 Optimization of Installation Temperature

Within the expected range of maximum to minimum operating temperatures, an optimum installation temperature can be selected such that buckling and tensile fracture and fatigue are avoided. The procedure is illustrated with an example. The parameters used in this example assume worst case thermal conditions:

Sheet material:	6061 aluminum
Min sheet temperature in winter:	253K (-4°F)
Max ambient temperature:	316K (109°F)
Sheet width:	1m (39.37 in.)
Sheet thickness:	0.013m (0.5 in.)

The procedure to calculate the optimal installation temperature is as follows. The procedure is illustrated in Figure 4-2.

1. For the sheet material used, determine the maximum allowable weldment tensile stress, assuming long life (>1,000,000 cycles) from S-N data. For 6061 aluminum, this is approximately 68.9 MPa (10 ksi).

2. From this maximum stress level and the assumed minimum temperature of the sheet in cold weather, determine the maximum installation temperature allowed ($T_{o_{max}}$), as given by

$$T_{o_{max}} = T_{min} + \frac{\sigma}{E\alpha}$$

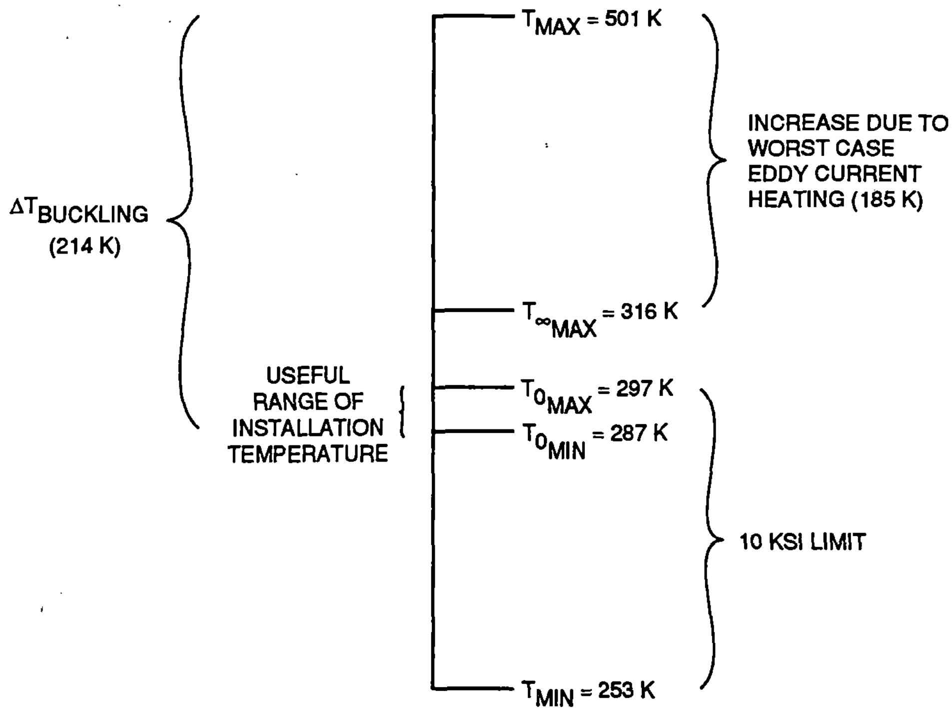

Figure 4-2. Example Optimization of Installation Temperature

$$T_{o_{max}} = 253\text{K} + \frac{68.9 \text{ Mpa}}{E\alpha} = 297\text{K}\ (24°\text{C})$$

$T_{o_{max}}$ is considered to be the maximum allowable installation temperature. Installing the CSG at higher temperatures will result in daily winter thermal stresses exceeding the desired limit of 10 ksi. However, if the sheet installation temperature is too low, then it may be difficult to avoid sheet buckling at the temperature extremes caused by eddy current heating. From a practical standpoint, a range of useful installation temperatures is needed, rather than a specific value. An initial range (of 10K) is assumed here:

$297\text{K} \geq T_0 \geq 287\text{K}$ $(75°\text{F} \geq T_0 \geq 57°\text{F})$

3. From the calculations of eddy current heating, determine the maximum sheet temperature increase above ambient, $T - T_\infty$. For an assumed average speed of 20 m/s near a Maglev station, the maximum expected temperature increase above ambient (from Figure 3-8) is approximately $T - T_\infty = 185\text{K}$ (333°F). For the maximum value of T_∞ expected, the maximum expected sheet temperature, T_{max}, is then calculated as

$$T_{max} = 185K + T_{\infty max}$$
$$= 501K\ (442°F)$$

T_{max} represents the maximum expected sheet temperature due to the effects of eddy current heating under worst case conditions (high passenger capacity near a Maglev station).

4. To avoid buckling in service, the sheet must be able to withstand an expected in-service temperature of T_{max} (from step 3) without buckling. This implies that the sheet must withstand a temperature increase from neutral of $\Delta T_{BUCKLING}$, as calculated from

$$\Delta T_{BUCKLING} = T_{max} - T_{o_{min}}$$
$$= 501 - 287 = 214K \qquad (385°F)$$

The sheet and fastener spacing must be designed so as to avoid buckling at this worst case temperature increase.

5. The sheet fastener spacing must be such that buckling will not occur at the maximum expected temperature increase defined in step 4 above. The required fastener spacing is determined from the buckling charts, or is calculated using the equations presented in Section 3. The required fastener spacing for avoidance of buckling in this example is approximately 44 cm (17.3 in.); to provide some margin for worn out fasteners, an even smaller pitch of 22 cm (8.7 in.) must be used.

6. If the installation temperature range and resulting fastener pitch are not satisfactory, the above procedure can be repeated using different sheet materials or dimensions until a practical design and installation temperature range are converged upon.

Thus it is possible to optimize the sheet installation temperature so that buckling and fatigue failure will theoretically not occur. Increasing the installation temperature from this optimal range could result in reduced fatigue life; decreasing the installation temperature from this range could result in reduced buckling strength. The primary driving factor here is the eddy current heating, which requires very short (and expensive) fastener pitch for the avoidance of buckling. This method does, however, have the potential problem of defining too high an installation temperature. If this temperature exceeds 300K, (81°F) it will probably not be practical. In such a case, the procedure should be repeated using a lower range of T_o. This, however, will result in a larger $\Delta T_{BUCKLING}$, and hence, a smaller value for the allowable fastener pitch.

4.2.3 Novel CSG Attachment Techniques and Expansion Joints

The CSG buckling problem may be substantially mitigated through the use of a novel continuous attachment technique, such as bonding.

Extensive Foster-Miller experience indicates that bonding the CSG directly to the concrete substructure is practical due to the porosity of the concrete and the extensive development of epoxies for use with aluminum. Bonding would provide continuous CSG support, high longitudinal resistance and sufficient flexibility for thermal and mechanical fatigue if a high toughness epoxy is utilized.

A major concern of bonding is environmental and fatigue degradation. Recent testing at Foster-Miller has evaluated a new developmental high toughness epoxy which may be suitable for this application. These tests, conducted under another program, have demonstrated both high resistance to environmental degradation and excellent adhesion to aluminum.

Several joint designs have been reviewed here. While the electrical adequacy of these designs has been well studied in the literature, the mechanical adequacy needs to be properly evaluated. The more novel joints reviewed include the angled sliding joint, the flexure support, and the grooved joint under development at Argonne National Laboratories (ANL). The angled sliding joint (Figure 4-3) provides the simplest solution by permitting segmented sheets to overlap. This solution is an improvement in continuity over the straight gap method. However, substantial drag and loss of lift will still result from such a joint. Straps or wires may be added across the joint for improved electrical performance. However, the added complexity will increase costs while reducing reliability. Further, attachment of this type of CSG presents problems. Fasteners must have sufficient longitudinal resistance to react the vehicle propulsion loads while permitting thermal expansion within the segment to make use of the joint. These conflicting requirements significantly complicate design of such a system. The low speed Maglev at the Birmingham airport in England uses a type of angled sliding joint. However, this system is not suitable for high speed Maglev.

The flexure support (Figure 4-4) permits thermal expansion while maintaining a CSG with no gaps. Since the CSG is supported on thin, flexible webs, it is free to expand and contract apart from the primary structure. While this concept may effectively mitigate thermal stresses, significant design difficulties exist. The vehicle levitation loads will induce potentially high bending in the CSG without the direct support of the understructure. The design requirement for a

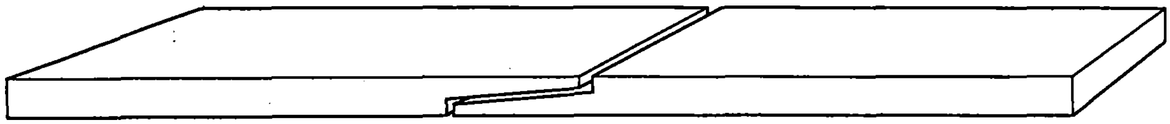

Figure 4-3. Angled Sliding Joint

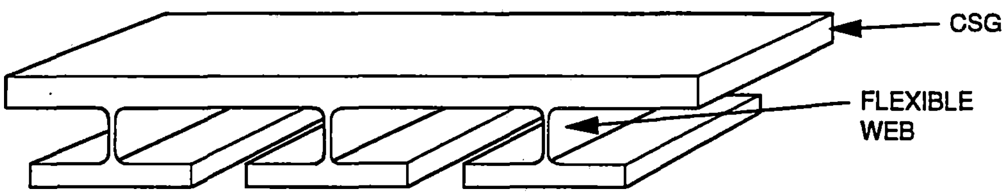

Figure 4-4. Flexure Support

flexible web may dictate a limited fatigue life. Most significantly, the fabrication and installation of such a complex structure would likely be cost prohibitive.

Research is ongoing at Argonne National Laboratories (ANL) to develop a novel joint. This joint (Figure 4-5) employs a grooved section which will flex to relieve stress in the sheet. While the electrical advantages of such a joint have apparently been demonstrated at ANL, the mechanical fatigue needs to be tested.

The advantages of leaving even a thin section of continuous material at an expansion joint were demonstrated in scaled testing (1). The lift and drag force transients due to the gap were found to be substantially less for even a 99 percent thickness groove than for a through cut. Based on this

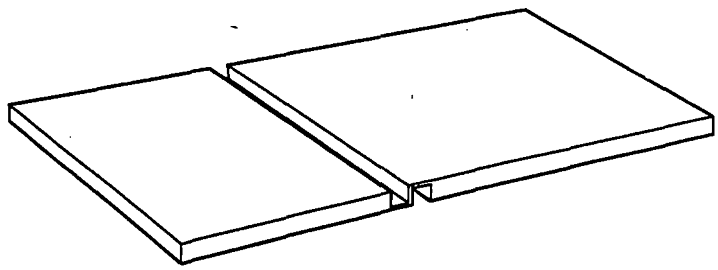

Figure 4-5. ANL Thermal Expansion Joint

testing, a pair of grooves, one on the top surface and one, slightly offset, on the bottom surface, was recommended.

The mechanical fatigue of this joint should be tested in the laboratory. Thermal cycling of the CSG will likely result in deflections sufficient to cause substantial fatigue damage. For example, for a joint pitch of 12m, free thermal expansion at the joint would be approximately 9 mm for an aluminum CSG with a 30K daily temperature cycle. This deflection of similar magnitude to the CSG thickness, could result in low fatigue life.

4.2.4 Active Temperature Control

Cooling water can be ducted under the guideway sheet using brazed or welded channels as shown in Figure 4-6. The water will remove the solar and eddy current heat from the guideway sheet when an appropriate temperature is reached. The heated water can then be used for consumption or heat storage tanks at stations, or the water can be recirculated in a closed loop. This method will also effectively prevent heat from transferring between the sheet and the primary guideway structure. Combined with white coatings on the guideway, this method could effectively mitigate thermal effects in both the guideway sheet and the supporting structure.

Active cooling can also be done through air circulation by fans. Figure 4-7 shows an arrangement in which the air cells are transverse to the vehicle direction.

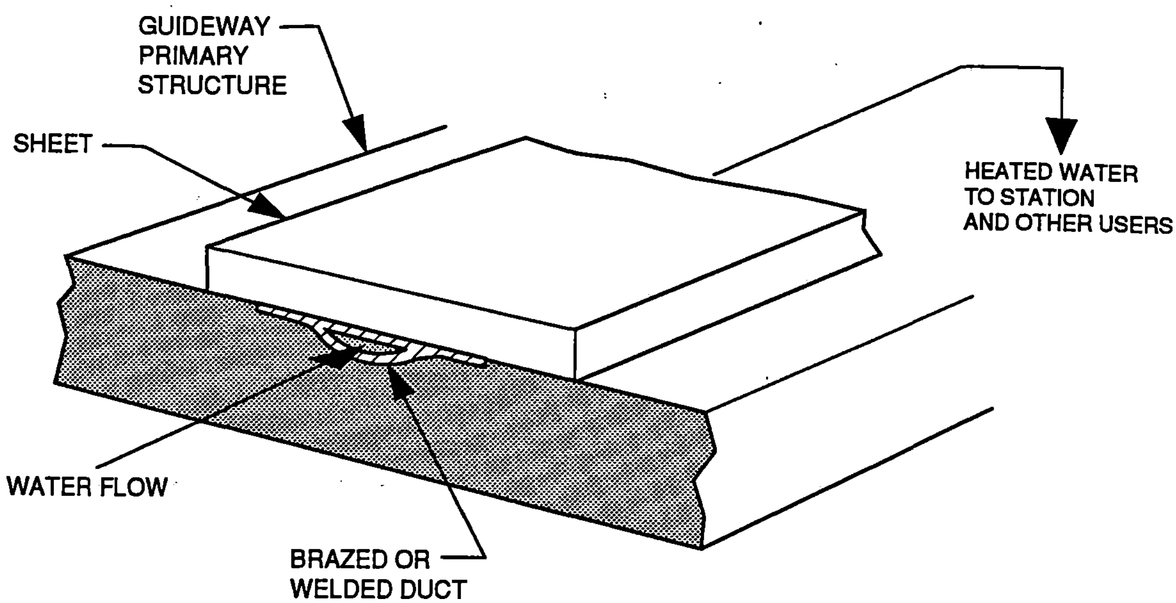

Figure 4-6. Active CSG Temperature Control

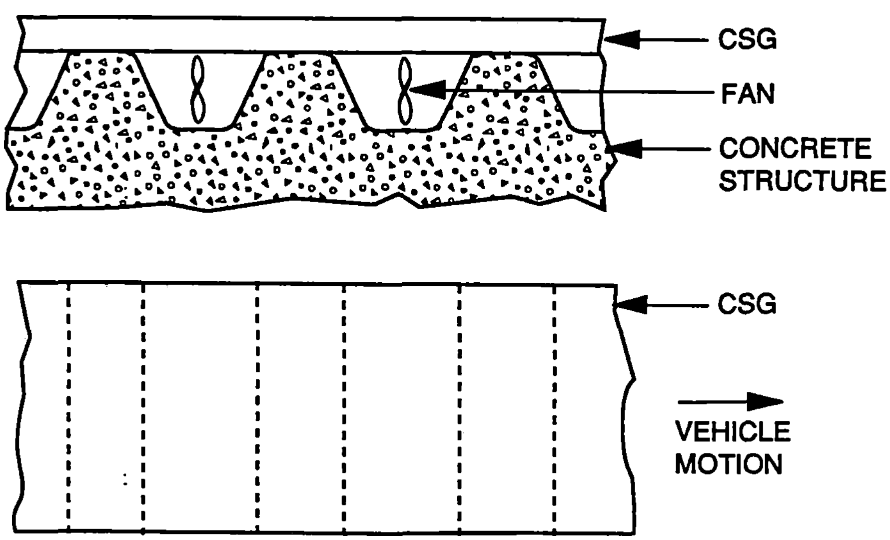

Figure 4-7. Active Fan Cooling of CSG

4.2.5 Passive Temperature Control

The temperature of the CSG can be controlled in a passive manner through the use of white paints (polymer based) or through the use of fins. A finned CSG (Figure 4-8) would have to be made as an extrusion and can be expensive. Attachment of a finned CSG can also be complicated.

4.3 Summary of Mitigation Methods

A summary of mitigation methods is presented in Table 4-1.

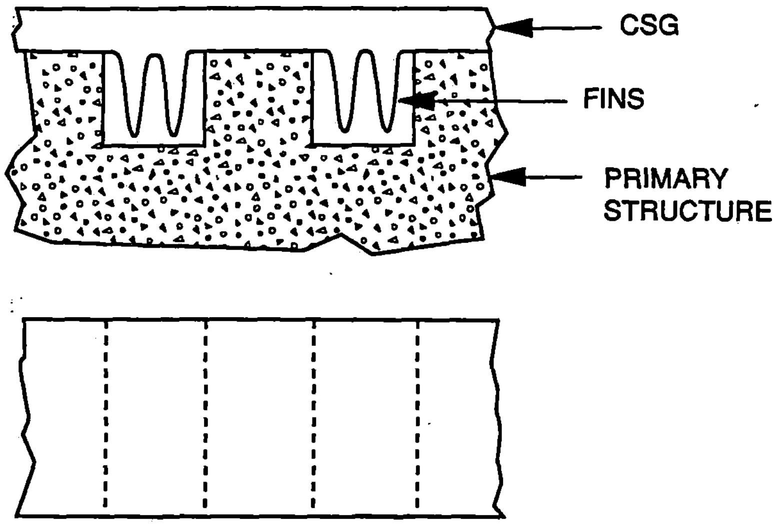

Figure 4-8. Finned CSG

Table 4-1. Summary of Mitigation Methods

Technique	Advantages	Disadvantages
Alternating Continuous Span	• Deflection reduction	• Higher bending stress • Potential higher cost
White Coatings and Insulating Concrete	• Thermal gradient reduction • Deflection reduction	• Added cost
Active Guideway Cooling	• Temperature control	• Substantial cost and maintenance
Expansion Joints	• Thermal stress relief • Low cost solution	• Ride comfort degradation • Potentially high maintenance
Neutral Temperature Optimization	• Lower maintenance • Design solution	• Potentially very small and expensive fastener pitch
Novel Attachment Techniques	• Continuous CSG support • Thermal expansion flexibility	• Potential environment degradation
Innovative Joints	• Thermal stress relief • Electrical continuity	• Potential fatigue problems • Added cost
Active Temperature Control	• Temperature control • Isolation of CSG	• Substantial cost and maintenance
Passive Temperature Control	• Temperature control • Less complex than active	• High CSG fabrication costs

5. DESIGN DATA AND TEST REQUIREMENTS

A computer software for the mechanical design of segmented or continuous sheet guideway can be developed after evaluation of potential installation and attachment techniques, and validation of basic theoretical analyses developed in the previous sections. The recommended tests are presented later in this section. First, the design data requirements for the development of software are discussed.

The software will contain the following modules integrated to provide a comprehensive design tool. The design methodology is illustrated in Figure 5-1.

- *Heat Transfer Module* - The temperature distribution in the guideway structure erected in a given geographical location will be evaluated on the basis discussed in Section 3. The seasonal and diurnal variations can be predicted using the finite element method for the parameters identified in this section. Data on these parameters are available in the literature.

- *Eddy Current Heating Module* - An in-house computer software is available for the prediction of eddy current power loss in the sheet guideway. The required parameters are magnet characteristics, gap height, CSG material, width, vehicle speed, number of magnets and headway or frequency. From the calculated power loss, the temperature rise in CSG will be determined, as shown in Section 3.

- *Buckling Module* - A buckling temperature evaluation model has already been developed, and computer software is written as a part of this work. This requires the following input parameters: longitudinal resistance by fasteners or other attachment methods, CSG thickness, width, fastener pitch, material modulus, and coefficient of thermal expansion. Except for the longitudinal resistance of certain fastener systems, data on other parameters are available in the literature. The buckling module will determine the allowable temperature rise over the installation temperature for a chosen CSG design, which must be larger than the expected increase due to solar and eddy current heating calculated in the heat transfer and eddy current modules.

- *Fatigue and Fracture Module* - Fatigue damage in welded CSG needs to be estimated on the basis of SN Curve. Data on weldable metals is available in the literature. Component stresses arising from diurnal cooling, eddy, current transient heating, vehicle induced stress due to strain transfer from primary structure can be quantified, and using the Miner's

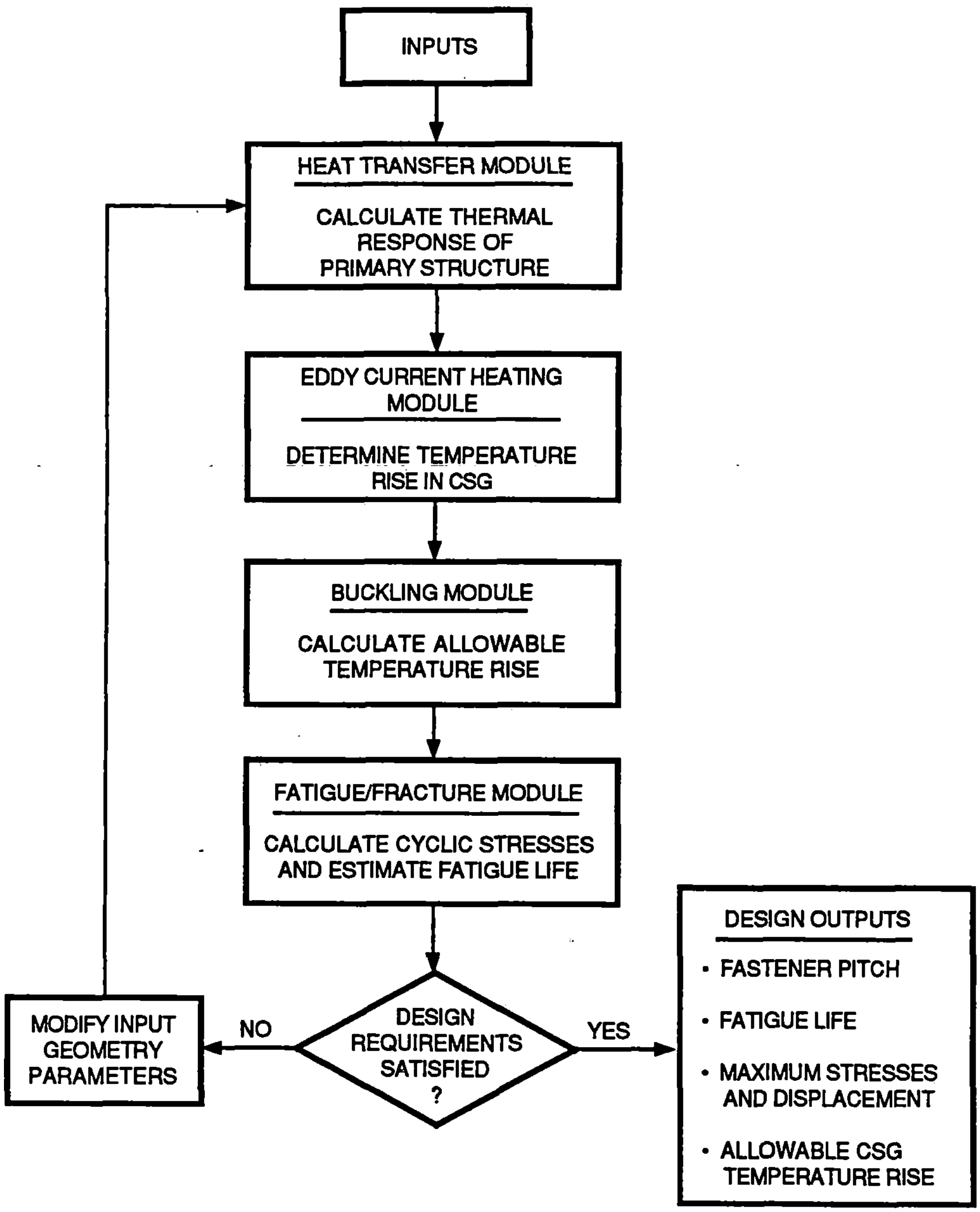

Figure 5-1. Flow Chart for CSG Design Software

cumulative damage rule the fatigue life is calculated in this software module. The module will also determine maximum expected tensile stress and provide allowable limits for the weldments.

For the development of the computer software to facilitate future reliable CSG designs, the following test program is recommended.

5.1 Heat Transfer Model Validation for Primary Structure

5.1.1 Objective

This test of a scaled concrete guideway support structure is proposed to validate the heat transfer model and to evaluate the effect of different heating resistant surfaces for potential application in Maglev structures.

5.1.2 Technical Discussion

A thermal analysis of the guideway primary structure has been conducted (see subsection 3.1.1) to define the expected depthwise temperature gradient for the candidate Foster-Miller guideway design. The complex cross section of this guideway necessitated use of a transient 2-D finite element analysis. Evaluation of the expected worst case condition yielded a predicted maximum temperature differential of 37K which compares well with the 32K specified by the New Zealand design code. While deflections resulting from this substantial gradient are typically acceptable for standard transportation vehicles, they may be unacceptable for Maglev systems.

The temperature gradient may be reduced by the application of a heating resistant surface. The effects of two such mitigation techniques were analyzed with the model. As was shown in Figure 3-3, a surface layer of aerated insulating concrete actually made the gradient more severe while a white surface coating significantly reduced the gradient. These analytical results, including the baseline temperature gradient, should be compared with data from laboratory experimentation to validate the model.

5.1.3 Test Plan

The proposed testing should be conducted outdoors on a concrete beam. This beam is expected to be a commercially available cross section such as shown in Figure 5-2. The sizing

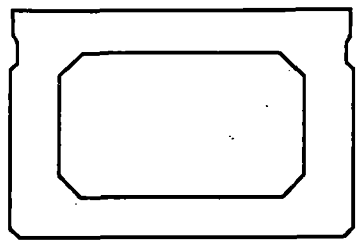

Figure 5-2. Typical Noncomposite Box Beam

should be selected to minimize cost by using a standard hollow section. It is expected that a beam depth of 0.5m would be sufficient to set up a meaningful temperature gradient. Thermocouples should be mounted about the cross section at several different spanwise stations. Data should be collected throughout several high solar radiation days. These data should be compared with model predictions and should also be used to verify the similarity of the spanwise stations and ensure that the temperature distribution does not vary along the span.

Following completion of the "as-is" temperature distribution tests, several heat resistant surfaces will be evaluated. It is recommended that these surfaces, summarized in Table 5-1, be applied at the different gauged spanwise stations as shown in Figure 5-3. This simultaneous testing setup should be used to permit direct "same day" comparisons of the surfaces. As shown, data should also be taken at "as-is" stations for direct comparison.

Table 5-1. Heat Resistant Surfaces for Primary Structure

Surface	Thickness (mm)	Mass (kg/m^2)	Solar Absorbtivity	Thermal Conductivity (w/m-K)
Insulating Concrete	25-50	14-28	0.25-0.50	0.2-0.5
White Paint	0.2	negligible	0.1-0.3	-
Metallic Paint	0.2	negligible	0.35-0.55	-

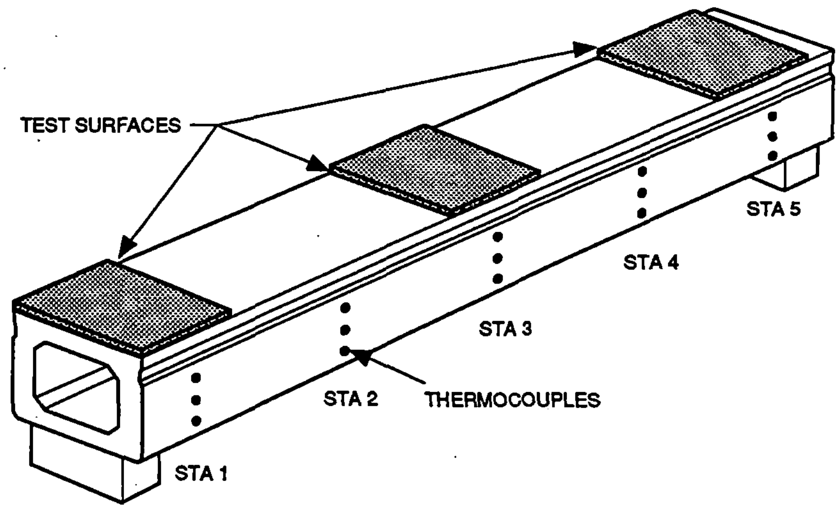

Figure 5-3. Test Facility for Heat Resistant Surface Evaluation

Due to the comparatively small depth (0.5m) of the test beam, the design maximum temperature differential of 32°C from the New Zealand code may not be achieved in these applications. The data from the tests of these surfaces may also be used to derive, if required, an adaptation of the fifth power distribution which would account for the heat resisting effects of these surfaces.

5.2 CSG Eddy Current Heating Analysis Validation

5.2.1 Objective

This test should be conducted on a CSG structure to quantify the eddy current induced heating due to vehicle passage for validation of the analysis.

5.2.2 Technical Discussion

An analysis of the heating due to vehicle passage has been conducted (see subsection 3.1.2). This vehicle passage will induce eddy currents along the CSG resulting in significant transient heating of the sheet.

The eddy current heating from one vehicle passage has been calculated to raise the CSG temperature by several degrees at high speeds. In the most severe low speed condition, the CSG temperature may be increased by as much as 30K by the passage of one eight-car vehicle. This effect will be greatly magnified by multiple vehicles with short headways. This substantial cyclic heating can result in thermal fatigue of the CSG. More significantly, the temperature rise, when compounded with solar heating, may result in CSG buckling. Eddy current induced heating has apparently not been quantified by testing. As this analysis identifies this process as a potentially severe problem, such a test program is recommended to validate the analysis.

5.2.3 Test Plan

The proposed testing should be conducted on a CSG structure exposed to a passing magnet. Analysis indicates that the induced heating is highly dependent on the vehicle speed. Thus, the facility must be able to create controlled relative movement between the magnet and the CSG. Two potential facility designs are presented in Figures 5-4 and 5-5. The CSG should not be longitudinally restrained by the supporting structure. As the purpose of these tests is to quantify eddy current heating and not buckling potential, restraint of the CSG will only result in facility alignment problems.

The CSG structure should be instrumented with thermocouples to record the temperature. As a standard thermocouple would not function properly in the presence of the strong magnetic field, care must be taken to properly design the instrumentation system. Tests should be conducted at various vehicle representative speeds to quantify the effect of this parameter. The gap between the CSG and the magnet must be precisely maintained as proper scaling of the results will depend on this distance. The heating recorded under the various test conditions should be compared with the predictions of the eddy current heating analysis.

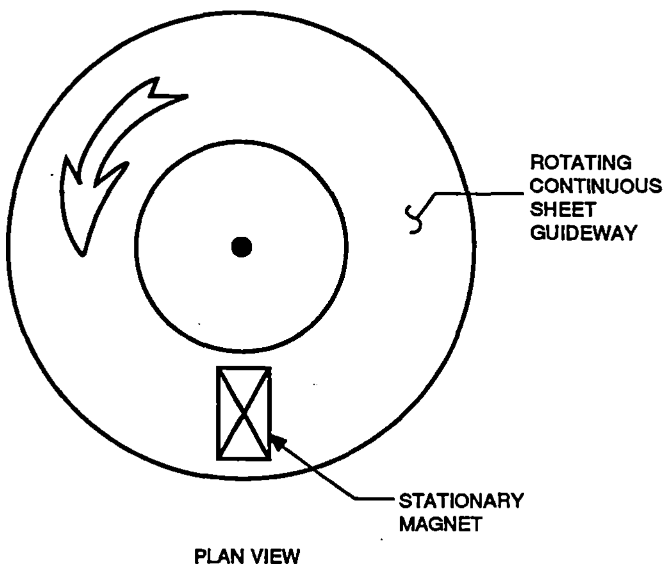

Figure 5-4. CSG Eddy Current Heating Test Facility (Turntable Concept)

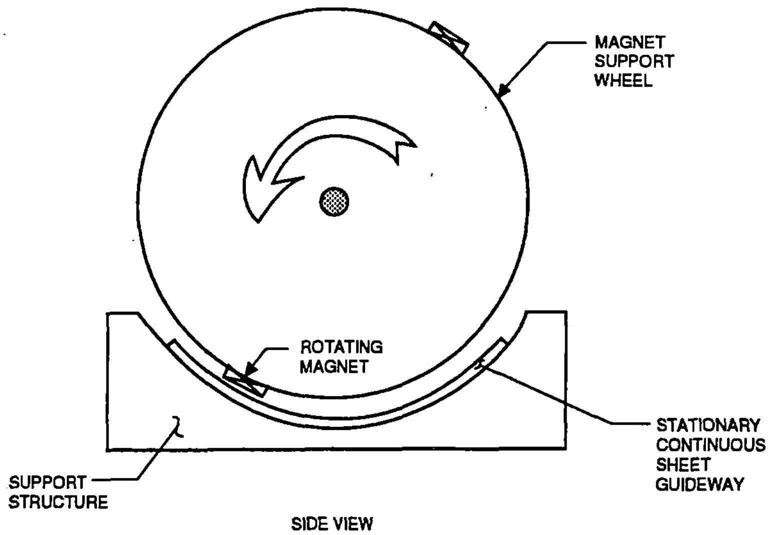

Figure 5-5. CSG Eddy Current Heating Test Facility (Wheel Concept)

5.3 Primary Structural Response Laboratory Validation

5.3.1 Objective

This test of a scaled Maglev guideway is proposed to validate the primary structural response model.

5.3.2 Technical Discussion

An analysis of the guideway primary structure has been conducted to determine the stresses and deflections due to the temperature gradient defined by the heat transfer analysis (see subsection 3.2.1). Several candidate guideway systems have been evaluated. Analytical results showed significant deflections for each candidate structure with the EMS steel guideway being a severe case. Further analyses calculated the significant influences of the maximum temperature gradient and the support conditions. The predicted deflections which may be unacceptable for Maglev operations must be validated. Therefore, a laboratory test on a representative guideway structure is recommended.

5.3.3 Test Plan

The proposed testing should be conducted in the laboratory using a scale model similar to the Transrapid steel guideway. It is recommended that the scale be selected as the minimum practical size which will deflect sufficiently under laboratory applied heating. For an expected deflection measurement system resolution of ±0.05 mm (0.002 in.) a simplified analysis estimates that a 1/10 scale model of the cross section may be sufficient over a span length of 6m. However, all the dimensions cannot be proportionately reduced as the material thicknesses would not be practical. A significant temperature gradient can be established in a test article of this size. Therefore, sufficient thermal stresses and deflections would be recorded to examine the validity of a theoretical model of the reduced scale guideway.

The test article should be supported on both ends of its span by a concrete footing with attachment points similar to the actual guideway. Simulated solar heating should be introduced to the guideway along its entire span with infrared heat lamps. The position of these lamps should be adjustable to provide uniform spanwise heating and allow for testing at various solar inclinations. The proposed test facility is shown in Figure 5-6.

The specimen should be heated from different simulated solar inclinations. Deflection transducers, thermocouples, and strain gauges should be recorded at regular time intervals.

The distance from the heating lamps to the test specimen can be adjusted such that the maximum top surface temperature attainable is approximately 55°C (130°F) which is the expected maximum summer surface temperature that would occur in Florida. This surface temperature should be maintained until the cross section temperature gradient remains unchanged. The heat source should then be removed and data recorded during cooling.

The data collected from these tests should be compared with the predictions of the primary structural response model. As this model is given a fifth power temperature distribution as an initial condition, the actual measured temperature distribution should be used as input if it varies significantly from the fifth power model.

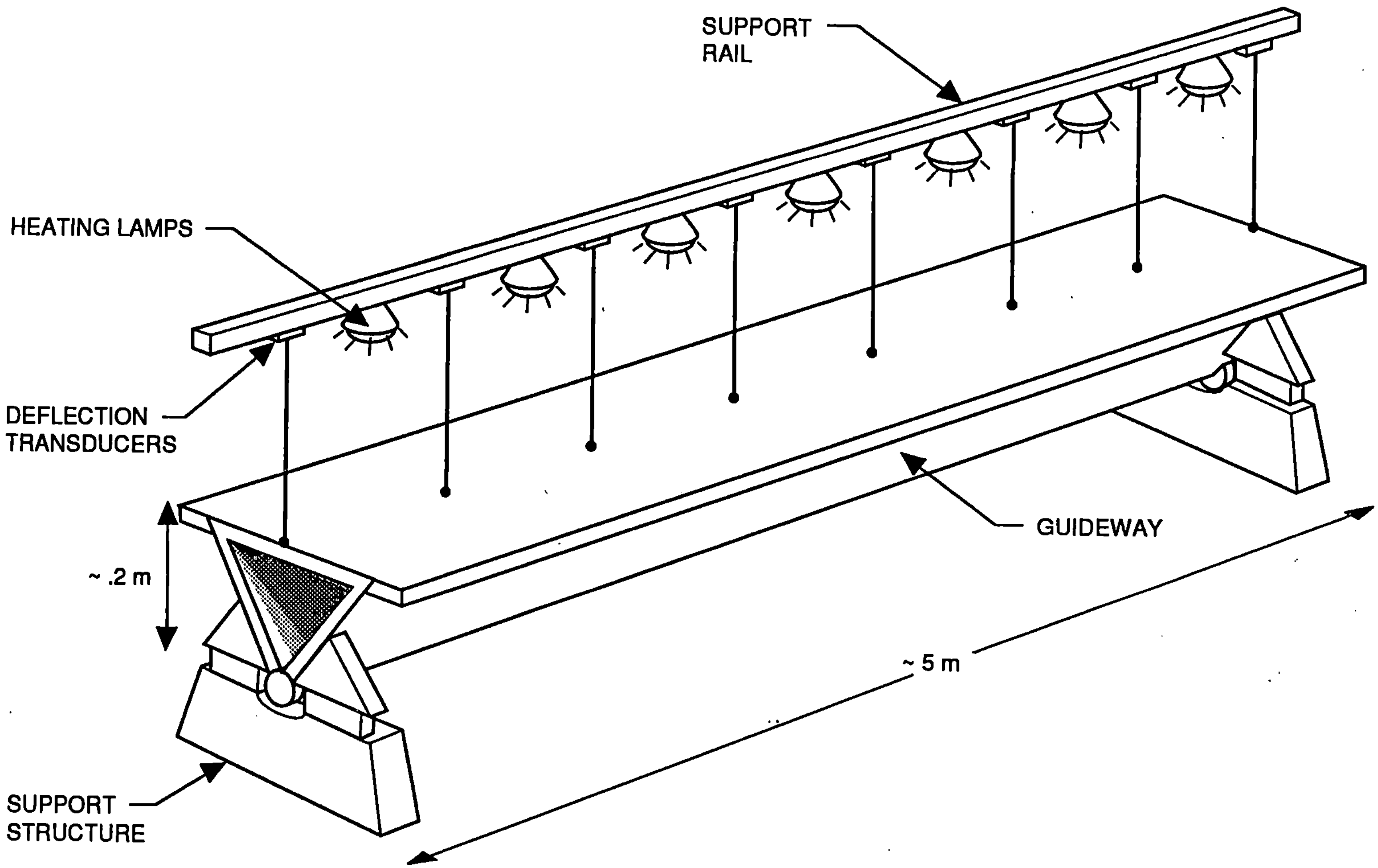

Figure 5-6. Proposed Testing Facility

5.4 CSG Buckling Model Validation

5.4.1 Objective

This test of a continuous sheet guideway is proposed to validate the buckling model and to evaluate CSG attachment methods.

5.4.2 Technical Discussion

An analysis was developed (see subsection 3.3.1) to evaluate the CSG buckling potential and to quantify the influence of such variables as CSG material and cross section, and fastener pitch and longitudinal resistance. A parametric study was conducted to determine the best combination of these variables based on the buckling analysis. The results of this study indicate that the use of CSG and discrete fasteners may not be cost effective as buckling is likely to result without thick CSG cross sections or very small fastener pitch.

The analysis of subsection 3.3.2 further indicated that segmented sheet guideway is not practical for several reasons. Consequently, CSG appears to only be practical if a superior attachment method is identified or if appropriate thermal stress mitigation methods are developed. A laboratory test program should be initially conducted to validate the CSG buckling model. Further testing should evaluate alternative attachment techniques.

5.4.3 Test Plan

The proposed testing should be conducted outdoors on a concrete slab. As this test is conducted to evaluate the performance of the CSG and its fasteners, the concrete slab need not be end supported across a span. The CSG is recommended to be a continuous aluminum plate of rectangular cross section. Several tests should be set up on the same slab to provide direct "same day" comparison between fasteners.

Initial tests should be conducted to validate the model. The CSG should be attached using edge clamps set at a consistent pitch.

Temperature and strain should be monitored in the CSG throughout several high solar radiation days to collect baseline data. Additional infrared heating lamps may later be used to induce buckling, if solar heating is not sufficient. The strains and temperatures recorded should be compared to the predictions of the buckling model.

Following these initial tests, novel attachment techniques, including bonding and other developmental techniques, should be evaluated in side-by-side testing (Figure 5-7). As discussed previously these methods may mitigate the thermal problems which result from the use of discrete fasteners. The previous CSG heating tests should be repeated with these novel attachments. Additionally, longitudinal test loading of the CSG must be applied to determine the resistance of these techniques. Testing is also recommended to evaluate the durability of these techniques under in-service environmental conditions. The results of these tests should clearly demonstrate the potential of these novel attachment techniques.

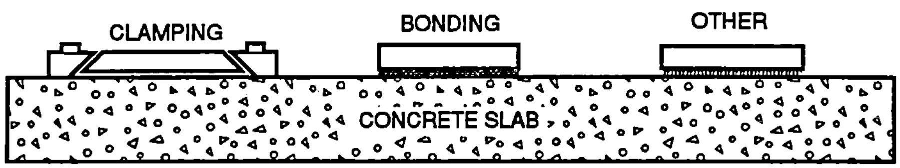

Figure 5-7. Proposed CSG Attachment Testing

6. CONCLUSIONS AND RECOMMENDATIONS

On the basis of the work performed in Sections 1 to 4, the following conclusions are drawn.

6.1 Conclusions

1. Both sheet guideways and supporting primary structures experience thermal effects due to temperature change. Temperature change in sheet guideways is due to eddy current and solar heating. The sheet guideways experience constrained thermal expansions, which can result in local out-of-plane buckling, or tensile fracture at weldments. This can result in loss of vehicle levitation and guidance. The primary structure will undergo transverse deflection due to the temperature gradient through the cross section of the guideway. If proper mitigation measures are not implemented, the thermal gradient induced deflection in the primary structure can exceed the tolerance limits used in EMS Maglev guideways, and ride quality can be significantly affected by these deflections.

2. The temperature distribution in the depth direction in primary structures is not adequately represented by many existing codes excepting the one developed in New Zealand. A fifth degree equation has been proposed for this in the New Zealand code, which is in reasonable agreement with the unsteady state heat transfer calculations presented in this report. The fifth degree equation should be adopted for elevated Maglev guideway design. Linear temperature distributions are non-conservative, and should not be used in the thermal analysis of Maglev guideway structures.

3. There are tradeoffs between single span and multiple span designs for the primary elevated Maglev structures. Alternating continuous support conditions (i.e., multiple spans), reduce maximum thermal deflections, but increase bending stress, which may contribute to reduced fatigue life, particularly in flexible guideway designs.

4. White coating on the primary structure can reduce the severity of the thermal gradient problem. Use of insulation concrete has marginal benefits in this regard.

5. Design of continuous sheet guideways is involved. Close fastener spacing will be required to increase buckling strength. Unduly high installation temperatures may also be required, which can cause tensile fractures at weldments. Mitigation of these effects through optimization of parameters is involved and may not be satisfactory in practice due to the

11. Kish, A. and G. Samavedam, "Dynamic Buckling of CWR Tracks: Theory, Test and Safety Concepts," Proceedings of TRB on Lateral Track Stability, 1991, pp. 23-28.

12. Elbady, M.M. and Ghali, A., "User's Manual and Computer Program FETAB," University of Calgary, Canada, 1982.

13. Prestressed Concrete Institute, *PCI Manual for Structural Design of Architectural Precast Concrete*, Chicago, IL, 1977.

14. Hayes, W.F., "High Speed Electrodynamic Maglev Guided Ground Transportation System Conceptual Design Study," National Research Council of Canada, Sept. 1977.

15. Grumman Corporation, "New York State Technical and Economic Maglev Evaluation," June, 1991.

16. CIGGT, "Thermal Analysis of Transrapid Maglev Guideway Proposed for Elevated Structure in Las Vegas - Southern California Corridor," Report No. 86-13, Kingston, Ontario.

17. Philco-Ford Corporation, "Conceptual Design and Analysis of the Tracked Magnetically Levitated Vehicle Technology Program (TMLV) Repulsion Scheme," Vol. I, Technical Studies, prepared for Federal Railroad Administration, DOT-FR-40024, 1975.

18. Timoshenko, S. and Gere, J., *Theory of Elastic Stability*, second edition, McGraw-Hill, NY, 1961.

19. Atherton, D.L. and Eastham, A.R., "Electrodynamic Suspension and Linear Synchronous Motor Propulsion for High Speed Guided Ground Transportation," CIGG Report No. 77-13, Kingston, Ontario, September, 1977.

20. Ooi, B.T. and O.P. Jain, "Force Transients at Guideway Butt Joints in Repulsive Magnetic Levitation System." IEEE Transactions, Vol. PAS-98, No. 1, 1979.

Thermal Effects and Mitigation Methods for Continuous Sheet Guideways, US DOT, FRA, NMI, G Samavedam, A Purple, 1992 -